



UvA-DARE (Digital Academic Repository)

Spectral analysis of blood stains at the crime scene

Edelman, G.J.

Publication date

2014

Document Version

Final published version

[Link to publication](#)

Citation for published version (APA):

Edelman, G. J. (2014). *Spectral analysis of blood stains at the crime scene*. [Thesis, fully internal, Universiteit van Amsterdam].

General rights

It is not permitted to download or to forward/distribute the text or part of it without the consent of the author(s) and/or copyright holder(s), other than for strictly personal, individual use, unless the work is under an open content license (like Creative Commons).

Disclaimer/Complaints regulations

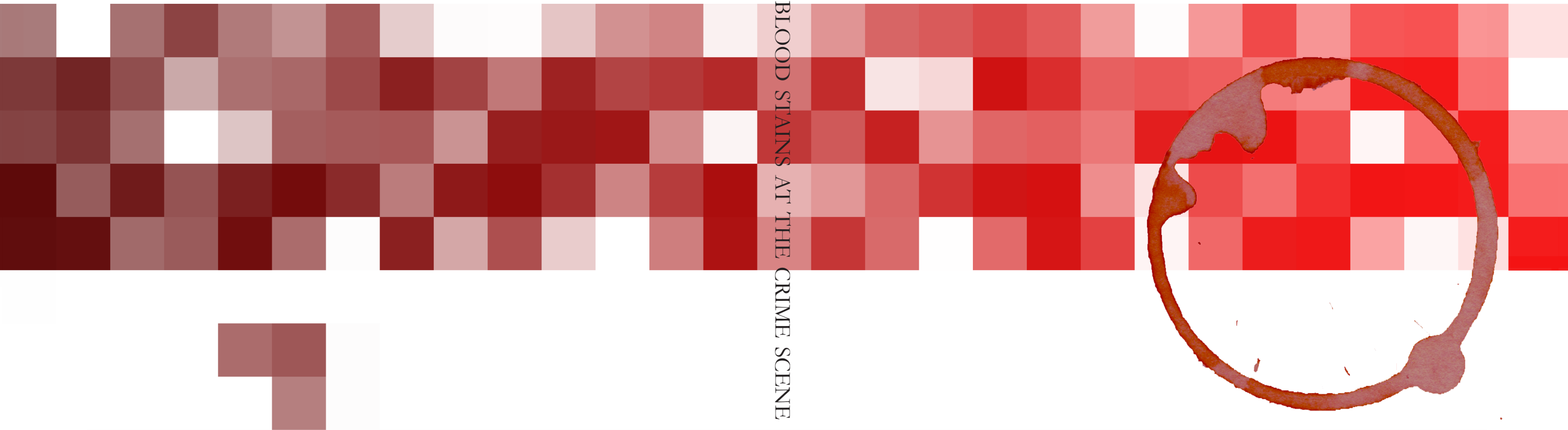
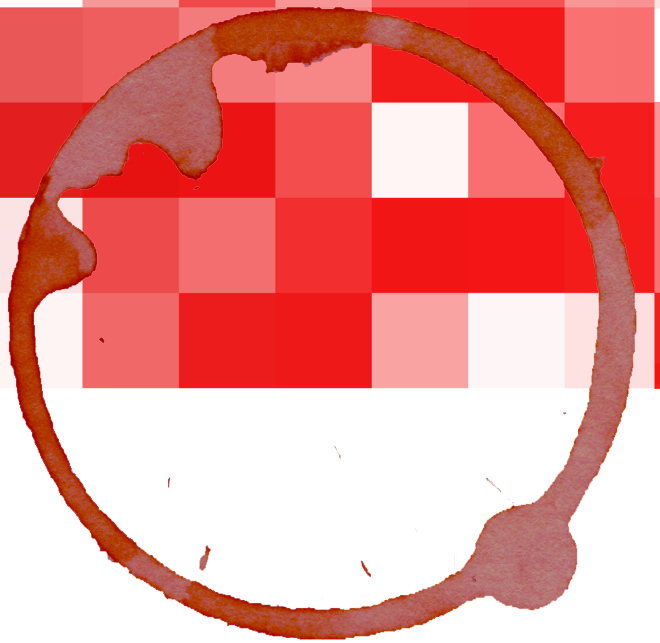
If you believe that digital publication of certain material infringes any of your rights or (privacy) interests, please let the Library know, stating your reasons. In case of a legitimate complaint, the Library will make the material inaccessible and/or remove it from the website. Please Ask the Library: <https://uba.uva.nl/en/contact>, or a letter to: Library of the University of Amsterdam, Secretariat, P.O. Box 19185, 1000 GD Amsterdam, The Netherlands. You will be contacted as soon as possible.

SPECTRAL ANALYSIS OF BLOOD STAINS
AT THE CRIME SCENE

Gerda Edelman

Gerda Edelman

SPECTRAL ANALYSIS OF BLOOD STAINS AT THE CRIME SCENE



SPECTRAL ANALYSIS OF BLOOD STAINS

AT THE CRIME SCENE

Spectral analysis of blood stains at the crime scene
PhD thesis, University of Amsterdam, The
Netherlands

Publication of this thesis is kindly supported by:



Author: Gerarda Johanna Edelman

ISBN: 978-90-6464-764-2

Printing: GVO drukkers & vormgevers B.V. |
Ponsen & Looijen

Copyright 2014 © Gerarda Johanna Edelman,
Amsterdam, The Netherlands. All rights reserved.
No part of this publication may be reproduced,
stored in a retrieval system, or transmitted in any
form or by any means, electronic, mechanical,
photocopying, recording or otherwise, without the
prior permission of the copyright owner.

SPECTRAL ANALYSIS OF BLOOD STAINS

AT THE CRIME SCENE

ACADEMISCH PROEFSCHRIFT

ter verkrijging van de graad van doctor
aan de Universiteit van Amsterdam
op gezag van de Rector Magnificus
prof. dr. D.C. van den Boom
ten overstaan van een door het college voor promoties ingestelde
commissie, in het openbaar te verdedigen in de Agnietenkapel
op dinsdag 15 april 2014, te 12.00 uur

door

Gerarda Johanna Edelman

geboren te Ede

Promotiecommissie

Promotores:

Prof. dr. M.C.G. Aalders

Prof. dr. A.G.J.M. van Leeuwen

Overige leden:

Prof. dr. A.D. Kloosterman

Prof. dr. R.J. Oostra

Prof. dr. A.K. Smilde

Prof. dr. ir. R.M. Verdaasdonk

Prof. dr. A.C. van Asten

Prof. dr. C. Weyermann

Faculteit der Geneeskunde

TABLE OF CONTENTS

1 - Introduction.....	- 7 -
2 - Hyperspectral imaging for non-contact analysis of forensic traces.....	- 13 -
3 - Reflectance spectroscopy and hyperspectral imaging for the identification of blood stains.....	- 43 -
4 - Hyperspectral imaging for the age estimation of blood stains at the crime scene.....	- 63 -
5 - Practical implementation of blood stain age estimation	- 79 -
6 - Visualization of latent blood stains using visible reflectance hyperspectral imaging and chemometrics.....	- 97 -
7 - Identification and age estimation of blood stains on coloured backgrounds by near infrared spectroscopy.....	- 111 -
8 - Infrared imaging of the crime scene: possibilities and pitfalls.....	- 131 -
9 - Discussion.....	- 149 -
10 - References.....	- 169 -
11 - Summary	- 189 -
12 - Samenvatting	- 191 -
13 - Curriculum vitae.....	- 195 -
14 - Portfolio	- 196 -
15 - List of publications	- 198 -
16 - Dankwoord.....	- 201 -

1 - INTRODUCTION

This introductory chapter emphasizes the need for innovative techniques which aid crime scene investigations. Techniques used at the crime scene are ideally portable, rapid, and non-destructive. Because existing spectroscopic techniques meet these criteria, they are highly suitable for crime scene analysis. In this thesis, we propose the use of several optical techniques for the detection, identification, and age estimation of blood stains. We explored the visible, near infrared, and mid infrared wavelength range for this purpose, as outlined in this chapter.

1.1. CRIME SCENE INNOVATION

Crime scene investigators play a vital role in most criminal cases. They have the responsibility to detect, document and analyze evidence, and to select, collect and package traces for further analysis in the laboratory. All further forensic investigations depend on the quality of the initial investigation at the crime scene. If traces are overlooked or destructed, they will not be analyzed and therefore will not be used as evidence in the court of law. This problem denotes the importance of techniques which aid crime scene investigators in their search for relevant traces.

Due to technological improvements, techniques traditionally used in laboratories are getting faster, more portable and more informative. These innovations induce new possibilities for the detection and analysis of traces at a scene of crime, within their original context. Techniques already used in forensic laboratories may be explored for this purpose. Likewise, exploration of technologies developed in other disciplines may also lead to interesting forensic innovations. Existing techniques from outside the forensic world, e.g. the spectral analysis of blood, can possibly be adapted for crime scene investigation purposes. Recently, Bremmer et al¹ demonstrated how a method routinely used in medicine for blood oxygen saturation measurements could be adapted to a forensic application. They were able to relate the concentration change of oxyhaemoglobin, methaemoglobin and hemichrome – all reaction products of haemoglobin – to the age of blood stains in a laboratory setup, based on diffuse reflectance spectroscopy. Spectroscopic age estimation of blood stains is an innovative technique giving an estimation of the moment blood was shed, information currently not available to the investigator. Just like medicine, forensic science benefits from non-invasive techniques like optical spectroscopy. Ideally, diagnostic techniques in medicine are applied *in vivo*, rather than in the laboratory, which requires the tissue to be removed from the body. Similarly, it is profitable to analyse forensic traces non-invasively within their original context at the crime scene.

The transition from laboratory measurements to crime scene analysis, however, brings some challenges, typical for forensic casework. While in a

laboratory setup ideal substrates are used, many different and far from ideal substrates can be encountered at a crime scene. Also, measurements are preferably performed without touching the trace. To deal with these circumstances, we can use techniques developed for remote sensing applications, or for the pharmaceutical and food industries. The need for high speed online processing in these industries has driven the development of fast methods for both data acquisition and analysis, which can also be valuable at the crime scene.

1.2. AIM

In this thesis, we describe several methods for the analysis of blood stains. Blood stains are among the most important types of evidence in forensic investigations. Analysis of blood stains can provide insight in *what* happened, as blood stain patterns inform investigators about the activities needed to create the stains, *who* was involved, by subsequent DNA-analysis, and spectral analysis may even indicate *when* the blood was shed. At a crime scene, however, some blood stains may be visible with the naked eye, while others are indiscernible, thus motivating the need for technology increasing the contrast between a stain and its background. After the detection of a stain, an identification test is needed to indicate the nature of the stain. When a blood stain identification test is positive, it is interesting to know when the stain was created in order to create a timeline of events. Our aim was to develop methods for:

1. the detection of latent blood stains;
2. the identification of blood stains;
3. the age estimation of blood stains,

which can be applied at the crime scene. Driven by the importance of non-destructive analysis we evaluated several optical techniques for these purposes. We explored the visible wavelength range and beyond.

1.3. OUTLINE

In **Chapter 2**, we describe the advantages and challenges of hyperspectral imaging for forensic applications. Because hyperspectral imaging integrates conventional imaging and spectroscopy to obtain both spatial and spectral information from a sample, it enables investigators to analyze the chemical composition of traces and simultaneously visualize their spatial distribution. The technique therefore offers significant potential for the detection, visualization, identification and age estimation of forensic traces. The application of this technique for the visualization and chemical analysis of forensic traces is reviewed.

Chapter 3 demonstrates the applicability of spectroscopy and hyperspectral imaging as a non-destructive indicative test for the identification of blood. By deducing the presence of haemoglobin oxidation products from reflectance spectra of blood stains, blood can be distinguished from other red and brown samples visually mimicking blood. Measurements were first performed using a fibre optic probe and a spectrometer in a controlled laboratory setup. Based on the results, the spectral processing steps were adapted to minimize the influence of non-chemical factors as the measurement distance and angle. With the adapted analysis, the identification method was shown to be suitable for a less-controlled hyperspectral imaging setup. The sensitivity and specificity of the technique were investigated, and the practical applicability was demonstrated in forensic casework.

The spectral analysis of blood stains was expanded to include age estimation in **Chapter 4**. Based on the reflectance spectra of blood stains, not only the presence of haemoglobin oxidation products can be assessed, but their relative concentrations can be calculated simultaneously. As described above, the amount of oxyhaemoglobin, methaemoglobin and hemichrome in a blood stain can be used to estimate the age of the stain. However, the technique described by Bremmer et al using a spectroscopy setup, was highly sensitive to small changes in the geometry of the setup, which complicated the use at the crime scene. We demonstrated that an improved spectral analysis greatly extended the applicability. Using a hyperspectral imaging system we

were able to estimate the age of different blood stain patterns at a simulated crime scene. When applied in criminal casework, this new technique provides investigators with information useful to determine the moment a crime was committed, or to select relevant stains for further analysis.

The above described method is hampered by coloured backgrounds, as these absorb visible light, and thereby disturb the measured reflectance spectra of blood stains. **Chapter 5** addresses this problem. We proposed an adapted algorithm to correct for background absorptions. Additionally, we described a statistical approach to calculate an age interval for a questioned blood stain. The applicability of the new technique for blood stain age estimation in forensic casework and its possible value for crime investigations is demonstrated in **Chapter 5**. In a case report we described a shooting incident in which 3 bodies were found dead in a living room. For crime reconstruction purposes, bloodstain pattern analysis was performed at the scene. As an innovative aid to the crime scene analysis, the absolute and relative age of different groups of bloodstains were measured using visible reflectance spectroscopy. Combined with other evidence, the results could lead to a better reconstruction of the timeline of events, useful for the verification of possible scenarios.

On dark objects, the visualization of latent stains is already challenging in forensic practice. **Chapter 6** covers the detection of blood stains on black backgrounds using visible hyperspectral imaging, which is useful for bloodstain pattern analysis, or to aid the collection of traces for further tests, e.g. blood stain identification or DNA analysis. This chapter shows that blood stains can be distinguished from many black fabrics based on the different absorption properties. Several chemometric methods are tested to optimize the contrast.

When the absorption of light is dominated by the background material, visible spectroscopy is hampered. Therefore we explored the wavelength range beyond the visible for the analysis of blood stains. In **Chapter 7** we successfully identified blood stains on coloured and black backgrounds and estimated their age using near infrared (NIR) spectroscopy. Compared to visible spectroscopy, NIR spectroscopy provides more information about the chemical structure of samples, as NIR absorptions are caused by specific

molecular vibrations. However, apart from the chromophores oxyhaemoglobin, methaemoglobin and hemichrome, several other components present in blood contribute to the absorption of NIR light, which complicates the analysis. For this reason, we used correlation analysis and partial least squares regression analysis for the identification and age estimation of blood stains using NIR spectroscopy.

A final interesting wavelength range explored in this thesis is the mid infrared, or thermal wavelength range. As a result of improvements in technology and a decrease in cost, mid infrared imaging is an emerging technique for law enforcement and forensic investigators. All objects radiate infrared energy, invisible to the human eye, which can be converted into visible images by mid infrared cameras, thereby visualizing differences in temperature and/or emissivity of objects. The rapid, non-destructive and non-contact features of mid infrared imaging indicate its suitability for a wide range of forensic applications, including the detection of latent bloodstains. **Chapter 8** provides an overview of the principles and instrumentation involved in mid infrared imaging. Difficulties concerning the image interpretation are addressed. Reported forensic applications are reviewed and supported by practical illustrations.

To conclude, all topics described above are discussed from a forensic practical point of view in **Chapter 9**. Emphasis is laid on further steps needed for the actual implementation of the described innovative techniques in standard forensic practice.

2 - HYPERSPECTRAL IMAGING FOR NON-CONTACT ANALYSIS OF FORENSIC TRACES

Forensic Science International 2012;223(1-3):28-39

Hyperspectral imaging integrates conventional imaging and spectroscopy, to obtain both spatial and spectral information from a sample. This technique enables investigators to analyze the chemical composition of traces and simultaneously visualize their spatial distribution. Hyperspectral imaging offers significant potential for the detection, visualization, identification and age estimation of forensic traces. The rapid, non-destructive and non-contact features of hyperspectral imaging mark its suitability as an analytical tool for forensic science. This chapter provides an overview of the principles, instrumentation and analytical techniques involved in hyperspectral imaging. We describe recent advances in hyperspectral imaging technology motivating forensic science applications, e.g. the development of portable and fast image acquisition systems. Reported forensic science applications are reviewed. Challenges are addressed, such as the analysis of traces on backgrounds encountered in casework, concluded by a summary of possible future applications.

2.1. INTRODUCTION

The detection and identification of forensic traces are crucial in crime scene investigations. For this purpose a wide range of techniques is available, including chemical enhancement techniques and the use of light sources with 15 to 30 nm bandwidths, which increase the contrast between a trace and its background. Many of these techniques are, however, either destructive or subject to human interpretation. Hyperspectral imaging is suitable for the non-contact identification of evidence, thus minimizing the risk of contamination and destruction of traces. Hyperspectral imaging integrates conventional imaging and spectroscopy to obtain a three dimensional data set containing both spatial and spectral information of a specimen. In addition, analysis of the temporal behaviour of spectra can give insight in the chemical changes within the specimen, which can be used for age estimation purposes. Estimation of the age of forensic traces provides investigators with valuable information, which can assist the reconstruction of the timeline of events.

Hyperspectral imaging was originally developed for remote sensing applications utilizing satellite imaging data of the earth² but has since found application in such diverse fields as food science³, pharmaceuticals⁴ and medical diagnostics⁵. Hyperspectral images are analogous to a stack of images, each acquired at a narrow spectral band. Like spectroscopy, hyperspectral imaging can be applied in different parts of the electromagnetic spectrum, e.g. ultraviolet (UV), visible (Vis), near infrared (NIR), mid infrared (IR) or even the thermal infrared range. In these regions reflectance, transmission, photoluminescence, luminescence or Raman scattering can be recorded by hyperspectral cameras with a spectral resolution similar to miniature spectrographs. Spatial resolutions can be adapted to the application, which range from microscopic to landscapes. Advantages of hyperspectral imaging include speed of data acquisition, reduction of human error, no destruction of traces, no specimen preparation, and the ability to illustrate the results.

Hyperspectral imaging is a powerful emerging tool for the analysis of forensic traces. Latent traces can be detected and visualized by using spectral differences to obtain optimal contrast between a trace and its background.

Individual spectra give information about the chemical composition of the specimen, which is useful for identification and quantification purposes, and the spatial distribution of traces is simultaneously recorded. In the last decade, hyperspectral imaging has proven to be a valuable technique for the imaging of latent fingerprints and the detection of trace materials within these prints. Hyperspectral imaging is also emerging in other fields of forensic science and has shown its value in comparative research of materials including fibres, paint chips, or inks, where the question arises whether two traces share common origin. The possibility of viewing spectral and spatial information side by side is advantageous in these cases.

Recent developments in hyperspectral imaging technology offer added potential for forensic science investigations. Because hyperspectral imaging systems are becoming increasingly portable, they may be used at the scene of investigation, where traces can be viewed and interpreted in the original context. The development of fast scanning systems enables investigators to scan a complete scene, which reduces the workload in forensic laboratories and quickly provides investigators with valuable information which can lead the investigation.

This chapter gives an overview of the principles, instrumentation and analytical techniques involved in hyperspectral imaging, followed by a review of recent forensic science applications. We limited our scope to hyperspectral imaging applications using reflectance, photoluminescence, transmission or Raman scattering. Because forensic traces are typically encountered in many different environmental circumstances, their analysis brings specific challenges, which are also addressed. To conclude, possible future applications are summarized.

2.2. HYPERSPECTRAL IMAGING

2.2.a INTERACTION OF LIGHT AND MATTER

The interaction between light and a specimen is determined by the optical properties of the specimen and the incident light. As hyperspectral imaging

measures such interaction, it may be used to characterize the material. In practice this involves illumination of the object under investigation. Commonly, the first interaction will be on the specimen surface where part of the light will be reflected (Figure 2.1a). This part contains no to little information from within the medium but is governed by the index of refraction difference between media. Upon entering the material, the light can be scattered or absorbed.

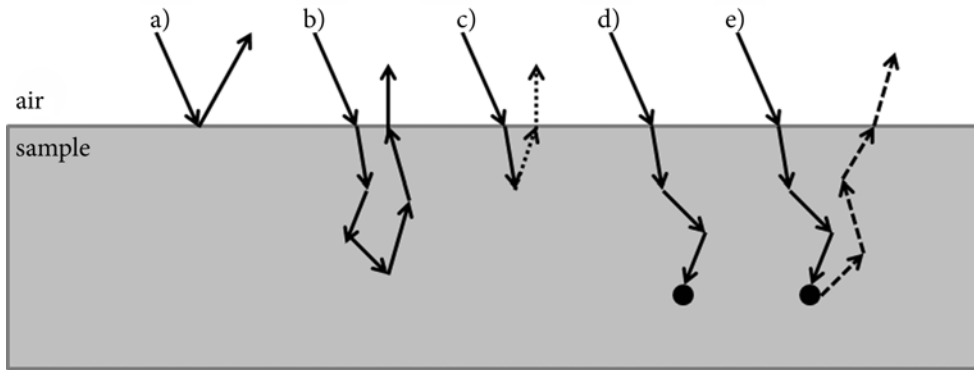


Figure 2.1. The interaction of light with a specimen may lead to a) specular reflection, b) elastic scattering followed by diffuse reflection, c) inelastic scattering followed by emission of Raman shifted light (dotted lines), d) absorption, and e) absorption followed by photoluminescence emission (dashed lines).

Scattering is the process by which light interacts with structures in a specimen and causes a change in direction of propagation, depending on the wavelength, size of the particle and index of refraction differences (Figure 2.1b). The majority of light is scattered at the identical wavelength of the incident light, a process referred to as elastic scattering. There may also be a small fraction that will be inelastically scattered (Raman scattering) which will cause wavelength shifts corresponding to the vibrational states of the molecules in the specimen (Figure 2.1c). Raman scattering can be measured to chemically analyze the scattering specimen.

The absorption properties of a chemical compound are wavelength dependent. Absorption in the visible wavelength range corresponds to the electronic states of the molecule, while absorption in the NIR and IR is

determined by the vibrational modes. Upon relaxation, return to the ground state, the energy will be released in the form of radiation (heat or photoluminescence) or by transfer to another molecule. So both the spectral absorption and, if present, the induced photoluminescence can be measured to identify the chemical contents of a specimen using hyperspectral cameras in reflectance, or transmission mode (Figure 2.1d/e). Quantitative analysis, however, is complicated because the length of the path travelled by the detected light depends on the optical properties of the specimen⁶.

2.2.b HYPERCUBE FORMATION

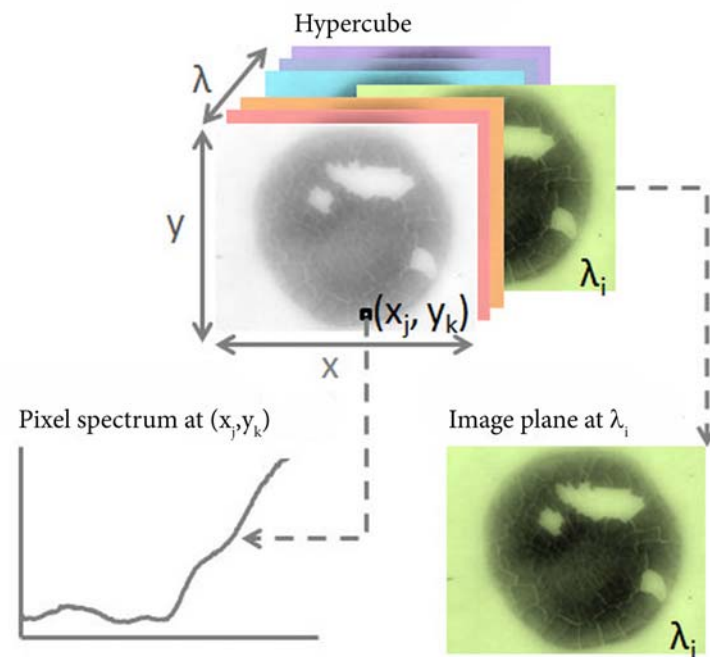


Figure 2.2. Hypercube of a blood stain, with two spatial (x,y) and one wavelength (λ) dimension. From the hypercube an image plane is shown for one wavelength (λ_i) and a spectrum is obtained from one pixel (x_j, y_k) .

Hyperspectral images are analogous to a stack of images, each acquired at a narrow spectral band. The resulting data set is a three-dimensional block of data, the so-called hypercube, with two spatial (x,y) dimensions and one wavelength (λ) dimension (Figure 2.2). This hypercube provides images for each wavelength (λ_i) and a spectrum can be obtained from each individual pixel (x_j,y_k), as depicted in Figure 2.2.

Obtaining information in all three dimensions of a hypercube simultaneously is currently not feasible; hyperspectral instruments can only capture two dimensions at a time. Temporal scanning is needed to create a three-dimensional hypercube by stacking the two-dimensional data in sequence. There are three ways of acquiring a hypercube (Figure 2.3), commonly known as point scanning (or whiskbroom), line scanning (or push broom), and area scanning (or stare down). These descriptive names refer to the hardware methodology used to acquire the hypercubes:

- In a point scanning system, a complete spectrum is acquired at a single point. Light originating from this point enters the objective lens and is separated into different wavelengths by a spectrometer and detected by a linear array detector. Once spectral acquisition is completed, the spectrum of another point can be recorded. Scanning has to be performed in both spatial directions to complete the hypercube.

- In the case of line scanning systems, the spectra of all pixels contained in one image line are acquired simultaneously. The light is dispersed onto a two dimensional charge coupled device (CCD) detector. This way, a two dimensional data matrix with the spectral dimension and one spatial dimension is acquired. The second spatial dimension of the hypercube is achieved by scanning across the specimen surface in a direction perpendicular to the imaging line. This means that relative movement between the object and detector is necessary, which may be achieved either by moving the specimen (e.g. using a translation stage or a conveyor belt) and keeping the hyperspectral camera in a fixed position or by moving the camera and keeping the specimen fixed.

- An area scanning system also acquires a two-dimensional data matrix but in this case the data represent a more conventional image with two

spatial axes. A complete hypercube is obtained by collecting a sequence of these images for one wavelength band at a time. The wavelength of incoming light in this configuration is typically modulated using a tuneable filter.

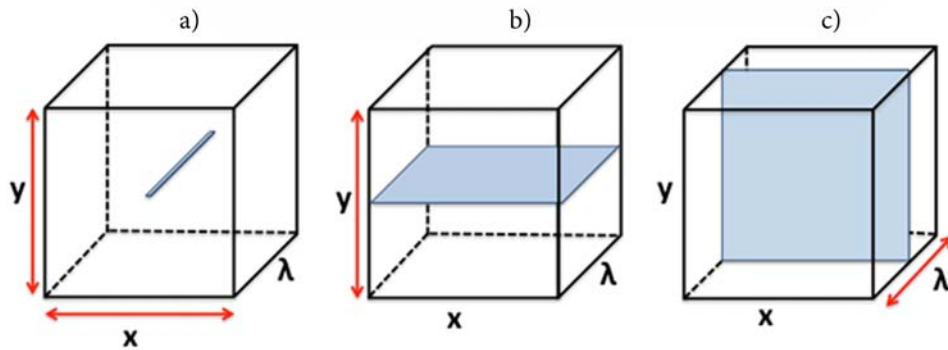


Figure 2.3. Methods for acquiring three-dimensional hypercubes: (a) point scanning, (b) line scanning, and (c) area scanning. Hypercubes contain two spatial (x,y) and one spectral (λ) dimension. Blue areas represent data acquired by one scan. Red arrows represent temporal scanning required to complete the hypercube.

2.2.c SYSTEM OPTIMISATION FOR FORENSIC SCIENCE APPLICATIONS

Typical hyperspectral imaging systems contain the following components: objective lens, wavelength modulator, detector, illumination, and acquisition system (Figure 2.4). All these components can be adjusted to the requirements of the application. The forensic environment of analysis may range from laboratory to field conditions, whereas the areas of interest may range from the microscopic to landscapes. As for conventional imaging, different objective lenses can be chosen to obtain the right spatial resolution for each application, e.g. macroscopic lenses, zoom lenses, wide angle lenses etc. For analysis on a microscopic scale, the hyperspectral imaging system can be coupled to a microscope.

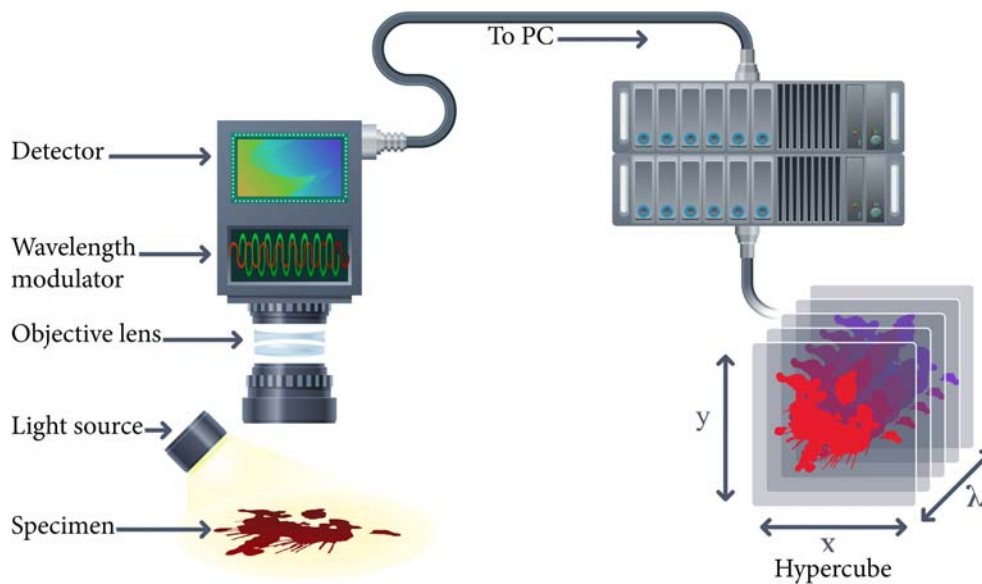


Figure 2.4. Schematic showing components of a hyperspectral imaging system, resulting in a hypercube of the specimen.

Acousto-Optic Tuneable Filters (AOTFs)⁷ and Liquid Crystal Tuneable Filters (LCTFs)⁸ are the two most common wavelength modulators employed. Major drawbacks of these filters are their size and costs. Recently, hyperspectral imaging systems have been developed and commercialised using Fabry-Pérot filters (Innopharmalabs, Ireland). Another recent innovation employs the use of a tuneable laser system based on Optical Parametric Oscillator (OPO) technology⁹, which replaces the broadband light source, thus removing the need for a wavelength modulator. The benefits of Fabry-Pérot filters and tuneable lasers compared to tuneable filters are their small size and weight, speed of wavelength tuning and high optical throughput. The development of these new technologies offers potential for low cost, hand held, portable hyperspectral imaging with the desired resolution for trace analysis in forensic science applications.

After the light is separated into different wavelengths the detector, e.g. a charge coupled device (CCD), measures the intensity of the collected light. The pixels in the CCD sensor can be arranged in one-dimensional or two-

dimensional arrays, resulting in line detectors and area detectors¹⁰. Detectors for the mid-infrared region are also available, such as lead selenide (PbSe), indium antimonide (InSb), and mercury cadmium telluride (MCT). To ensure sensitivity of the detector to low light intensities in the infrared regions, the detector may have to be cooled. The CMOS image sensor is another detector that has the potential to compete with CCD. Typical advantages as high speed, low cost, low power consumption, and small size for system integration make them prevail in the consumer electronics market (e.g. low-end camcorders and cell phones). However, the dynamic range and the sensitivity are lower than those of CCD detectors¹⁰.

The choice of the light properties (broadband vs. monochromatic, specular vs. diffuse, etc.) and consequently the illumination source (halogen, LED, laser, etc.) and lighting arrangement are crucial for the performance and reliability of the system. Halogen lamps, commercially available in various forms, are most common broadband illumination sources used in hyperspectral applications. Halogen lamps can be used directly to illuminate the target (like room lighting) or can be delivered through an optical fibre. Light emitting diode (LED) technology has advanced rapidly during the past few years, and both narrowband and broadband light generators are currently available in the market. This technology is a relatively inexpensive, robust and reliable alternative to halogen lighting, and its use for hyperspectral imaging is likely to expand in the near future, with particular benefits for portable systems. Unlike broadband illumination sources, lasers are powerful directional monochromatic light sources, which make them interesting candidates for photoluminescence and Raman applications. The use of aforementioned tuneable light sources is still limited in hyperspectral imaging applications but they offer promising scope for specific applications including trace analysis. The implementation of digital micro-mirror devices (DMDs) is another recent development in hyperspectral imaging¹¹. In this setup, only the region of interest is illuminated. Such systems reduce variations in the spectra arising from scattered light from the background and nearby objects.

Finally, the image acquisition system can be optimized for the application. The desire for on-line monitoring within the process industries has

seen the emergence of real-time online systems typically employing line-scanning approaches. This line scanning setup also offers potential for large-scale forensic science applications, where instead of using a moving stage or conveyor to pass a specimen or product past the detector, the detector itself is moved over a large stationary area of interest such as a wall, a floor or an entire scene of investigation (see Figure 2.5).



Figure 2.5. Hyperspectral imaging system at a simulated crime scene.

2.2.d DATA ANALYSIS

Upon detection, analysis of the data provided in the hypercube is required. Grahn and Geladi detail the types of treatment that can be applied¹². A summary of processing steps is given below.

Calibration

The raw data in a hypercube not only result from the chemical composition of a specimen, but also from the illumination intensity, the sensitivity of the detector and the transmission of the optics¹³. The influence of these factors is a function of wavelength, but may also show spatial variations. Spectral and spatial calibration is required to compensate for this. Calibration measurements

typically performed for reflectance measurements consist of acquisition of the dark response of the system, measured while covering the lens and dimming the light source, and the response of a uniform, high reflectance reference. Using these data, the reflectance (R) can be calculated as follows:

$$R = (I_{\text{specimen}} - I_{\text{dark}}) / (I_{\text{reference}} - I_{\text{dark}}),$$

where I_{specimen} is the intensity of the reflectance measurement of the specimen, I_{dark} the intensity of the dark response, and $I_{\text{reference}}$ the intensity of the uniform reference.

It is considered good practice to carry out calibration on a daily basis, as small changes in electrical power sources, illumination, detector response and system alignment may result in changes in the detected response. Inclusion of internal reference standards in each hyperspectral image acquired is also recommended, which allows monitoring the performance of the system over time.

Spectral pre-processing

Spectral information can be used to gain knowledge about the chemical composition of a specimen. However, several non-chemical origins cause systematic variations between spectra, unrelated to the chemical composition of a specimen, including specular reflections, scattering effects due to surface inhomogeneities, varying object – illumination distances and random noise. A number of spectral pre-processing techniques can be applied to reduce these variations, e.g. smoothing, offset correction, normalization, mean centring, standard normal variate (SNV) correction¹⁴, multiplicative scatter correction (MSC)¹⁵, and Savitzky-Golay differentiation¹⁶. The effect of MSC and differentiation is demonstrated in Figure 2.6; MSC removes variation resulting from scattering effects, first and second order differentiation eliminate a constant offset or linear baseline, respectively, and can be used to resolve overlapping peaks originally appearing as shoulders.

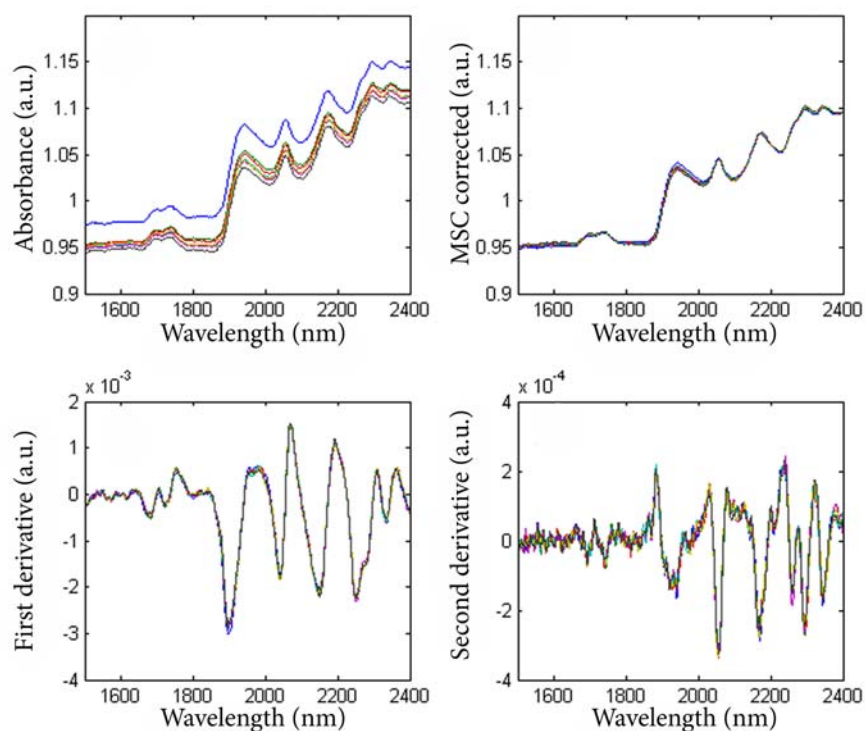


Figure 2.6. Spectra of several blood stains of the same age before and after pre-processing: a) absorbance spectra, b) spectra after applying multiplicative scatter correction (MSC), c) first derivative spectra, d) second derivative spectra.

Spectral analysis

Spectral data analysis attempts to address what different components are present in the hypercube, in which concentration and how they are distributed. In some cases the intensity at a single wavelength, the integrated intensity (area) under a spectral peak, or ratios of intensities at different wavelengths can be sufficient for the analysis. However, using these methods, the large amount of spectral information available is not completely exploited. To reduce the amount of variables, while keeping the maximum of variation in the data,

Principal Component Analysis (PCA) can be applied, which is a popular multivariate chemometric method.

In general, spectra are compared to other spectra in the hypercube or to reference spectra from an external library using a similarity measure, e.g. the Euclidean distance, Pearson's correlation coefficient or the spectral angle¹⁷. Spectral unmixing can be applied to decompose a measured spectrum into a collection of constituent spectra¹⁸⁻²⁰. Clustering and classification techniques use the spectral information contained in the hypercube and identify regions with similar spectral characteristics. Clustering techniques are unsupervised methods, e.g. k-nearest neighbors²¹, which require no a priori information about the dataset to achieve clustering. Supervised classification methods, including partial least squares discriminant analysis²², and spectral angle mapping²³, require the selection of well-defined and representative calibration and training sets for classifier optimization. On the other hand, hyperspectral image regression enables the prediction of constituent concentrations at the pixel level, thus enabling their spatial distribution in a specimen to be visualized. Numerous approaches are available for the development of regression models (e.g. partial least squares regression, principal components regression¹⁵).

Image processing

Image processing is performed to convert the contrast developed by the previous steps into a picture showing the component distribution. Additionally, a single wavelength image can be selected showing the highest contrast between different components. Greyscale or colour mapping with intensity scaling is frequently used to display compositional contrast between pixels in an image. False colour mapping, in which two or more images at different wavebands are combined to form a new colour image may be employed to enhance apparent contrast between distinct regions of a specimen.

An interesting other approach for presenting the results was demonstrated by Alsberg et al²⁴, who projected the results of hyperspectral

imaging analysis back onto the scene to highlight chemical differences otherwise invisible to the naked eye. This non-destructive technique provides information similarly to traditional forensic methods, e.g. the use of luminol to highlight blood stains at a scene of investigation, and can be useful to guide investigators in their search for traces.

2.3. FORENSIC SCIENCE APPLICATIONS

Although hyperspectral imaging has mainly been used for the analysis of fingerprints, studies are also reported on several other forensic traces, including drugs, hair, dentin, bruises, blood stains, condoms, inks, tapes, firearm propellants, paints and fibres. These applications are described in more detail below.

2.3.a FINGERMARKS

Latent fingerprints are a complex mixture of eccrine deposits from the finger and sebaceous deposits resulting from touching other body parts, such as the face²⁵. Eccrine deposits mainly consist of amino acids, inorganic compounds, and proteins, while sebaceous material consists primarily of fatty acid esters²⁶. The chemistry of these residues varies among individuals and it shows increasing amounts of sebaceous deposits with age^{27, 28}. Fingerprint detection techniques aim to create contrast between the ridge details of a latent fingerprint and the background on which it is located.

Detection and enhancement of untreated fingerprints

Several authors recently evaluated the possibility of detecting untreated latent fingerprints using hyperspectral imaging. Exline et al used visible reflectance and photoluminescence hyperspectral imaging to detect untreated latent fingerprints on plastic and paper²⁹. Resulting images were compared to images created with a conventional forensic imaging system, in which different excitation and observation wavelengths could be chosen. While both methods succeeded in visualizing latent fingerprints on plastic, hyperspectral imaging

showed enhanced contrast on paper surfaces. Processing tools used included background division, offset correction, normalization and PCA. In a further study Payne et al optimized this visualization technique by using different processing tools to achieve an improved image³⁰.

Unlike visible hyperspectral imaging, NIR and IR hyperspectral imaging yield information about the vibrational modes of a molecule, and thus give additional information about the chemical composition of the material being studied. Bartick et al were the first to show the application of NIR and IR hyperspectral imaging for imaging latent fingerprints, using spectral bands indicative of the chemical components of the deposited material²⁷. They successfully visualized fingerprints deposited on aluminium coated microscope slides.

Crane et al demonstrated the ability of IR hyperspectral imaging to detect latent untreated fingerprints on various porous backgrounds (copier paper, cigarette butt paper, U.S. dollar bill, postcard) and non-porous backgrounds (trash bags, a soda can, tape)²⁸. Fingerprints on the soda can and a black trash bag were clearly visible when viewing the intensity band image at 9842 nm (asymmetric O-C-C stretch ester) (see Figure 2.7). On other backgrounds, more complicated processing tools were required, like PCA, and second derivatives. Processing with these tools rendered most prints clearly visible, even on paper-based porous surfaces. However, the position of the fingerprints was known before collecting the images.



Figure 2.7. Cut and flattened Dr. Pepper's soda can with fingermark deposit. (A) Soda can imaged by a document scanner. B) Infrared image of the outlined area obtained by plotting the band intensity at 9842 nm (1016 cm^{-1}). Reprinted from *Journal of Forensic Sciences*, 52/1, Nicole J. Crane, Edward G. Bartick, Rebecca Schwartz Perlman, Scott Huffman, *Infrared Spectroscopic Imaging for Noninvasive Detection of Latent Fingerprints*, 48-53, Copyright (2012), with permission from John Wiley and Sons²⁸.

In two papers, Tahtouh et al also described the application of infrared hyperspectral imaging to the visualization of untreated fingerprints^{31, 32}. Results indicated that the infrared spectra of many untreated fingerprints show peaks due to C-H stretching vibrations around 3333 nm, mainly due to fatty acid residues. These peaks are common to most organic compounds, but they can

be used to visualize fingerprints against some backgrounds, like metals, minerals, and ceramics, that do not contain C-H bonds. For fingerprints on other backgrounds, they stated that some type of chemical enhancement technique is required prior to hyperspectral imaging.

Bhargava et al described an approach to use IR hyperspectral imaging to reveal latent fingerprints overlaid on top of one another, each made under different hand washing conditions³³. Differences observed in the absorbance of the C-H stretching mode and other vibrational modes in the spectra indicated that the two prints had different chemical compositions. Because of this variation, linear unmixing applied to the spectral content of the data could be used to provide images revealing both superimposed fingerprints.

Detection and enhancement of treated fingerprints

Conventionally, fingerprints are treated with chemicals to increase sensitivity and/or contrast with the background. On porous surfaces such as paper, ninhydrin and DFO (1,8-diaza-9-fluorenone) are often applied, which both react with amino acids present in fingerprint ridges, causing a purple colour or photoluminescence respectively³⁴. On non-porous surfaces such as glass and plastic, cyanoacrylate (superglue) is the most widely used method³⁴. Cyanoacrylate fumes polymerize in the presence of moisture and greasy component of the fingerprint. The contrast of fingerprints treated with cyanoacrylate can be further enhanced by various methods including luminescent staining.

Exline et al²⁹ and Payne et al³⁰ investigated the potential of hyperspectral imaging to increase the contrast and visual quality of treated fingerprints compared to traditional methods of detection. Using visible hyperspectral imaging they investigated fingerprints treated with ninhydrin, DFO, cyanoacrylate, and fluorescent dyes. In some cases, hyperspectral imaging showed significant enhancement over the traditional method, which was mainly due to the suppression of a highly fluorescent background or isolation of the developed latent impression. Hence, the minutiae details were visible using hyperspectral imaging where they were not with the traditional

method. Such examples were examined and compared to the original donor's prints by a certified fingerprint examiner. This process verified that the enhanced detail coincides with actual naturally occurring detail. The added information brought by hyperspectral imaging could sometimes be sufficient for exclusion purposes, whereas the traditional examination would lead to an inconclusive result. In a similar study Miskelly and Wagner used hyperspectral imaging to image chemically treated fingerprints deposited on a newsprint and an aluminium soda can³⁵. They showed that background correction is an important step in the visualization of fingerprints on difficult backgrounds.

Although visible hyperspectral imaging is an improvement compared to traditional techniques, it is not always possible to obtain acceptable fingerprint images, for example when the background is highly fluorescent, coloured or patterned. However, most dyes that absorb or fluoresce strongly in the visible region are reflective in the NIR³⁶. This means that background interferences from dyed surfaces should be reduced when working in the NIR, compared to visible imaging. Maynard et al systematically imaged latent fingerprints on porous, non-porous and semi-porous surfaces³⁶. Next to a wide variety of conventional chemical and physical treatments, NIR laser dyes were tested for their ability to produce NIR photoluminescence. Both absorption and photoluminescence properties of the treated marks were examined using NIR hyperspectral imaging. The most suitable enhancement techniques depend on the type of surface. Fingerprints on coloured, printed or watermarked surfaces were imaged in the NIR region without interference from the background colour, both in absorbance and in photoluminescence modes. In these cases, imaging in the NIR region provided advantages over imaging in the visible region.

Background interference problems in the visible region can also be solved by showing differences in chemical composition of the print and the background using mid-infrared hyperspectral imaging, as shown by Tahtouh et al^{31, 32}. Infrared hyperspectral imaging of chemically treated fingerprints was carried out on several challenging backgrounds. It was found that infrared hyperspectral imaging gives high quality images of cyanoacrylate-fumed fingerprints on polymer banknotes and aluminium drink cans, regardless of the

printed background. Attempts to acquire images of fingermarks on paper-based porous surfaces treated with established reagents such as ninhydrin were all unsuccessful due to the swamping effect of the cellulose constituents of the paper.

In addition to the chemicals commonly used to create contrast between fingermarks and backgrounds, Tahtouh et al tested four novel chemicals which can be visualized with IR hyperspectral imaging³⁷. These were chosen for their potential to produce a strong, isolated infrared spectral band. Each chemical polymerized selectively on fingermark ridges and high quality images were obtained of fingermarks on difficult backgrounds.

Detection and identification of trace contaminations in fingermarks

Next to eccrine and sebaceous deposits, fingermarks may be contaminated by exogenous substances of various sources. These substances might include drugs of abuse, traces of explosives or gunshot residue. Traces found at the scene of investigation can be directly related to an individual by its presence in the fingermark. Many of the approaches involved in collecting traces are destructive. For example, swabbing objects destroys fingermark deposits within the area. Because of its non-destructiveness, hyperspectral imaging can be used to simultaneously image a latent fingermark and detect trace information contaminating it.

In 2005, Grant et al had volunteers handle a mixture of common materials before giving fingermarks³⁸. When looking at the fingermarks under a visual light microscope, it was impossible to distinguish particles from different materials. However, by using infrared hyperspectral imaging, vibrational spectra of individual particles were obtained and identified by comparison with a spectral library.

In a similar study, Bhargava et al examined traces of explosives within a latent print, using an infrared hyperspectral imaging system³⁹ (Figure 2.8). They used spectral subtraction to eliminate the effects of latent material on traces. Unique spectral features of the traces were used to provide images of the distribution of these traces. From pixels dominated by the material the full

spectrum of the traces was obtained and compared to databases for identification.

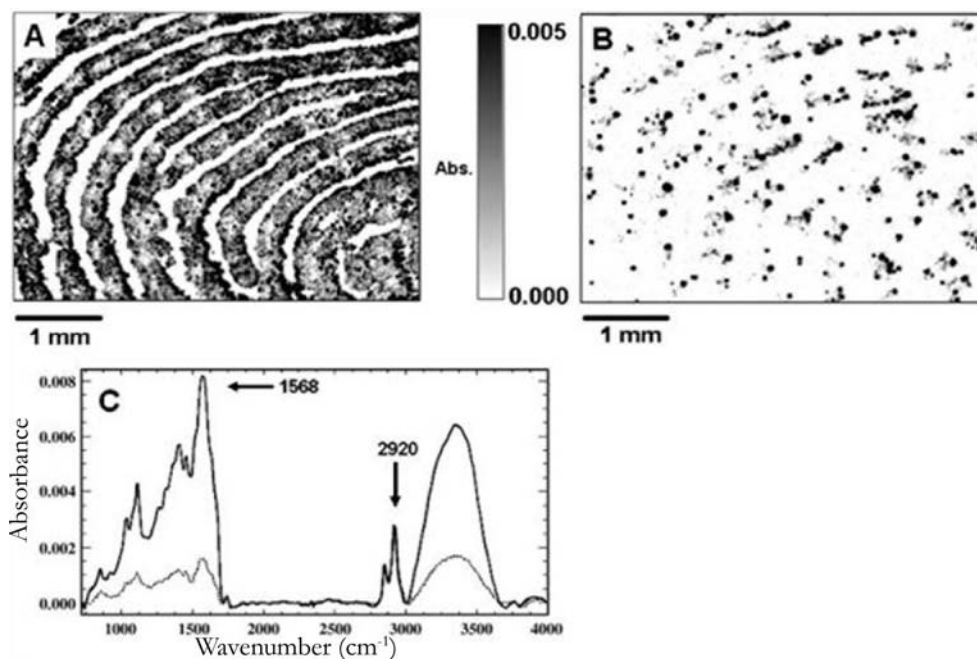


Figure 2.8. Images of a latent fingerprint developed by using different vibrational modes to highlight different aspects of the chemical composition of the deposited material. a) Print image developed by the absorbance magnitude at 2,920 cm⁻¹. and b) print image developed by absorbance magnitude at 1,568 cm⁻¹. c) Example spectra from the oil-rich region (top, dark line) and flake rich region are shown. Reprinted from Analytical and Bioanalytical Chemistry, 394/8, Rohit Bhargava, Non-invasive detection of superimposed latent fingerprints and inter-ridge trace evidence by infrared spectroscopic imaging, 2069–2075, Copyright (2012), with permission from Springer³⁹.

Ng et al tested different spectral searching algorithms for their efficacy in finding targeted substances deposited within fingerprints²⁵. Out of a range of algorithms which included conventional Euclidean distance searching, the spectral angle mapper and correlation algorithms gave the best results when used with second-derivative image and reference spectra. Aspirin, diazepam,

caffeine, and explosive components were successfully detected and located in a fingerprint.

Emmons et al used Raman hyperspectral imaging to examine fingerprints contaminated with traces of explosives (532 nm excitation)⁴⁰. To determine if explosives were present in the fingerprints measured, the resulting spectra of each pixel were compared to a spectral library of pure reference specimens of explosives. A false colour picture was created which indicated the possible presence of explosives. Significant differences in the spectra could be used to differentiate between different types of explosives.

Chen et al applied IR hyperspectral imaging and principal component analysis to distinguish between overlapping fingerprints based on exogenous compounds⁴¹. After creating a blank fingerprint containing natural secretions, a second finger contaminated with an explosive solution was printed on top of it. Although trace residues of the explosives trapped between the fingerprint ridges could be clearly detected, it was not evident which fingerprint these chemicals belonged to in cases with overlapped prints.

All the above studies examined fingerprints left on surfaces, which are ideal for infrared reflection analysis. In a forensic science scenario, reflective substrates such as a doorknob, knife blade, or handle should be relatively straightforward for analysis similar to the laboratory situation²⁵. However, surfaces such as glass, plastic, wood, paper, cloth, etc., will all have their own (sometimes strong) infrared absorptions. These IR absorptions of the underlying surface will mask some parts of the spectrum, rendering these regions unusable for spectral identifications. The effectiveness of finding foreign materials within latent fingerprints in these cases will be dependent on having enough identifying spectral features outside these spectral regions³⁸.

2.3.b OTHER TRACES

Apart from the analysis of fingerprints, the benefits of hyperspectral imaging can be exploited for the analysis of many other traces of importance in forensic science. Latent traces can be detected and visualized by using spectral differences to obtain optimal contrast between a trace and its background.

Individual spectra give information about the chemical composition of the specimen, which is useful for identification, quantification, or age estimation. The possibility of viewing spectral and spatial information side by side is an advantage in comparative research of e.g. fibres, paint chips, or inks, where the question arises whether two traces share common spectral features. Several applications described in literature are reviewed below.

Kalasinsky et al were the first to demonstrate the value of infrared hyperspectral imaging for determining drugs of abuse in hairs⁴². By examining only the interior portion of the hair, drugs exclusively resulting from human ingestion were measured and distinguished from drugs that made contact with the outside of the hair. After microtoming the hair, IR hyperspectral images were obtained of the cortex and the medulla. Drug free hairs of different sources all correlated with standard spectra of proteins. A hair of a chronic drug abuser of hydromorphone was analyzed similarly. Subtraction of the drug free reference spectra yielded a strong indicative band at 5824 nm, which was also present in reference hydromorphone spectra. An intensity band image at 5824 nm showed that the drug was concentrated in the centre of the hair. This way, relative drug concentrations across the hair could be successfully determined and visualized. In a further study, Kalasinsky showed the distribution of drugs in human hairs, which is critical information to validate drug testing data⁴³. IR hyperspectral imaging on hairs doped with 6-acetyl morphine (a metabolite of heroin) and cocaine, showed that hydrophobic drugs tend to bind to the medulla of the hair while hydrophilic drugs tend to be spread throughout the cortex of the hair.

Hair colour is basically determined only by eumelanin and pheomelanin, whose varying ratios produce the observed colour. In forensic science casework, hair colour is normally classified through visual comparison with standardized plates. Birngruber et al investigated the possibility to objectively distinguish hairs from different persons using hyperspectral imaging in the Vis-NIR range⁴⁴. They demonstrated an extreme intra-individual variability in the spectra of single hairs from an individual. Because of this, hairs undistinguishable on the basis of morphology could not be distinguished based on the hyperspectral images.

The chemical composition of the dentinal part of the tooth evolves with increasing age. Tramini et al measured 30 human teeth with Raman hyperspectral imaging (with 632 nm laser excitation) and were able to identify a very small quantity of dental material coming from skeleton debris or biological remains, and determine which kind of tissue it was⁴⁵. They created a PLS regression model to predict the age of an individual based on Raman spectra of his teeth. The model was tested on four teeth, and an age estimation was obtained with a mean error of 5 years.

The analysis of bruises, or aging of bruises in particular, can give important evidence in cases of domestic violence or child abuse. Several studies have been performed as initial steps towards the aging of bruises using hyperspectral imaging. A bruise is formed after blunt trauma, which results in blood being present in the skin. In time, haemoglobin in the blood is degraded into other products, including bilirubin. Both haemoglobin and bilirubin have typical spectral features in the visible region⁴⁶. Payne et al showed the possibility to use hyperspectral imaging to differentiate pure blood from blood with bilirubin based on these spectral features⁴⁷. Randeberg et al presented hyperspectral images of bruises on porcine and human skin⁴⁶. They used minimum noise fraction transform, a statistical method similar to PCA, to classify the injuries. Stam et al described how hyperspectral imaging can be used to accurately determine the areas covered by haemoglobin and bilirubin in the bruise, by fitting pixel spectra with a combination of reference spectra of chromophores present in bruises⁴⁸.

Similarly, reflectance spectra of blood stains can be spectrally unmixed to derive the relative amounts of oxyhaemoglobin, methaemoglobin and hemichrome within the blood stains^{18, 49}. By comparison of spectra derived from hyperspectral imaging data with a non-linear least squares fit of the theoretical spectra of the haemoglobin derivatives, blood stains were identified in a simulated crime scene and could be distinguished from similarly coloured substances, as demonstrated in **Chapter 3**¹⁸. Additionally, the temporal behaviour of the amount of haemoglobin derivatives provided insight in the chemical changes occurring in time, and could be used to estimate the age of

blood stains in **Chapter 4**⁴⁹. Figure 2.9 shows a simulated crime scene in which fresh and older blood stains were distinguished using this method.

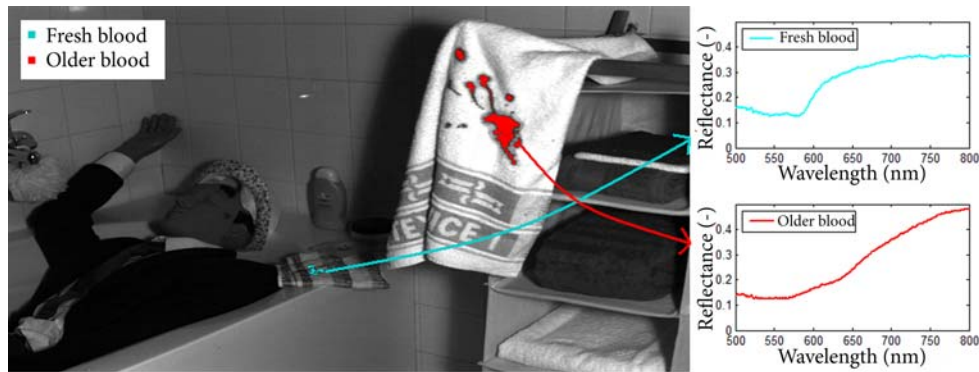


Figure 2.9. Simulated crime scene, in which fresh and older blood stains were automatically detected and distinguished (left) based on their reflectance spectra (right).

Important evidence pertaining to sexual assault cases can be provided by the identification of condom lubricant components. In an exploratory study, Wolfe and Exline showed that some of the most common materials found in condom lubricants can be accurately characterized by Raman hyperspectral imaging (with 532 nm laser excitation) without the extensive specimen preparation inherent to other analytical methods⁵⁰. Using the CH stretching region of the Raman spectrum, they were able to generate contrast based on spectral differences.

To demonstrate the potential of hyperspectral imaging in forensic investigations, Payne et al compared hyperspectral imaging to point measurements performed with traditional spectrometers⁵¹. They used Vis/NIR hyperspectral imaging to differentiate between a set of tapes and adhesives, a set of inks (Figure 2.10) and two brands of firearm propellants, based on reflectance and photoluminescence properties. They conclude that hyperspectral imaging offers significant advantages, mainly because a large number of specimens can be analyzed at once. This makes comparisons of different specimens easier and reduces the analysis time.



Figure 2.10. Third principal component of blue ink set, indistinguishable with the human eye. Reprinted from *Talanta*, 67/2, Gemma Payne et al, Visible and near-infrared chemical imaging methods for the analysis of selected forensic specimens, 334–344 Copyright (2012), with permission from Elsevier⁵¹.

In the same paper photoluminescence spectra of two multi-layered paint specimens were compared using hyperspectral imaging⁵¹. Because both spectral and spatial data were gathered, differences in paint layers could easily be highlighted visually, as an alternative to a spectral comparison. This was also shown by Flynn et al who analyzed more multi-layered paint specimens using IR hyperspectral imaging⁵². They presented several ways to display hyperspectral data, which make chemical differences and similarities between heterogeneous specimens easy to visualize and understand for the layperson (such as a juror). The same applies to the visualization of differences in bicomponent fibres, as described in⁵³. This study showed that infrared hyperspectral imaging can provide spatially resolved chemical information for those bicomponent fibres where it is possible to detect spectral differences between the two components present. As well as yielding characteristic IR spectra of each component, the technique also provided images clearly illustrating the side-by-side configuration of these components in the fibre. However, in 5 of 11 bicomponent fibres no spectral differences were found

using integrated peak intensities. Multivariate statistical analysis may improve these results. Markstrom and Mabbott also demonstrated the advantages of using hyperspectral imaging for the comparison of fibers⁵⁴ and addressed that the ability to compare fibres simultaneously in one measurement minimizes the chance for errors.

Miskelly and Wagner attempted to improve the visualization of chemically treated soil shoe marks using hyperspectral imaging³⁵. The standard chemical enhancement technique for such marks is an acidic thiocyanate solution which reacts with iron (III) oxides in the soil to form a coloured iron (III) thiocyanate complex. Unfortunately, this complex has a broad absorption band in the visible spectrum. They point at the necessity of enhancement chemicals with narrow absorption bands, as these can often be readily enhanced relative to the underlying background.

A forensic science application of remote sensing technology was demonstrated by Kalacska et al⁵⁵, who used airborne hyperspectral imaging for the detection of mass graves. Analysis of the spectra using Minimum Noise Fraction transform showed a clear separation between an experimental grave, a refilled empty grave, grass and forest. This indicates that airborne hyperspectral imaging can be used to detect the existence of suspicious decomposition properties, i.e. mass graves, which lead to differences in soil chemistry and vegetation.

2.4. TYPICAL CHALLENGES

As demonstrated above, the application of hyperspectral imaging in forensic science casework brings specific challenges. In contrast to pure specimens usually analyzed in the laboratory, traces from casework can consist of complex contaminated mixtures. Next to this, the chemical composition of biological traces may change in time. Although these changes can be used for age estimation purposes^{1, 45}, the influence of environmental conditions like temperature, humidity, precipitations and light should be studied. For example the influence of temperature and humidity on the aging of blood stains is shown by Bremmer et al⁵⁶.

Also, traces are typically not found on ideal neutral reflecting backgrounds used in laboratories (see Figure 2.9). In casework, all possible backgrounds can be encountered (e.g. different materials, porous, non-porous, coloured, patterned, etc.) which may complicate the measurements^{28-32, 36}. Comparison of spectra on different backgrounds typically requires advanced system calibration and data analysis. Miskelly and Wagner and Tahtouh et al examined the spectral properties of enhancement chemicals and experimented with new chemicals for the visualization of shoe marks³⁵ and fingermarks³⁷ respectively dedicated for the use of hyperspectral imaging. Although the use of chemicals is not preferred, this may help finding evidence.

The above mentioned challenges are not just characteristic for hyperspectral imaging, but are also valid for conventional spectroscopy. The transition from spectroscopy to hyperspectral imaging, however, is not straightforward. While specimen optical properties are independent of the spectral measurement system, the transition from spectroscopy to spectral imaging involves a drastic change in the illumination–collection geometry of the measurement system. Gebhardt et al showed that this change in measurement setup results in a disparity between measured spectra, which is dependent on the optical properties of the specimen and the optical path length⁵⁷. Spectral data bases created for the identification of forensic traces like fibres or printer toners^{58, 59} may therefore need to be adapted to hyperspectral imaging applications.

Moving hyperspectral imaging from the laboratory to the scene of investigation brings further complications. Advances in wireless technology and sealed operating units are desirable to prevent contamination. Investigating scenes where chemical, biological, radiological, or nuclear (CBRN) events have occurred poses dangers to investigators. In these cases, a remotely controlled robotic hyperspectral imaging system could provide important information instantly. However, these scenes have even more decontamination requirements.

The complex nature of crime scenes makes for challenging image analysis. Next to this, sunlight, external light sources, shadows and reflections from nearby objects all change the apparent illumination on an object. This

variation can cause large variability in the measured spectra for a fixed object, a problem regularly encountered in remote sensing⁶⁰. Algorithms are needed to distinguish this spectral variability due to non uniform illumination from spectral variability between objects.

2.5. FUTURE APPLICATIONS

Despite the challenges, hyperspectral imaging offers great potential for providing new, valuable information in forensic science casework. hyperspectral imaging can be applied to detect traces by optimizing the contrast between a trace and its background, or to differentiate between traces, based on spectral differences. To create contrast between a trace and its background, crime scene investigators traditionally use commercially available light sources with different excitation and barrier filters to isolate regions of the spectrum where traces of interest have high absorption or photoluminescence. This way, e.g. semen and blood traces can be detected (**Chapter 6**)⁶¹. For laboratory purposes, dedicated forensic imaging systems are available with different light sources, excitation and barrier filters. These systems are mainly used in document analysis, e.g. for differentiating inks^{62, 63}, but can also be applied in other fields, e.g. the visualization of gunshot residue patterns on dark clothing⁶⁴. For all these purposes hyperspectral imaging can be used instead. Because hyperspectral imaging systems filter the light in many small bandwidths, maximum spectral differences can be calculated automatically and the choice of one specific filter is no longer necessary, which reduces the risk of human errors.

Many applications currently performed with conventional spectroscopy may also be enhanced with a spatial component using hyperspectral imaging, similar to the way presented for the identification (**Chapter 3**)^{18, 65}, and age estimation of blood stains (**Chapter 4**)^{1, 49, 66-68}, as shown in Figure 2.9. In these applications, the added spatial information is crucial, as the blood stain pattern may reveal useful information for the reconstruction of a crime⁶⁹. The spectroscopic identification of other body fluids⁷⁰ will also benefit from hyperspectral imaging, as the traces can then be

interpreted in their original context. The spatial distribution of components may be less important in fields like illicit drug analysis. However, using hyperspectral imaging instead of spectroscopic point measurements for the identification of drug components⁷¹ may speed up the process, as many specimens can be imaged at once. The improved speed of hyperspectral imaging compared to spectroscopy, is particularly of advantage in hazardous environments. In explosives investigations especially, the ability to measure specimens without contact or specimen preparation is beneficial, as many accidents occur even when trained personnel handle explosives⁷².

In 2000, Malkoff and Oliver proposed some interesting applications in forensic medicine which are not yet put into practice, like the analysis of patterned injuries (e.g. a tire print on the body of a victim), scanning of body and clothes for toxins, the aging of wounds through the spectral evaluation of local inflammation and repair, and the estimation of the time of death of a victim⁷³. They also draw the attention to the need for crime scene reconstruction for operational planning, hazard identification, training etc. Crime scenes are often digitally captured using photography, and panoramic and 3D scanning techniques. These data can be used for a virtual crime scene reconstruction. The addition of hyperspectral imaging data to this reconstruction can give information about the chemical composition of traces and their distribution in the scene. Malkoff and Oliver claimed, this may help in body localization and retrieval, or the characterization of biological or chemical threats⁷³. Using hyperspectral imaging, the chemical properties of the scene of investigation can be captured quickly without much disturbance to the scene and analysis can be performed afterwards in the original context.

2.6. CONCLUSION

Recent technological developments in hyperspectral imaging components have opened up the approach to forensic science applications. Fast acquisition, portable, high resolution systems are emerging facilitating the transfer of hyperspectral imaging from the laboratory to the field. Several forensic science applications of hyperspectral imaging were recently explored successfully.

Challenges typically encountered in forensic science casework, e.g. contaminated traces found on non-ideal backgrounds in varying environmental circumstances, emphasize the necessity to modify existing techniques and instrumentation. Key steps in the research process are refining and validating the data to meet the needs of the legal and scientific communities. When introduced in forensic science casework, hyperspectral imaging can help investigators detecting, visualizing and identifying useful traces non-destructively.

3 - REFLECTANCE SPECTROSCOPY AND HYPERSPECTRAL IMAGING FOR THE IDENTIFICATION OF BLOOD STAINS

Partly published in:

Journal of Forensic Science 2011;56(6):1471-5

Proc. SPIE 8743 2013;doi:10.1117/12.2021509

We demonstrated the feasibility of reflectance spectroscopy and hyperspectral imaging to detect and identify blood stains remotely at the crime scene. Blood stains outside the human body comprise the main chromophores oxyhaemoglobin, methaemoglobin and hemichrome. Consequently, the reflectance spectra of blood stains are influenced by the composite of the optical properties of these individual chromophores. Using the coefficient of determination between a non-linear least squares multi-component fit and the measured spectra, blood stains were successfully distinguished from other substances visually resembling blood (e.g. ketchup, red wine and lip stick) with a high sensitivity and specificity. The practical applicability of this technique was demonstrated at a mock crime scene, where blood stains were successfully identified automatically. Finally, the described technique was applied in a case example, in which a stain on a paint can was tested for the presence of blood.

3.1. INTRODUCTION

Identification of blood stains at a crime scene is of critical importance in criminal investigations. Extraction of DNA from the stains may lead to the identification of victims or suspects, and the blood stain pattern can reveal useful information about the activities needed to produce these patterns. To avoid contamination and destruction of traces, there is a need for techniques that allow for remote, non-contact identification of blood. Ideally, traces are judged and interpreted in the original context, so techniques are preferably applied at the crime scene⁷⁴.

Various screening tests, routinely used in forensic practice, use chemical or optical methods for the identification of blood and to discriminate it from other body fluids or red substances. Most chemical tests, including tetrabase⁷⁵ and Kastle-Meyer, employ peroxidase activity of haemoglobin molecules. The peroxidase either causes a colour change or induces chemiluminescence. A commonly used example of the latter is the luminol test. By spraying luminol onto the suspected area, the reactant will glow in the presence of blood⁷⁶. This test is especially appropriate for recovering stains after cleaning attempts. All tests described above are presumptive in nature, not confirmative, since several other substances are reported to catalyze this peroxidase reaction⁷⁷. More reliable, confirmatory tests are based on haemoglobin derivative crystals^{78, 79} or RNA markers in blood⁸⁰. However, these tests require advanced sample preparation and microscopic observation, and are therefore not applicable for interpreting traces in their original context, at the crime scene.

Recently, optical techniques have been suggested for blood stain identification^{70, 81}. Haemoglobin has specific absorption bands at 420 (known as the Soret band), 540 and 576 nm (attributed to the α and β chains in a haemoglobin molecule)⁸²; it fluoresces at 465 nm, when excited at 321 nm⁸³; and haem provides Raman shifts⁸⁴ at 1.222 and 1.542 cm^{-1} . Because of these specific optical features of haemoglobin, spectroscopic techniques, e.g. visible reflectance, fluorescence or Raman spectroscopy, have the potential to allow on field identification of blood. However, despite the promising results, these

techniques have not been reported to be implemented in forensic practice yet. Accordingly, all these techniques have their own drawback. Measuring Raman signals is highly complicated by interference with the fluorescence signal of the traces and its background. A fluorescence signal is difficult to measure, because of the high absorption properties of haemoglobin in the ultraviolet and visible wavelength range. The value of the absorption properties for blood stain identification has been demonstrated by Kotowski *et al* in a microspectrophotometry setup⁸⁵; De Weal *et al* recently confirmed their findings⁸¹. Their microscopic setup however, required sample preparation and a laboratory environment for accurate measurements.

In this study, we investigated whether blood stains can be detected and discriminated from other body fluids and substances visually mimicking blood, based on their visible reflectance spectra. In a laboratory setup, the reflectance spectra of a set of blood samples and a set of mainly red/brown coloured substances were measured using both conventional probe based optical reflectance spectroscopy and hyperspectral imaging. Hyperspectral imaging combines spectroscopy with imaging, thereby obtaining both spatial and spectral information from all objects in the field of view. When analyzing blood stains, the added spatial information is interesting, as the blood stain patterns can reveal useful information for the reconstruction of a crime and all stains can be interpreted in their original context. Hyperspectral imaging also improves the speed of the process compared to spectroscopy, as many samples can be recorded and analysed at once.

The spectral analysis applied in this chapter was based on the expected presence of haemoglobin derivatives in blood. Blood stains outside the human body comprise mainly the chromophores oxyhaemoglobin, methaemoglobin and hemichrome¹. We used a physical light transport model and a fitting algorithm to find a combination of haemoglobin derivatives leading to a reflectance spectrum most similar to the measured spectrum. Assuming that all blood stains contain a mixture of these haemoglobin derivatives, the fitted spectra were expected to resemble all measured spectra of blood stains. Worse fits were expected for non-blood samples. Therefore, the goodness-of-fit was evaluated as a measure to distinguish blood from other samples. The sensitivity

and specificity of this method were analyzed in a laboratory setup, both for the probe based spectroscopy and the hyperspectral imaging setup. Based on experiences using the spectroscopy setup, the data analysis was slightly improved for the hyperspectral imaging setup. At a mock crime scene, we investigated the practical applicability of this technique using hyperspectral imaging. Finally, the spectroscopy setup was applied in a forensic case, to determine whether an unknown stain on a paint can was blood or not.

3.2. PROBE BASED SPECTROSCOPY

3.2.a MATERIALS AND METHOD

Samples

To test the sensitivity and specificity of the blood stain identification task using spectroscopy, two sample sets were prepared: a set of blood samples and a set of blood mimicking samples and different body fluids. The blood samples, forty in total, were obtained from eight healthy male donors. These samples were prepared by deposition of a small drop of blood onto a piece of white cotton, creating a stain with a diameter of 21 ± 4 mm. We performed 1200 measurements on the forty blood samples, covering a period of a few seconds after deposition until a year after deposition; this resulted in thirty measurements per sample, to monitor possible influences of ageing.

The second set contained 35 non-blood samples (specified below in Figure 3.4). Among these samples were 31 samples mimicking blood visually, including ketchup, red wine and fake blood; and four body fluids commonly found at crime scenes: saliva, semen, urine and perspiration. All samples were created, similar to the blood stains, onto a piece of white cotton.

Measurement setup

Reflectance measurements were performed with a combination of a spectrograph (USB 4000; Ocean Optics; Duiven, the Netherlands), a tungsten-halogen light source (H-2000; Ocean Optics; Duiven, the Netherlands) and a

non-contact probe (QR400-7-UV/BX; Ocean Optics; Duiven, the Netherlands). This probe contains six 400 μm core diameter delivery fibres, circularly placed around a similar central collecting fibre. Figure 3.1 shows the schematic of the setup. The probe is positioned 1 cm above the specimen. During measurements, light emitted by the delivery fibres is scattered and partly absorbed in the sample, and the remitted light is collected with the central fibre.

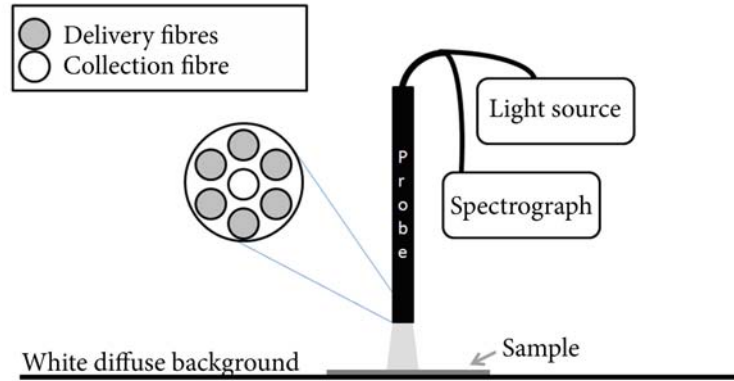


Figure 3.1. Schematic of the measurement setup. The reflection probe tip shows six delivery fibres, placed around a central collection fibre. The delivery fibres are connected to the light source and the collection fibre is connected to the spectrograph.⁶⁵

Pre-processing

Spectral analysis was limited to the wavelength range of 500 – 700 nm, because of the low detector sensitivity and low power of our light source beyond this range. First, the dark response ($I_{dark}(\lambda)$) of the detector was subtracted from each spectrum. Next, to account for the intensity spectrum of the light source, we divided by the background response of white cotton at all wavelengths ($I_{white}(\lambda)$):

$$R(\lambda) = \frac{I(\lambda) - I_{dark}(\lambda)}{I_{white}(\lambda) - I_{dark}(\lambda)}, \quad (3.1)$$

where R is the reflectance and I is the intensity.

Blood stain identification

The reflectance spectra were analyzed with a multi-component linear least squares fit. The absorption spectra of the three components present in blood, i.e. oxyhaemoglobin, methaemoglobin and hemichrome (Figure 3.2) were used as input.

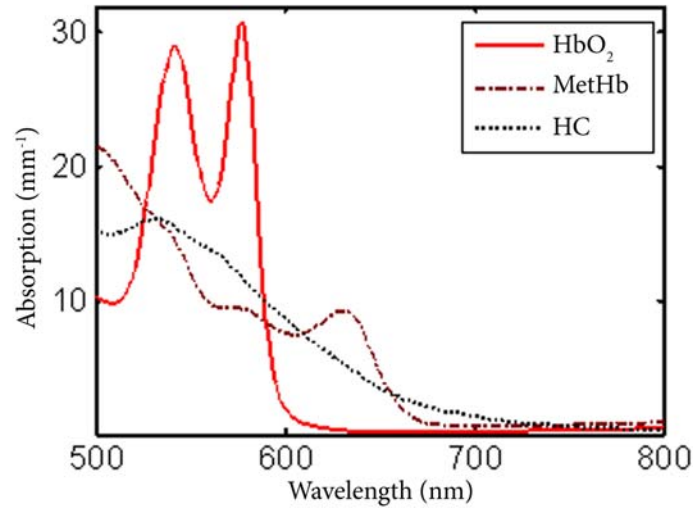


Figure 3.2. Absorption spectra of oxyhaemoglobin (HbO_2), methaemoglobin (MetHb) and hemichrome (HC)

A one-dimensional solution of the radiative transport theory was employed to translate these spectra into a reflectance spectrum:

$$R = 1 - \frac{K}{S} \left(\sqrt{1 + \frac{2S}{K}} - 1 \right), \quad (3.2)$$

where R (-) is the reflectance, S (mm^{-1}) is derived from the scattering coefficient, and K (mm^{-1}) from the absorption coefficient^{86, 87}. This model

assumes a homogeneous blood layer of infinite thickness interacting with incoming diffuse light. The fitting algorithm varies the amplitudes of the three absorption spectra, in order to find the combination with a minimum of difference between the theory and the diffuse reflectance spectrum¹.

Assuming that all blood stains contain a mixture of haemoglobin derivatives, the non-linear least squares fit was expected to resemble all measured spectra of blood stains. Worse fits were expected for non-blood samples. The goodness of fit was determined using the coefficient of determination R^2 and the sensitivity and specificity of the identification tasks were studied.

To test on differences in R^2 values within the total blood stain population three individual, one way ANOVA tests were taken on samples ($n=40$), donors ($n=8$) and ageing. For ageing testing, we grouped the blood stains in four categories: age < 1 day; 1 day < age < 1 week, 1 week < age < 1 month and age > 1 month. Significance is found if $p < 0.05$.

3.2.b RESULTS

The left hand side of Figure 3.3 shows a typical diffuse reflectance spectrum of a blood sample of one day old, measured with the spectroscopy setup. The spectrum shows two distinct dips, at 540 nm and 576 nm, corresponding to the oxyhaemoglobin absorption maxima⁸². The calculated coefficient of determination between the blood reflectance spectrum and the blood component fit is very high: $R^2=0.996$. The reflectance spectra of all blood samples were obtained and all corresponding coefficients of determination were calculated. For the total of 1200 measurements we found an average R^2 of 0.986 ± 0.012 .

Three one-way ANOVA tests were performed to test on differences in sample, donor and ageing. The outcome of the test shows that at a 0.05 level, no significant difference is found among sample variation (F-value = 0.8014, prob >F = 0.8040) and donor variation (F-value = 0.8215, prob >F = 0.569). However, for ageing, a significant difference is found (F-value = 64.4, prob >F = 0). For both ages smaller than one day and ages between a day and a week R^2

$=0.99\pm0.01$; for ages between a week and a month and older than one month $R^2 = 0.98\pm0.01$. This difference in R^2 -value between stains measured within a week and after a week of deposition is found significant at a 0.05 level.

The right hand side of Figure 3.3 shows a reflectance spectrum of a blood mimicking sample: ketchup. The agreement between the sample's reflectance spectrum and the blood-fit is poor, especially for $\lambda < 600$ nm. The poor agreement results in a low coefficient of determination: for the total population of 35 non-blood samples the average $R^2=0.67\pm0.21$ was found.

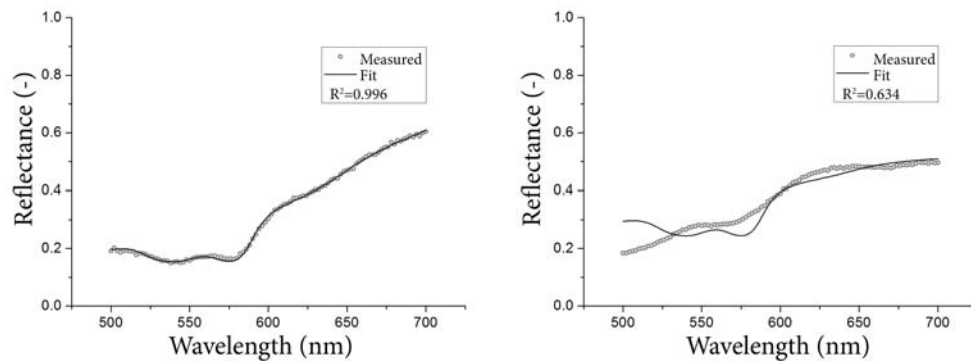


Figure 3.3. Diffuse reflectance signal (grey dots) with corresponding blood-fit (black line). Two typical measurements are shown: a) a blood sample of one day old and $R^2=0.996$ b) a non-blood sample: ketchup, $R^2=0.634$.⁶⁵

Figure 3.4 shows the coefficients of determination of four typical blood stains and all non-blood samples. The blood samples, coloured in black in Figure 3.4, have the following coefficients of determination: immediately after deposition, $R^2=0.997$; after one day: $R^2=0.996$; after one month: $R^2=0.982$ and after one year: $R^2=0.984$. The non-blood samples are coloured in grey. The non-blood samples with highest R^2 are coloured lip gloss: $R^2=0.961$ and red wine: $R^2=0.954$. Non-red body fluids, shown on the right side of figure 3, score low correlations, saliva: $R^2= 0.199$, semen: $R^2=0.476$ perspiration: $R^2=0.669$ and urine: $R^2= 0.381$. The patterned column on the far right resembles the measured R^2 of the case study, which will be discussed in detail below.

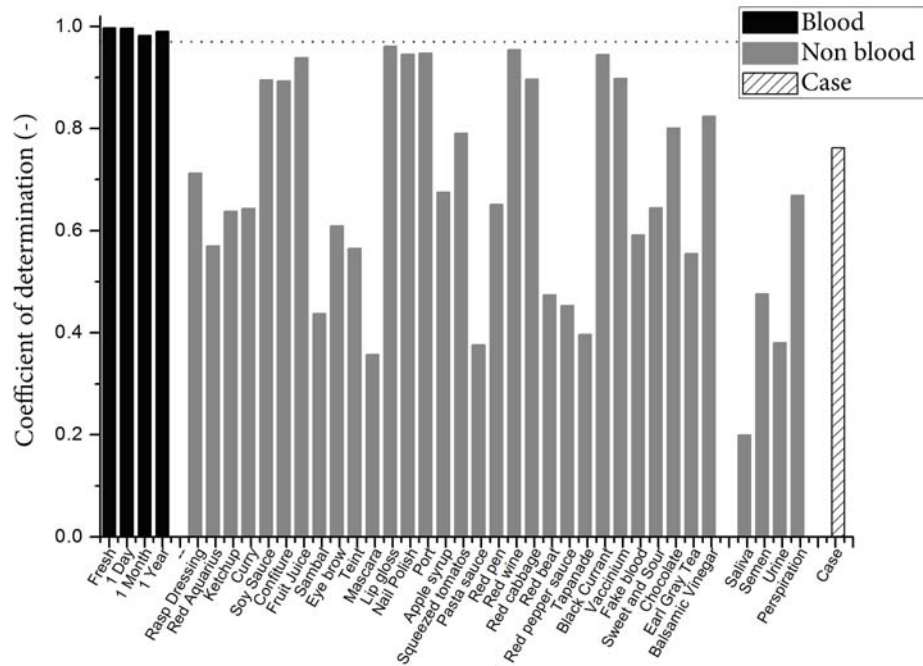


Figure 3.4. Column plot of coefficients of determination of four typical blood samples (black), all non-blood samples (grey) and case study (patterned).⁶⁵

Figure 3.5 plots the distribution of the obtained R^2 -values for all samples. The boxes show the distribution of 25%, 50% and 75% of the samples, the whiskers show 1% and 99% of samples. The coefficient of determination in Figure 3.5 is plotted on a logarithmic scale to enable visualization in both blood and non-blood samples.

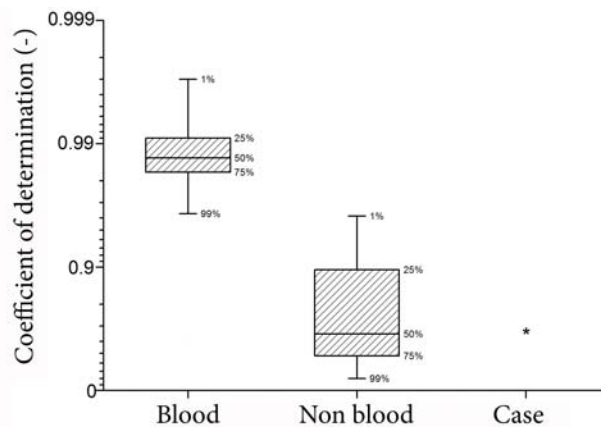


Figure 3.5. Box plot of the distribution of observed coefficients of determination of all blood measurements (n=1200) and all non-blood samples (n=35). On the right the outcome of the case example described below.⁶⁵

A possible threshold for the separation of blood and non-blood samples would be at $R^2=0.97$. At this level, the specificity is 100% and the sensitivity 98.1%, i.e. no non-blood samples were reported with $R^2>0.97$ and only 1.9% of the blood samples were found to have $R^2<0.97$.

3.2.c CASE EXAMPLE

Materials and method

The spectroscopy method presented in this chapter was applied for investigational purposes in a case where someone was suspected of multiple burglary cases. The paint can found at one of the crime scenes contained latent traces of a fingerprint, possibly printed in blood. Confirmation or exoneration of the nature of the stain was crucial for the processing of this particular crime. We measured the reflectance spectrum of the questioned stain and analysed it as described above to indicate whether it was blood. A tetrabase test was used for verification of the result.

Result

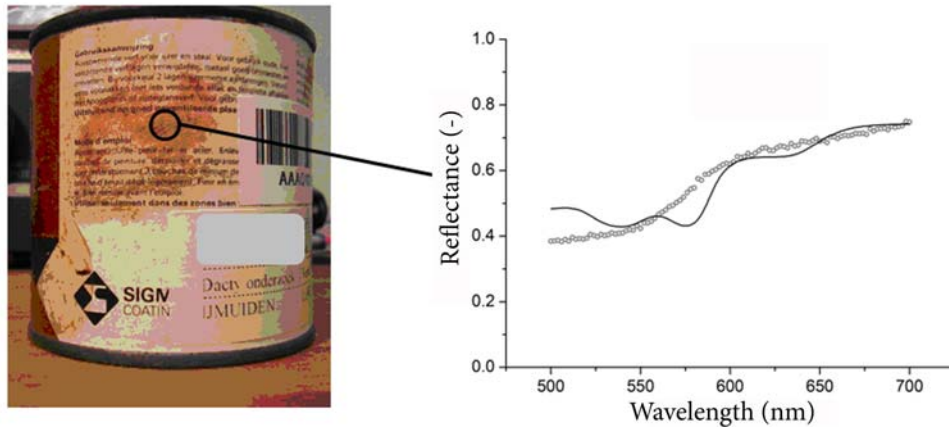


Figure 3.6. Left: Photograph of paint can of interest for blood test. The black line with open circle shows the spot where the reflectance spectrum is recorded. Right: Diffuse reflectance signal with corresponding linear least squares fit.⁶⁵

Figure 3.6 shows a photograph of a paint can found at the crime scene. We obtained a diffuse reflectance spectrum of a red stain on this can and found an R^2 -value of 0.672, which is much lower than the values found for blood (see Figure 3.5), indicating that the stain does not contain blood. To verify the optical presumptive test for this case example, an additional tetrabase test⁷⁵ was performed on the same spot. Tetrabase tests are routinely used in forensic practice in the Netherlands. According to the instructions, filter paper was used to sample a small amount of substance from the paint can. Thereafter the filter paper was treated with the tetrabase chemicals. The filter paper did not change colour after deposition of the tetrabase, indicating no presence of blood on the paint can. The tetrabase test was performed twice, once with dry filter paper, and once with wet filter paper. The results of the tetrabase test were in agreement with the outcome of the spectroscopic identification.

3.3. HYPERSPECTRAL IMAGING

3.3.a MATERIALS AND METHOD

Samples

The samples used to test the hyperspectral imaging setup were similar to the set described above. Again, blood stains on white cotton were analysed repeatedly (every day for 4 weeks, thereafter weekly until the age of 2 months). The 30 different non blood samples are specified in Figure 3.7. Instead of the bodily fluids analysed using spectroscopy, bleach was added to the set, as bleach is likely to be false positive when using the commonly used identification technique luminol.



Figure 3.7. Photographs of non-blood samples containing: 1) tea, 2) coffee, 3) red wine, 4) red grape juice, 5) black currant soda ('cassis'), 6) coke, 7) cherry coke, 8) red berry juice, 9) tomato juice, 10) ketchup, 11) curry, 12) Tabasco, 13) ketjap manis, 14) Worstershire sauce, 15) soy sauce, 16) balsamic, 17) Maggi aroma, 18) red wine, 19) cherry marmalade, 20) forest fruit marmalade, 21) apple syrup, 22) chocolate sauce, 23) red cabbage, 24) red beet, 25) bleach, 26) lipstick, 27) lipstick, 28) lipstick, 29) red food colourant, 30) red food colourant.

Measurement setup

The hyperspectral imaging system used was a push broom line-scanning system (Spectral Imaging Ltd., Oulu, Finland), consisting of a rotary stage, a hyperspectral camera operating in the visible- near infrared wavelength range (400-1000 nm) and a broadband halogen light source.

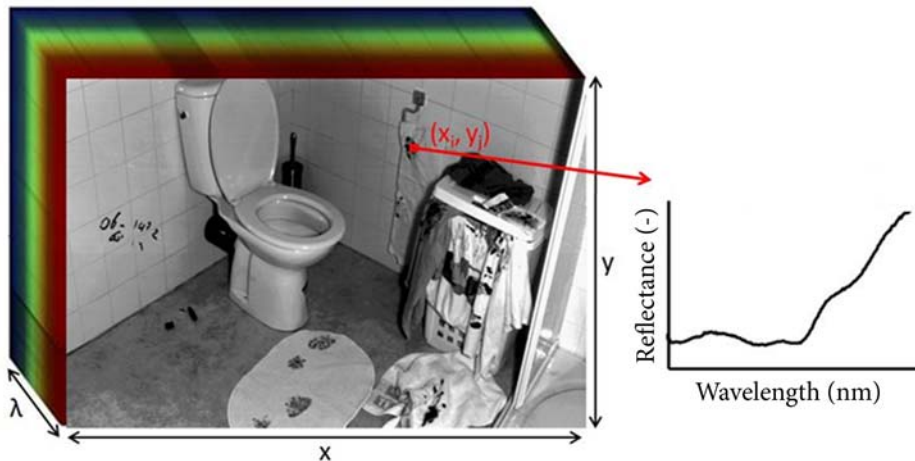


Figure 3.8. Hypercube of a mock crime scene, with two spatial (x, y) and one wavelength (λ) dimension (left). From the hypercube a reflectance spectrum was obtained from each pixel (x_i, y_i) (right).

Using this system, we recorded so-called hypercubes (explained in **Chapter 2**), containing two spatial dimensions (x, y) and a spectral dimension (λ) (see Figure 3.8). From these hypercubes, a region of interest of 10×10 pixels was cropped for each sample, corresponding to a sample size of approximately 1 cm^2 . Reflectance spectra were obtained for all these regions as described below.

Pre-processing

In the hyperspectral imaging setup, the wavelength range was expanded to 500 – 800 nm. The reflectance spectra for all samples were calculated as above, with corrections for the dark response and light source (formula 3.1). Now, an extra correction algorithm, the Standard Normal Variate algorithm¹⁴ was applied to normalize spectral variations caused by differences in sample-detector distance and variations in local light intensities:

$$R_{corr}(\lambda) = \frac{R(\lambda) - \mu}{\sigma}, \quad (3.3)$$

in which R_{corr} is the corrected reflectance, μ the average reflectance and σ its standard deviation.

Blood stain identification

The reflectance spectra of all samples were analyzed using the fitting algorithm described above (formula 3.2). To examine the goodness of fit between the measured reflectance spectra and the fitted light transport model, the coefficient of determination R^2 was calculated for each pixel of the different samples. A Receiver Operating Characteristic (ROC) curve was plotted, showing the sensitivity and specificity of the identification tasks at different thresholds of R^2 .

3.3.b RESULTS

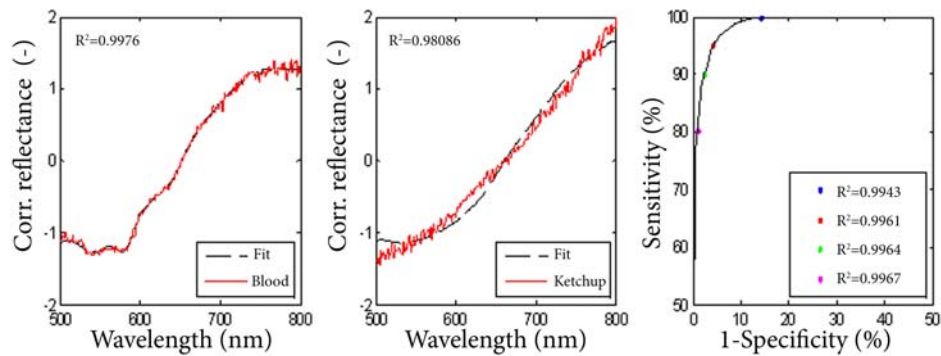


Fig. 3.9. a) Corrected reflectance spectra (red) of a single pixel depicting blood and the corresponding least squares fit (black). The R^2 value for this pixel is 0.9976. b) Corrected reflectance spectra (red) of a single pixel depicting ketchup and the corresponding least squares fit (black). The R^2 value for this pixel is 0.98086. c) ROC curve showing the sensitivity and specificity of the identification task at different thresholds. Coloured dots represent the sensitivity and specificity at several thresholds given in the legend (e.g. at $R^2=0.9943$ the sensitivity is 100% and the specificity is 85%).

Fig. 3.9 shows the corrected reflectance spectra of two pixels depicting blood (Fig. 3.9a) and ketchup (Fig. 3.9b), and the corresponding non-linear least squares fits of the haemoglobin derivatives present in blood stains. Please note that for both cases the coefficients of determination R^2 between the fits and the measured reflectance spectra approach one, but this coefficient was lower for most non-blood stains than for blood stains.

The ROC-curve (Fig. 3.9c) shows the sensitivity and specificity of the identification task at different thresholds. At a threshold of $R^2 = 0.9943$ we reached a sensitivity of 100% and a specificity of 85%. False positive pixels at this threshold contained ketjap manis, Worcestershire sauce, soy sauce, balsamic, red cabbage and bleach. The area under the curve (AUC) was 0.99.

3.3.c MOCK CASE EXAMPLE

Materials and method

Finally, we recorded a hyperspectral image of a mock crime scene (see Figure 3.10), in which red wine, lipstick and several blood stains of different ages were present. The pre-processing steps described above were applied to the data and all individual pixels were analysed using the non-linear least squares fitting algorithm. For each pixel the goodness of fit was measured using the coefficient of determination R^2 . All pixels with an R^2 value above a predetermined threshold were coloured red in a mask, which was overlaid onto a greyscale background depicting the scene (one waveband of the hyperspectral image). False positive and false negative pixels of the mock crime scene were evaluated.

Results



Figure 3.10. Greyscale image (one wavelength band of the hypercube), overlaid with red pixels showing identified blood stains at a threshold R^2 of 0.98.

At the mock crime scene a hypercube was recorded with 800 pixels in vertical direction, 1575 in horizontal direction and 424 spectral bands (2x2 binning), in less than two minutes. All individual pixels in the hypercube were analyzed as described above. At a threshold of 0.98, most blood stains were identified, as depicted in Figure 3.10. Several pixels which were later confirmed to contain blood on the blue T-shirt and on the cloth on the floor were not identified using hyperspectral imaging. False positive pixels contained 4 pixels of the lipstick on the wall and 6 pixels in the specular reflecting part on the waste pipe. Corrected reflectance spectra of 2 pixels correctly identified as blood, 2 false positives and 2 false negatives are depicted in Figure 3.11.

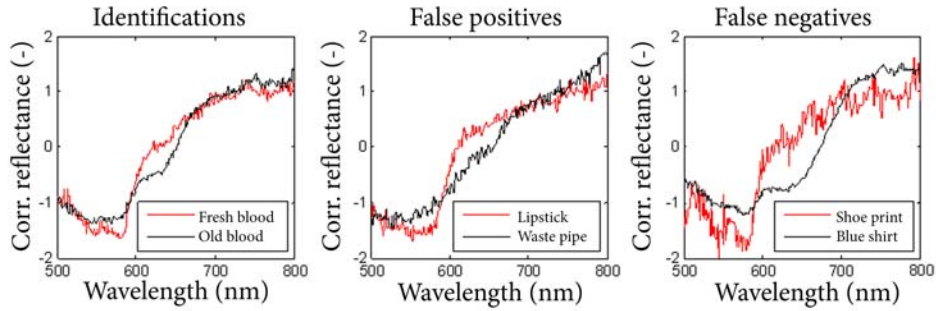


Figure 3.11. Corrected reflectance spectra of 2 pixels correctly identified as blood, 2 false positives and 2 false negatives.

3.4. DISCUSSION AND CONCLUSION

We demonstrated the feasibility to use spectroscopy or hyperspectral imaging to identify blood stains remotely. Based on their optical properties, both fresh and old blood stains from various donors were successfully distinguished from other samples, with a high specificity and sensitivity. No significant differences were found between blood stains for various samples or various donors. A small significant difference was found among blood stains with varying age. Yet, these differences did not hamper discrimination between blood and non-blood samples. In a case example, the absence of blood was determined using the described technique, which was confirmed by a tetrabase test. The practical applicability of this technique was demonstrated at a mock crime scene, where blood stains were identified automatically using hyperspectral imaging.

As illustrated by the ROC curve in Figure 3.9c there is a trade-off between sensitivity and specificity of this technique, which both depend on the choice of the threshold. In the spectroscopy setup for example, if no false positives are allowed, a possible threshold would be at $R^2=0.97$, resulting in a 100% sensitivity and a specificity of 98.1%. In forensic casework however, it seems more relevant to accept some false positives by choosing a threshold which leads to a 100% sensitivity, to prevent that blood stains are overlooked. When hyperspectral imaging was used, the specificity was 85% with a sensitivity of 100%. Because spectroscopy and hyperspectral imaging are non-

contact and non-destructive, all trace material is conserved and can be swabbed for subsequent confirmative identification tests in the laboratory.

The results of the identification task were somewhat better for probe based spectroscopy, compared to hyperspectral imaging, which can be explained by the larger sampled area. Averaging hyperspectral imaging data from multiple pixels covering the same area is expected to lead to better results. The R^2 values between measured reflectance spectra and non-linear least squares fits of the haemoglobin components were in general higher for the hyperspectral imaging measurements, which was expected as a result of the added Standard Normal Variate correction applied in this case. When using hyperspectral imaging, we observed higher R^2 values in the laboratory data than in the mock crime scene data, which may be explained by geometrical parameters like object to sensor distance and angle.

Regardless the results, hyperspectral imaging has benefits compared to probe based spectroscopy. Because both spectral and spatial information are recorded, traces can be analysed within their original context. Additionally, it is less labour-intensive and more time-efficient; an entire crime scene can be captured rapidly using a hyperspectral imaging system. The hyperspectral image of the mock crime scene presented in this study was recorded within two minutes. Although the subsequent pixel-based calculation time was several hours, this can easily be reduced using preliminary data reduction steps.

In casework traces are typically not found on ideal full-reflecting backgrounds used in laboratories, but all possible backgrounds can be encountered (e.g. different materials, porous, non-porous, coloured, patterned, etc.). Results of the mock crime scene showed that some backgrounds complicate the analysis. Several blood stains on the cloth on the floor, which appeared to be thinner, were not identified. This failure may be explained by the higher contribution of the background to the measured reflectance spectra in these pixels. Additionally, the absorption by the background complicated the measurements on the blue T-shirt. For dark backgrounds which absorb most visible light, near infrared spectroscopy can be used for the identification of blood stains, as shown in **Chapter 7**¹⁹. In **Chapter 5**, the influence of different

backgrounds and the limitations of the visible wavelength range will be explored.

Other errors in the hyperspectral imaging setup were caused by specular reflections. Sunlight, external light sources, shadows and reflections from nearby objects all change the apparent illumination on an object. This variation can cause large variability in the measured spectra for a fixed object, a problem regularly encountered in remote sensing. In this study, we applied a correction algorithm for differences in offset and intensity of the reflectance spectra, which greatly reduced the variability between samples measured at various distances from the sensor, where the local intensity of the light source varied⁶⁷. However, more algorithms may be needed to correct for other effects encountered in complex crime scenes.

We show the possibility to estimate the age of blood stains using hyperspectral imaging in **Chapter 4**⁴⁹. Combined with the technique described above, it is possible to simultaneously detect and identify blood stains and estimate their age non-destructively. When introduced in forensic casework, the described technique can help investigators to analyse traces in the original context at the crime scene, without the need to wait for results from the laboratory. This helps investigators to select most relevant traces, which reduces the workload in forensic laboratories.

3.5. ACKNOWLEDGEMENTS

Part of this research was developed in the project CSI the Hague, within the Pieken in de Delta program by the NL Agency of the Dutch Ministry of Economic Affairs, Agriculture and Innovation (project number PID082036).

4 - HYPERSPECTRAL IMAGING FOR THE AGE ESTIMATION OF BLOOD STAINS AT THE CRIME SCENE

Forensic Science International 2012;223(1-3):72-7.

The age estimation of blood stains can provide important information on the temporal aspects of a crime. As previously shown, visible spectroscopy of blood stains can successfully be used for their age estimation. In the present study we evaluated the feasibility to use hyperspectral imaging for this purpose. Visible reflectance spectra of blood stains were recorded using a push broom hyperspectral imaging system. From these spectra, the relative amounts of oxyhaemoglobin, methaemoglobin and hemichrome within the blood stains were derived. By comparison of the haemoglobin derivative fractions with a reference dataset, the age of blood stains up to 200 days old was estimated. The absolute error of the age estimation task increased with age, with a median relative error of 13.4% of the actual age. To test the practical applicability of this method, a simulated crime scene was analyzed, in which blood stains of several ages were deposited. Hyperspectral imaging combined with the proposed analysis provided insight in the absolute age of the blood stains. Additionally, the blood stains were clustered based on their haemoglobin derivative fractions, without the use of a reference dataset. Results demonstrated that the order of formation of blood stains can be determined, even under unknown environmental circumstances, when no proficient reference dataset is available. These findings are an important step toward the practical implementation of blood stain age estimation in forensic casework.

4.1. INTRODUCTION

Knowledge of the time of bleeding is highly significant in many forensic investigations, because this information can be used to determine the moment a crime was committed, or whether a blood stain is crime-related. In a recent murder case in The Netherlands where blood stain age estimation was requested, several blood stains were found in a suspect building. The main question was whether these blood stains all originated from a single event or from multiple events. Information about the blood stain ages would enable investigators to verify testimonies, and to adjust the direction of their investigation accordingly. Several techniques, including high performance liquid chromatography⁸⁸, electron paramagnetic resonance^{89, 90}, atomic force microscopy⁹¹ and RNA degradation measurements^{92, 93} have been investigated for this purpose, as reviewed by Bremmer et al⁹⁴. However, none of these methods is yet implemented in forensic practice; most require sample preparation and need to be performed in a laboratory.

Non-destructive blood stain age estimation can be performed using visible reflectance spectroscopy^{1, 67}. When blood exits the human body, oxyhaemoglobin (HbO_2) auto-oxidizes into methaemoglobin (MetHb), which in turn denatures into hemichrome (HC)¹. Previously we have shown that visible reflectance spectroscopy can be used to determine the relative fractions of the haemoglobin derivatives and estimate the age of blood stains by comparing these fractions to reference data¹. A different approach for processing of the spectral data was proposed by Li et al⁶⁷, who applied linear discriminant analysis to estimate the age of blood stains.

A drawback of using spectroscopy is that point measurements of all suspected stains at the crime scene can be time consuming and labour intensive. Hyperspectral imaging integrates conventional spectroscopy and imaging, thereby obtaining both spatial and spectral information from all objects in the field of view. As a result, spectral properties of all objects can be recorded together with information about their location and distribution within the scene, without the need for further documentation. Because current hyperspectral imaging systems are fast and portable, they can be transported to

the crime scene where traces can be analysed and interpreted in the original context, thereby reducing the workload in forensic laboratories and almost instantly providing investigators with valuable information. However, the transition from spectroscopy to hyperspectral imaging means a change in illumination-detection geometry⁵⁷, thus different processing of the spectra is required. In **Chapter 3**, we demonstrated the feasibility of hyperspectral imaging of the crime scene to detect and identify blood stains remotely¹⁸. In that study, blood stains were distinguished from other samples with a sensitivity of 100% and a specificity of 85% using hyperspectral imaging. Even small blood stains with a diameter of approximately 1 mm could be detected from 1.5 meter distance.

The aim of this study is to show the feasibility to use hyperspectral imaging for age estimation of blood stains. Thereto, visible reflectance spectra of blood stains were recorded and spectrally unmixed to obtain the relative fractions of HbO₂, MetHb and HC within the stains. The temporal behaviour of these fractions was used to estimate the age of blood stains up to 200 days old. We investigated the practical applicability of this method by the analysis of a simulated crime scene in which blood stains of several ages were deposited. By hyperspectral imaging, spectral unmixing, and comparison of the haemoglobin fractions to a reference dataset, the absolute ages of blood stains were estimated. Additionally, we proposed a method to determine the relative ages of blood stains, which is useful in forensic investigations where the environmental conditions are unknown.

4.2. DATA ACQUISITION AND ANALYSIS

4.2.a HYPERSPECTRAL IMAGING

Measurements were performed using a push broom line-scanning spectral imaging system (Spectral Imaging Ltd., Oulu, Finland). This system consisted of a rotary stage, a hyperspectral camera operating in the visible and near infrared wavelength range (400-1000 nm) and a halogen broadband white light source. Using this system, we recorded so-called hypercubes (see Figure 4.),

containing two spatial dimensions and a spectral dimension, as introduced in **Chapter 2**. Using the light intensities at all measured wavelengths, reflectance spectra were obtained from all pixels in the hypercube, as described below.

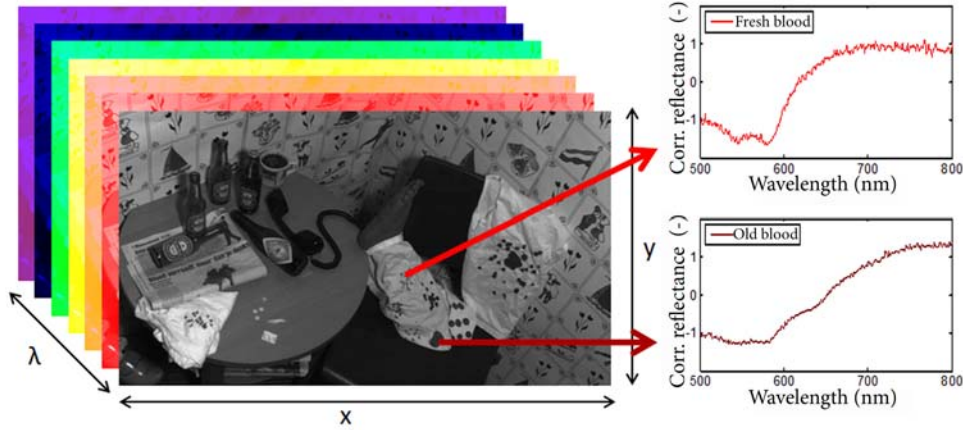


Figure 4.1. Hypercube of a simulated crime scene, with two spatial (x,y) and one wavelength (λ) dimension (left). From the hypercube a reflectance spectrum was obtained from each pixel (right).

4.2.b PRE-PROCESSING

Spectral analysis was limited to the wavelength range of 500-800 nm, because of the low camera sensitivity and low power of the light source beyond this range. The following pre-processing steps were applied to all spectra in the hypercube. First, the dark response ($I_{dark,ij}(\lambda)$) of the camera was subtracted. Depending on the system, this can be pixel and wavelength dependent. Next, to account for wavelength dependent intensity differences in the light source, we divided by the background response of a white reference plane at all wavelengths ($I_{white}(\lambda)$), previously corrected for the dark response:

$$R_{ij}(\lambda) = \frac{I_{ij}(\lambda) - I_{dark,ij}(\lambda)}{I_{white}(\lambda) - I_{dark,ij}(\lambda)},$$

where R is the reflectance, I is the intensity and i and j are horizontal and vertical pixel indices. Finally, all reflectance spectra were corrected using the standard normal variate algorithm⁹⁵. All data analysis was performed using custom-made scripts written in MATLAB (The Mathworks Inc., Natick, Massachusetts, USA).

4.2.c SPECTRAL UNMIXING

After the pre-processing procedure a non-linear spectral unmixing model was employed to find the relative fractions of HbO₂, MetHb and HC. Similar to the way described in **Chapter 3**⁶⁵, a one-dimensional solution of the radiative transport theory was employed to translate the measured corrected reflectance spectra into the absorption spectra of HbO₂, MetHb and HC^{82, 96}. A non-linear least squares fit was used to estimate the relative fraction of each haemoglobin derivative. The coefficients of determination R^2 between the measured spectra and the fit were used as a quality test. Measurements with an R^2 value below 0.99 were excluded from the further analysis.

4.3. MATERIAL AND METHODS

4.3.a REFERENCE DATASET

To build a reference dataset, blood was drawn from a healthy non-smoking volunteer, deposited on white cotton cloth and stored in a laboratory at room temperature. Hypercubes of the blood were recorded repeatedly for 200 days (almost daily in the first month, thereafter approximately once a month). After pre-processing of the data, a training set was selected consisting of 8 regions of 25 pixels for each age, which were averaged to obtain 8 reflectance blood spectra per age. The spectral unmixing procedure was applied to these spectra to find the fractions of HbO₂, MetHb and HC present in the blood, which were plotted against the age. In between data points, values were interpolated linearly.

4.3.b AGE ESTIMATION

The obtained reference dataset of haemoglobin fractions was used to estimate the age of a test set of 8 reflectance spectra of neighbouring blood stains, again all averaged over 25 pixels, and recorded up to 200 days. As above, the fractions of the haemoglobin derivatives were derived and compared to the reference dataset. A k -nearest neighbour (k -NN) algorithm was applied to find the age at which the Euclidean distance to the reference fractions was minimal ($k=1$)⁹⁷. All estimated ages were plotted against the actual age. The absolute and relative errors were calculated.

4.3.c CRIME SCENE ANALYSIS

A crime scene was simulated and recorded using the hyperspectral imaging system (Figure 4.2). The blood stains present in the scene were donated by 5 different healthy non-smoking volunteers (not including the volunteer whose blood was used to create the reference data set) and deposited on white cotton cloths 0.1, 2, 15, 40, and 200 days prior to the measurements. Before these blood stains were put in the scene, they were stored in a laboratory at room temperature, i.e. under similar conditions as the reference blood stains.

Pre-processing and spectral unmixing were applied to all spectra of the hypercube, as described above. Before analyzing the haemoglobin fractions, it was determined whether a spectrum resembled that of blood, using the automatic detection and identification method described in more detail in **Chapter 3**¹⁸. By thresholding the R^2 values between the corrected reflectance spectra and the least-squares fit of the absorption spectra of HbO₂, MetHb and HC, a mask was created to isolate all pixels depicting blood stains. For the subsequent age estimation task, two approaches were used, as described below.

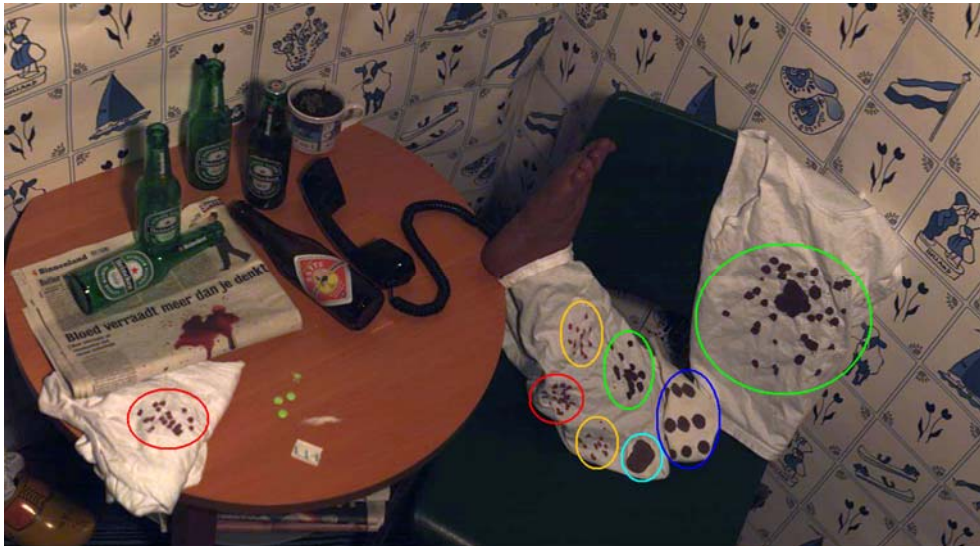


Figure 4.2. Colour image of the simulated crime scene, in which blood stains of various ages were deposited. The locations of blood stains are indicated with ellipses, of which the colour symbols the age; orange = 0.1 day, red = 2 days, green = 15 days, blue = 40 days, cyan = 200 days.

Absolute age

First, the absolute ages were estimated by comparing the fractions of HbO_2 , MetHb and HC for blood stains at the crime scene with those of the reference dataset. Within the mask depicting all blood stains, all connected pixels were grouped and labelled to analyse all individual blood stains separately. The reflectance spectra of all pixels within one stain were averaged and spectrally unmixed to find the haemoglobin fractions within the blood stain. For each stain, a k-NN algorithm was applied to find the age at which the Euclidean distance to the reference dataset was minimal ($k=1$)⁹⁷. Average estimated ages were calculated for each class and plotted against the actual age.

Relative age

In forensic practice, if blood stains are found in different or unknown environmental circumstances, the method described above may lead to wrong

age estimations, as both humidity and temperature are known to influence the chemical reactions within a blood stain⁵⁶. For those cases, we propose a method to estimate the relative age of blood stains. The averaged spectra of all blood stains in the simulated crime scene described above were analysed. K-means cluster analysis⁹⁸ was applied to find groups of blood stains with similar haemoglobin derivative fractions. Results were presented by depicting all clusters in different colours overlayed on a greyscale image of the scene. By analysing the haemoglobin fractions of the different clusters, the order of formation was determined.

4.4. RESULTS

4.4.a REFERENCE DATASET

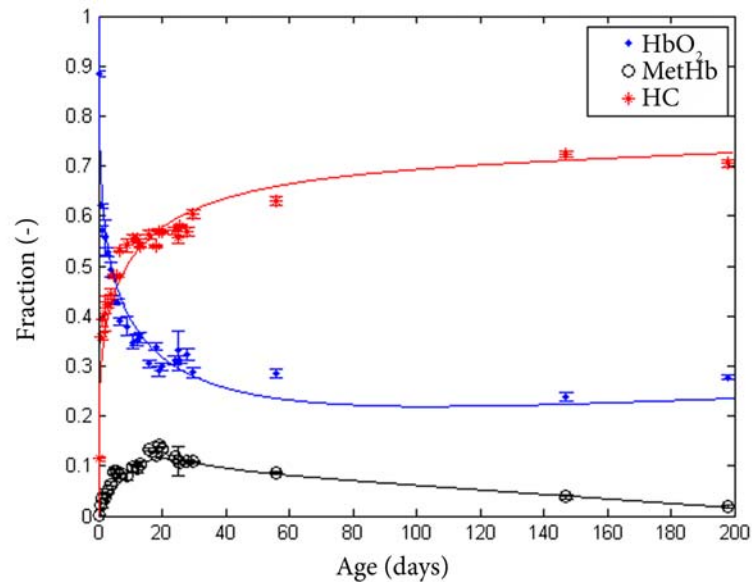


Figure 4.3. Calculated fractions of oxyhaemoglobin (HbO₂), methaemoglobin (MetHb) and hemichrome (HC) against the age of the blood stains. The lines through the data points are a guide to the eye.

Figure 4.3 shows the temporal behaviour of HbO₂, MetHb and HC fractions in blood stains up to 200 days old. Within the measured blood stains, the fraction of HbO₂ decreased with age, whereas the fraction of MetHb increased in the first three weeks, followed by a decrease, and the fraction of HC seemed to increase in time.

4.4.b AGE ESTIMATION

By comparison of the haemoglobin fractions with the reference dataset (Figure 4.3), the age of blood up to 200 days was estimated (Figure 4.4). The absolute error of the age estimation task increased with age (Figure 4.5). The median relative error was 13.4% of the actual age.

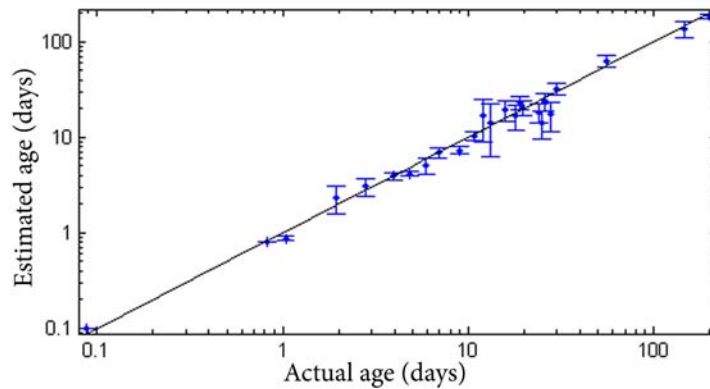


Figure 4.4. Mean estimated age of blood stains versus the actual age for blood stains up to 200 days old. Error bars depict the standard deviation. The solid line is the line of unity.

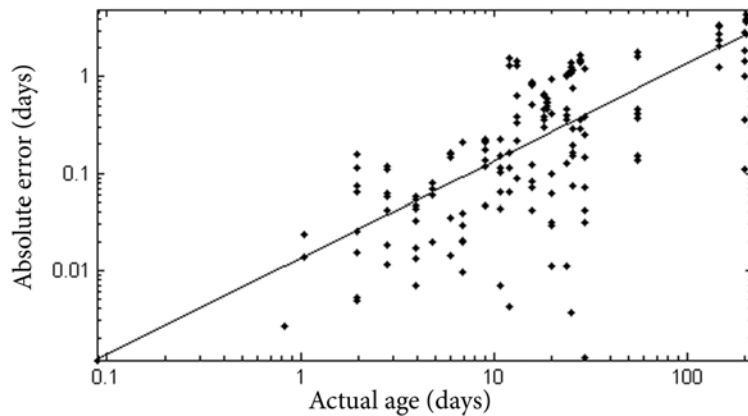


Figure 4.5. Absolute error of the age estimation task versus the actual age for blood stains up to 200 days old. The solid line depicts the median relative error of 13.4%.

4.4.c CRIME SCENE ANALYSIS

Absolute age

The mean estimated age for all blood stains at the simulated crime scene was plotted against the actual age in Figure 4.6. Error bars depict the standard deviation between different blood stains of the same age. An exception was made for the oldest blood stain; because only one stain of 200 days old had been deposited in the scene, 6 different regions within this stain were selected and used to calculate the mean estimated age and the standard deviation. The absolute errors of the age estimation task are given in Table 4.1.

Table 4.1. Actual ages, estimated ages and absolute errors of the age estimation task of blood stains in the simulated crime scene.

Actual age (days)	Estimated age (days)	Absolute error (days)
0.1	1.0	0.9
2	4.7	2.7
15	10.7	4.3
40	34.0	6.0
200	197.9	2.1

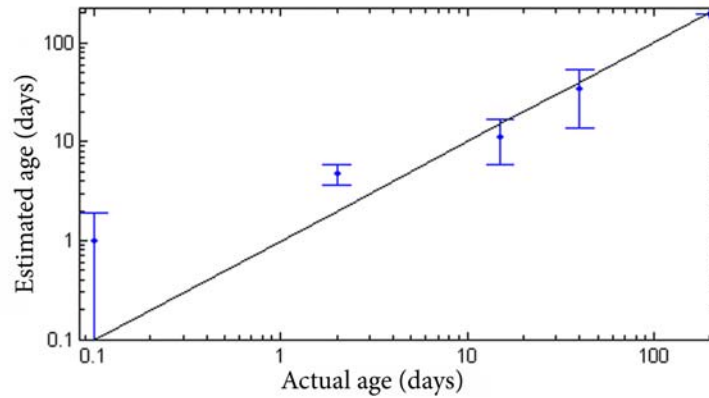


Figure 4.6. Mean estimated age of blood stains at the simulated crime scene versus the actual age. Error bars depict the standard deviation between different blood stains of the same age (0.1, 2, 15, and 40 days old), or the standard deviation between different regions within the stain (200 days old).

Relative age

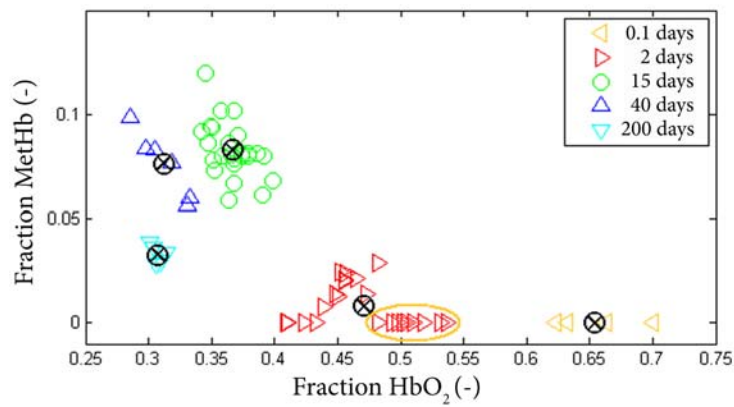


Figure 4.7. Scatter plot depicting the HbO₂ and MetHb fractions calculated for blood stains in the simulated crime scene. Each blood stain is assigned to a different colour, class number and marker type using k-means clustering. The majority of blood stains was assigned to the correct age group mentioned in the legend. Blood stains in the orange ellipses were incorrectly clustered in the group of 2 days old blood stains, while the actual age was 0.1 days.

The HbO₂ and MetHb fractions calculated for all blood stains in the simulated crime scene are plotted in Figure 4.7. Different marker types and colours in this figure indicate the results of a k-means cluster analysis, with k=5. The majority of blood stains was assigned to the correct age group mentioned in the legend. Data points within the orange ellipse belong to blood stains of 0.1 days old, but were incorrectly assigned to the cluster of 2 days old blood stains. The results are presented differently in Figure 4.8, where each cluster is indicated by a different colour. Again, the orange ellipses show the incorrectly clustered blood stains.



Figure 4.8. Results of the relative age estimation task. The haemoglobin fractions of all blood stains were clustered using k-means clustering. The majority of blood stains was assigned to the correct age group mentioned in the legend. Blood stains in the orange ellipses were incorrectly clustered in the group of 2 days old blood stains, while the actual age was 0.1 days.

Analysis of the HbO₂ fraction in the different blood stain clusters (Figure 4.7) indicates the order of formation of the blood stains. The average HbO₂ fractions for clusters 1 to 5, indicated by the crosses in Figure 4.7, were 0.65, 0.47, 0.37, 0.31, and 0.30 respectively. Assuming that the HbO₂ fraction

decreases in time, as shown in Figure 4.3, the correct order of formation could be predicted using the average cluster fractions.

4.5. DISCUSSION

We introduced the use of hyperspectral imaging for the age estimation of blood stains at the crime scene. The temporal behaviour of HbO₂, MetHb and HC fractions within blood was measured for blood up to 200 days old (Figure 4.3), and used to estimate the age of other blood stains with a median relative error of 13.4% (Figure 4.4). For stains previously identified as blood, the age estimation task was completely automatic and did not need any human interference. The practical applicability of this technique was demonstrated by the analysis of a simulated crime scene. Within this scene, the age of blood stains could be estimated successfully by comparison with a reference dataset of haemoglobin fractions (Figure 4.6). Additionally, without using any reference dataset, blood stains were clustered in groups with similar ages and the order of formation was determined successfully (Figure 4.8).

The described approach of splitting the spectra into the different chemical components has the advantage that the influence of temperature, humidity or other environmental circumstances can be studied. Bremmer et al demonstrated that the oxidation of HbO₂ is relatively independent of humidity, whereas the transition of MetHb into HC strongly depends on humidity⁵⁶. The influence of environmental factors at the crime scene will make precise estimation of the absolute age of blood stains challenging. If the environmental factors can be reconstructed we are able to study the kinetics of the haemoglobin derivatives, which can be used to estimate the absolute ages of blood stains. Additionally, even in unknown circumstances, we demonstrated the possibility to determine the relative age of different blood stains, under the assumption that they were exposed to similar environmental conditions. Because the fraction of HbO₂ decreases in time, this fraction can be used to determine the order of formation of different blood stains, as demonstrated by the analysis of the simulated crime scene.

To our knowledge, no other application of hyperspectral imaging for the age estimation of blood stains has been reported previously. Two prior studies were reported using a more controlled spectroscopy setup. An advantage of using hyperspectral imaging is the speed of acquisition; within a minute millions of spectra can be recorded. The time needed for the analysis depends on the size of the scene and the calculation power. In this particular case we needed several hours to analyze the scene. The accuracy of our age estimation improved compared to the accuracy reported by Bremmer et al, who used a fibre based spectroscopy device to estimate the age of blood stains¹. For example, at an age of 3 days, the ages estimated by Bremmer et al varied between 1.5 and 6 days. In comparison, at an age of 2.8 days, we estimated ages between 2.2 and 4 days. Although we cannot test this improvement on significance, it can be explained by the pre-processing procedure we applied prior to analysis, as suggested by Li et al⁶⁷. Application of the standard normal variate algorithm reduced the variance between spectra of blood stains of the same age.

Using spectroscopy combined with pre-processing and linear discriminant analysis, Li et al reported an error of less than one day for blood stains up to 19 days old, after which the accuracy decreased⁶⁷. Although it is expected that the accuracy decreases with age, as chemical changes are faster in the beginning of the aging process, the sudden decrease in accuracy after 19 days can be explained by analysis of the relative fractions of haemoglobin derivatives derived in our study. After an increase of approximately 3 weeks, the relative fraction of MetHb within a blood stain starts to decrease (see Figure 4.3b). This explains why a linear model can successfully be used to approximate the spectral behaviour in the first 19 days, but after that results become inaccurate. In the first three weeks, we achieved similar results as Li et al. However, using the fractions of haemoglobin derivatives, ages of older blood stains up to 200 days could also successfully be estimated. In practice, the accuracy will depend on the actual age of the blood stain and knowledge of the environmental conditions. How this influences the evidential value depends on the hypotheses relevant to the case.

A challenge under field operation is the ability to analyze complex crime scenes, where blood stains are typically recorded with varying distances to the camera, and under varying angles. In this study, the blood stains were randomly distributed throughout the crime scene, so the possible variation caused by different distances and angles was part of the error bars shown in this chapter (Figure 4.6). The exact influence of geometrical properties is subject of extensive further study. The mean absolute difference between actual and estimated ages of blood stains ranged between 0.9 and 6.0 days (Table 4.1). To estimate the relative ages of blood stains in the simulated crime scene, we used cluster analysis with prior knowledge of the number of clusters. Although this number will be unknown in forensic practice, advanced cluster analysis⁹⁸ combined with bloodstain pattern analysis may give more insight in the number of events that created the blood stains. Additionally, if prior information about blood stain groups is available (e.g. based on DNA analysis), the amount of errors may be reduced by replacing unsupervised cluster analysis by supervised classification, which makes use of a predefined training set.

Other challenges typically encountered in forensic casework, e.g. contaminated traces found on non-ideal backgrounds, emphasize the necessity to refine and validate the technique in forensic practice. When blood stains are deposited on coloured backgrounds, age estimation using visible hyperspectral imaging is expected to be hampered by the absorption of visible light by the background. The model we used in this study is a general model for light propagation in turbid media, in the limit of a non-absorbing background, in which the only chromophores are the haemoglobin components. Extension to other backgrounds requires adaptation of the boundary conditions. This requires an extensive further study presented in **Chapter 5**, in which both the scattering and absorption properties of the substrate will be accounted for. For some backgrounds, a switch to the near infrared wavelength range may be necessary (**Chapter 7**)¹⁹. Another topic for further research is the influence of carboxyhaemoglobin on our analysis. Because we analysed blood of healthy non-smoking volunteers who usually have only a small percentage (<4%) of carboxyhaemoglobin⁹⁹, the possible presence of this haemoglobin derivative was not taken into account. However, the increased level of

carboxyhaemoglobin expected for smokers, people suffering from sickle cell disease, fire victims or in cases of fatal carbon monoxide poisoning, may influence the results in forensic practice¹⁰⁰⁻¹⁰².

In conclusion, we demonstrated the feasibility to use hyperspectral imaging for the absolute or relative age estimation of blood stains at the crime scene, based on the relative amount of haemoglobin derivatives present in the blood stains. When applied in forensic practice, the described technique provides investigators with valuable information, which can be used to reconstruct the timeline of events.

4.6. ACKNOWLEDGEMENTS

The authors kindly acknowledge Aoife Gowen, for sharing her experience in the analysis of hyperspectral images. Additionally, we thank the volunteers for donating blood. An application of the results of this research is being developed in the project CSI the Hague, within the *Pieken in de Delta* program by the NL Agency of the Dutch Ministry of Economic Affairs, Agriculture and Innovation (project number PID082036).

5 - PRACTICAL IMPLEMENTATION OF BLOOD STAIN AGE ESTIMATION

In preparation

To enable the use of spectroscopy for the age estimation of blood stains in forensic practice, a method applicable for blood stains found on many different backgrounds is needed. We describe a one dimensional light transport model, which corrects for light absorptions of the background. Using this method, we calculate the relative amounts of HbO₂, MetHb and HC in blood stains on coloured backgrounds, based on their reflectance spectra. Additionally, we describe a statistical method to calculate an estimated age within a 95% confidence interval. The increased applicability in casework and its possible value for crime investigations is demonstrated in a case example of a shooting incident where 3 bodies were found dead in a living room. For crime reconstruction purposes, the absolute and relative age of different groups of blood stains were measured using visible reflectance spectroscopy. We analyzed blood stains at two distinct locations in the house: downstairs where the victims were found, and upstairs. The results indicated that the group of blood stains found upstairs was older than the blood stains found in the vicinity of the bodies downstairs. Thus, the blood stains upstairs were probably not related to the current crime. The age estimated for the blood stains downstairs was 1.5-3.2 days old. This time interval includes the moment gun shots were heard by a witness. Combined with other evidence, the age of blood stains may lead to a better reconstruction of the timeline of events.

5.1. INTRODUCTION

Blood stain age estimation techniques can provide valuable information for criminal investigators. Age information gives insight in the sequence of blood shedding events, or even the absolute time of deposition. This intelligence can be useful for the verification of suspect or witness statements, and for the selection of relevant samples for e.g. DNA analysis, reducing the workload in forensic laboratories. In **Chapter 4** it was shown that the age of blood stains on white backgrounds can be estimated using visible reflectance spectroscopy or hyperspectral imaging^{1, 49, 67, 68}. On coloured backgrounds, light absorption by the background influences the measured reflectance spectra. In this chapter, we describe a physical spectral processing model to correct for these background absorptions, which is demonstrated by a case example.

In the last decade several spectroscopic techniques, including visible reflectance spectroscopy (**Chapter 3, 4**)^{1, 18, 49, 65, 67, 68}, near infrared spectroscopy (**Chapter 7**)^{19, 66}, and Raman spectroscopy^{103, 104} have been explored for the analysis of blood stains in laboratory settings. The transition from laboratory measurements, with its ideal experimental conditions, to crime scene analysis however, is complicated by the wide variety of substrates on which the blood may be deposited¹⁰⁵. This problem is often encountered in case work, and may explain why no blood stain age estimation technique has yet routinely been applied in forensic investigations.

We demonstrated in **Chapter 4** how visible reflectance spectroscopy or hyperspectral imaging can be used to measure the concentration change of oxyhaemoglobin (HbO₂), methaemoglobin (MetHb) and hemichrome (HC) – all reaction products of haemoglobin – in a laboratory setup, without destroying or even touching the sample⁴⁹. A reference database of the relative amounts of HbO₂, MetHb and HC for blood stains of different ages stored under controlled ambient conditions (with known temperature and humidity) can in turn be used to estimate the age of a questioned blood stain.

In previous studies on age estimation of blood stains using spectroscopy, possible sources of spectral variation were often controlled or taken constant for all experiments^{1, 67, 68}, e.g. the background colour, the blood

stain thickness, and the sample-detector distance, which is impossible in forensic practice. We now describe a one dimensional light transport model for the calculation of the relative amount of HbO₂, MetHb and HC in the blood stains, which can be applied to correct for these variables, thereby increasing the applicability of blood stain age estimations in forensic practice. Additionally, we describe a statistical method to calculate an estimated age within a 95% confidence interval.

Using reflectance spectroscopy we repeatedly measured equally aged blood stains on a glass slide which were placed on top of several coloured backgrounds. The calculated haemoglobin derivative fractions for blood stains on different background colours were compared. Finally, we describe a criminal case where we estimated the age of blood stains using the light transport model. At the scene of a presumed double homicide followed by suicide, blood stains were found on several backgrounds at two distinct locations. The research questions were twofold. 1) What is the age of the blood stains surrounding the victims? This information gives insight in the moment the crime was committed. 2) Is there an age difference between the blood stains found at two different locations? The answer to the latter question can indicate whether a blood stain is related to the crime. Application of this technique in practice provided investigators with information currently not available, which could be used to create possible scenarios.

5.2. BLOOD STAIN AGE ESTIMATION

5.2.a LIGHT TRANSPORT MODEL

To find the relative fractions of HbO₂, MetHb and HC present in a blood stain a least squares fitting algorithm was employed in combination with a one-dimensional light transport model for multi-layered samples⁸⁶:

$$R = \frac{1 - R_b \cdot (a - b \cdot \coth(bST))}{a - R_b + b \cdot \coth(bST)}, \text{ with } a = \frac{S + K}{S} \text{ and } b = \sqrt{a^2 - 1}, \quad (5.1)$$

where R is the blood stain reflectance (-), R_b the reflectance of the background (-), S is derived from the scattering coefficient (mm^{-1}), and K from the absorption coefficient (mm^{-1}), which are all wavelength dependent^{1, 87}. T is the blood stain thickness (mm). This model describes the reflectance of a homogeneously coloured sample of fixed thickness on top of an absorbing substrate as a function of wavelength. Light is assumed to be diffuse in all directions after penetrating the sample, although the model considers only two net fluxes straight up and straight down. The model used in **Chapter 3 and 4** is the limit of formula 5.1, valid only for blood stains of infinite thickness.

Formula 5.1 is compared to the measured reflectance spectrum using a least squares fitting algorithm. Input data are the reflectance spectrum of the blood stain, the reflectance spectrum of the background, and the optical properties of the haemoglobin derivatives⁸². The output of the algorithm is the:

- relative amount of HbO₂ in the blood stain,
- relative amount of MetHb in the blood stain,
- relative amount of HC in the blood stain,
- blood stain thickness,

based on the best fit of the non-linear function to the measured reflectance spectrum. The relative amounts of haemoglobin derivatives change when blood stains are aging, as shown in **Chapter 4**^{6, 18}. The blood stain thickness determines how much the reflectance spectrum is influenced by light absorption of the background.

5.2.b STATISTICAL ANALYSIS

To estimate the age of a questioned blood stain, the calculated HbO₂ fractions are compared with a reference database of blood stains measured up to an age of 200 days old. The MetHb and HC fractions are disregarded, because of their sensitivity for humidity changes⁵⁶. Because first order reaction kinetics are expected, the HbO₂ fractions are plotted against the natural logarithm of the age in Figure 5.1. In this figure three different phases are observed, with age intervals of less than 1 day, from 1 to 20 days, and more than 20 days. In the first phase, the measured HbO₂ fraction decreases exponentially,

corresponding to the fast oxidation rate of HbO₂ observed by Bremmer et al in the first hours after deposition of the blood stain. After this phase, a slower exponential decay is observed for blood stains with ages between 1 and 20 days, again in agreement with Bremmer et al. The age interval of the third phase was not analysed in Bremmer's report, which explains his reference to a biphasic decay. The change after 20 days may be explained by the decreasing fraction of MetHb around this age, as shown in **Chapter 4**^{1,49}.

For each of the three age intervals, we calculated a linear regression model, which was used to relate the natural logarithm *age* (days) of blood stains to the HbO₂ fractions in order to estimate the age of questioned blood stains (denoted by the subscript q) based on measured HbO₂ fractions [HbO₂]_q:

$$\text{Phase 1) } \ln(\text{age}) = -11.7 \cdot [\text{HbO}_2]_q + 6.9 \quad (\text{adjusted } R^2 = 0.95) \quad (5.1)$$

$$\text{Phase 2) } \ln(\text{age}) = -6.1 \cdot [\text{HbO}_2]_q + 4.0 \quad (\text{adjusted } R^2 = 0.91) \quad (5.2)$$

$$\text{Phase 3) } \ln(\text{age}) = -22.7 \cdot [\text{HbO}_2]_q + 7.4 \quad (\text{adjusted } R^2 = 0.91) \quad (5.3)$$

Independent of the phase, a 95% confidence interval for the predicted age can be determined, as described by Maddala¹⁰⁶, by:

$$\ln(\text{age}) \pm t_{\alpha/2}(n-2) \sqrt{1 + \frac{1}{n} + \frac{([\text{HbO}_2]_q - \overline{[\text{HbO}_2]})^2}{S_{[\text{HbO}_2]}}}, \quad (5.4)$$

in which $\alpha = 0.05$, t is Student's t-value, n is the number of measurements in the reference database, $\overline{[\text{HbO}_2]}$ is the average HbO₂ fraction, and $S_{[\text{HbO}_2]}$ its standard deviation:

$$\overline{[\text{HbO}_2]} = \sum_{i=1}^n [\text{HbO}_2]_i / n,$$

$$S_{[\text{HbO}_2]} = \sqrt{\sum_{i=1}^n ([\text{HbO}_2]_i - \overline{[\text{HbO}_2]})^2 / (n-1)}$$

This confidence interval is influenced by the variability between different blood stains in the reference database.

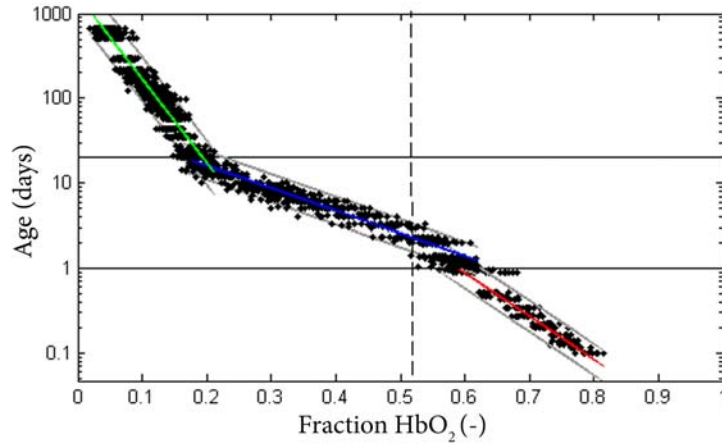


Figure 5.1. The age of blood stains from the reference database plotted against the measured fraction HbO₂ (black dots) on a semi-logarithmic scale. Green, blue and red lines depict the regression lines for three different phases, separated by the horizontal black lines. Their corresponding confidence intervals are plotted in grey. By drawing a vertical line at a measured HbO₂ fraction of a questioned blood stain, its age can be determined (e.g. the striped line).

5.3. LABORATORY TEST

5.3.a MATERIALS AND METHOD

To test background correction of the light transport model, six blood stains were applied onto glass slides, and placed on top of 5 pieces of cotton (white, yellow, pink, blue, and green) with the blood stain facing the cotton (see Figure 5.2). Reflectance spectra of all combinations of 6 blood stains and 5 background colours were measured using a CCD spectrometer (USB 4000; Ocean Optics; Duiven, the Netherlands), a tungsten-halogen light source (H-2000; Ocean Optics; Duiven, the Netherlands) and a non-contact probe (QR400-7-UV/BX; Ocean Optics; Duiven, the Netherlands). These measurements were repeated 10 times, from 2 hours up to 19 days old.

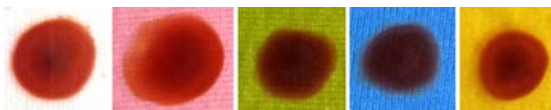


Figure 5.2. Photographs of the samples: blood stains on glass slides, placed on top of white, pink, green, blue and yellow cotton.

Next to the blood stains, reference measurements were collected of the background material. Spectral analysis was limited to the wavelength range of 450 – 800 nm, because of the low detector sensitivity and low power of our light source beyond this range. Each measured spectrum was corrected for dark noise and for intensity variations of the light source using the reflectance spectrum of a white reflectance standard (Spectralon). Reflectance spectra were normalized by applying the standard normal variate algorithm¹⁴. Data analysis was performed using custom-made scripts written in MATLAB (The Mathworks Inc., Natick, Massachusetts, USA).

All corrected reflectance spectra were analyzed using the multi-layer light transport model described above, in which the spectral reflectance of the background was incorporated. The coefficient of determination (R^2) between the measured spectrum and a haemoglobin derivative fit was used as a quality check. This R^2 value approaches 1 if the theoretical fit matches the measurement. Spectra with an $R^2 > 0.999$ were used for further analysis. For all measurements with an R^2 value exceeding this threshold, the relative amounts of haemoglobin derivatives were calculated and plotted against the age of the blood stains.

5.3.b RESULTS

For all combinations of blood stains and background colours, the fitting algorithm was used to deduce the relative amount of haemoglobin derivatives. Figure 5 shows two examples of measured spectra and their theoretical fits for a blood stain on a pink and blue background respectively. This figure demonstrates the difference in fit quality; on the pink background the fit shows a high correlation with the measured spectrum ($R^2 > 0.999$), while the fit clearly deviates from the reflectance spectrum on the blue background ($R^2 = 0.986$).

Based on the threshold of $R^2=0.999$ blood stains on the blue background were disregarded in the further analysis (range of R^2 values: 0.983-0.997). The same applied for blood stains on the green background, which likewise did not pass the quality check (range of R^2 values: 0.986-0.994), contrary to the blood stains on pink, yellow and white backgrounds.

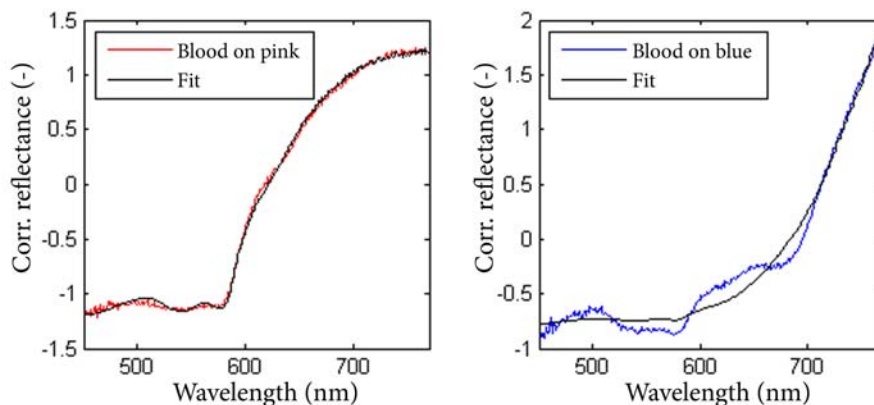


Figure 5.3. Examples of corrected reflectance spectra of a blood stain on a pink background (left, $R^2 > 0.999$) and a blue background (right, $R^2=0.986$) and their corresponding haemoglobin fits.

For these blood stains with an $R^2 > 0.999$ the calculated fractions of HbO_2 , MetHb and HC are plotted against the age in Figure 6. This figure shows overlapping error bars (one standard deviation) of the calculated fractions for the different background, supporting the use of the reference database of blood stains on white cotton for the other colours.

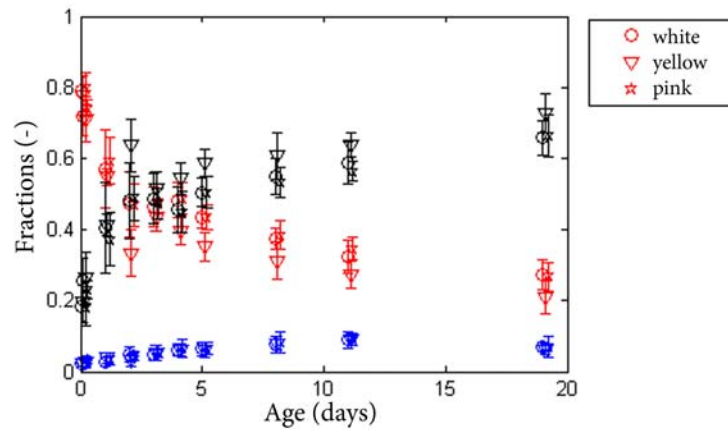


Figure 5.4. Calculated haemoglobin fractions for blood stains of different ages on white, yellow and pink backgrounds. Red data points depict HbO₂, blue corresponds to MetHb, and black data points show the fractions of HC. Error bars illustrate the standard deviations.

5.4. CASE EXAMPLE

5.4.a CASE DESCRIPTION

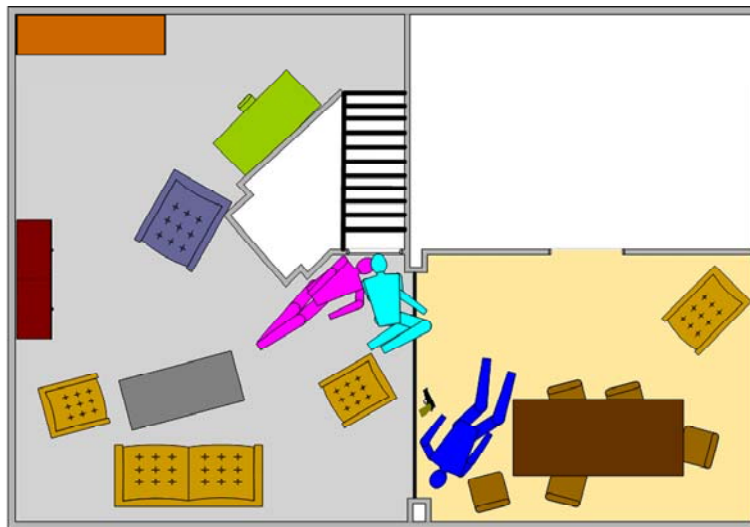


Figure 5.5. Digital sketch of the crime scene, showing three victims in the living room.

On a Sunday morning, a witness reported the sound of gun shots in the neighbouring residence. After entering the house through the attic window, police patrol found two dead men and a woman in the living room (Figure 5.5). A gun was found close to one of the men, who lived in the residence. Forensic investigators measured a rectal temperature difference between this man and the other two victims, indicating that he had died at a later moment. The question arose whether this was a triple suicide, a double murder followed by a suicide, or whether a fourth individual had been involved. In order to reconstruct the events taken place, the blood stain patterns were analyzed. Apart from the blood found around the victims downstairs, several stains were found upstairs (see Figure 5.6).

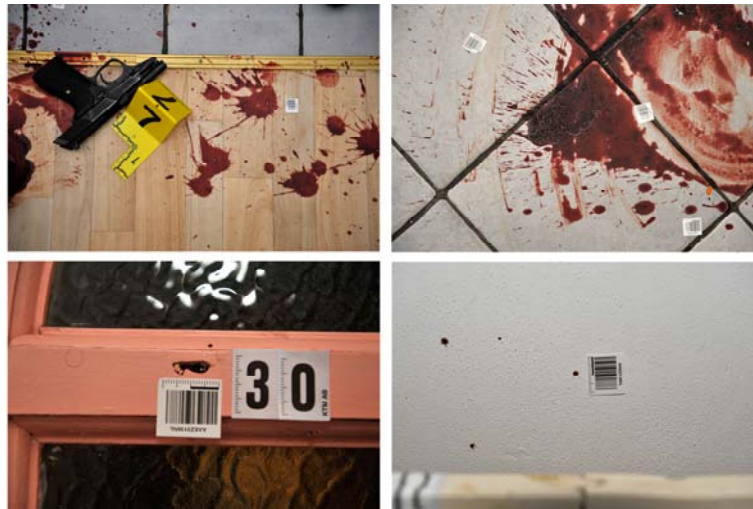


Figure 5.6. Photographs of blood stains found at the crime scene. Top: blood stains found downstairs (left: next to the man close to the gun, right: around the other two victims), bottom: blood stains found upstairs.

5.4.b MATERIALS AND METHOD

To determine whether these stains were related to the crime, the age of 19 blood stains was estimated using visible reflectance spectroscopy and the light transport model described above. Spectroscopic measurements on the blood

stains were performed 2,5 days after the reported gun shots. DNA evidence showed that the blood stains found upstairs all belonged to the man who lived there. Downstairs, not surprisingly, blood stains with DNA from all three victims were found. Both relative and absolute ages of the blood stains upstairs and downstairs were estimated.

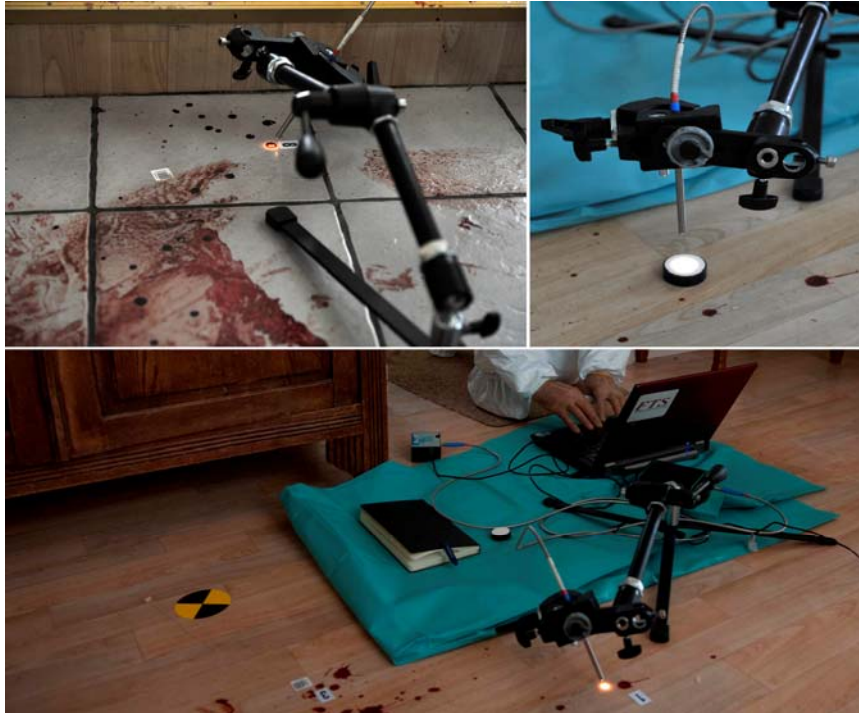


Figure 5.7. Photographs of the measurement setup during reflectance measurements of a blood stain (top left), a white reference (top right) and a clean background (bottom) at the crime scene.

5.4.c RESULTS

Of the 19 selected blood stains in the criminal case, 11 measurements (6 from downstairs, 5 from upstairs) produced an $R^2 > 0.999$ and thus passed the quality check for further analysis. Figure 5.8 (left) shows an example of a measured reflectance spectrum of a blood stain found downstairs and the

corresponding haemoglobin derivative fit. In this spectrum, the absorption characteristics of oxyhaemoglobin (dips at 540 and 576 nm) and methaemoglobin (a dip at 630 nm) are clearly visible. This indicates the relative freshness of the stain. The dip around 720 nm is due to light absorption of the background, which is corrected for. The right spectrum in Figure 5.8 has less characteristic features, indicating that the stain is older.

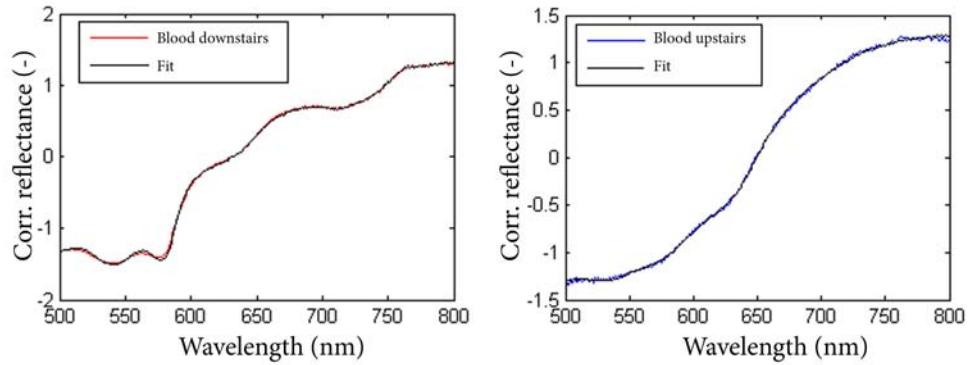


Figure 5.8. Examples of corrected reflectance spectra and their corresponding haemoglobin derivative fits for a blood stain found downstairs (left) and upstairs (right).

The calculated haemoglobin fractions are displayed in Figure 5.9. The error bars of the two blood stain groups do not overlap. This suggests that the blood stains were not created at the same time. More specifically, the lower amount of HbO_2 found for the blood stains upstairs indicates that these blood stains are older, as the amount of HbO_2 decreases in time.

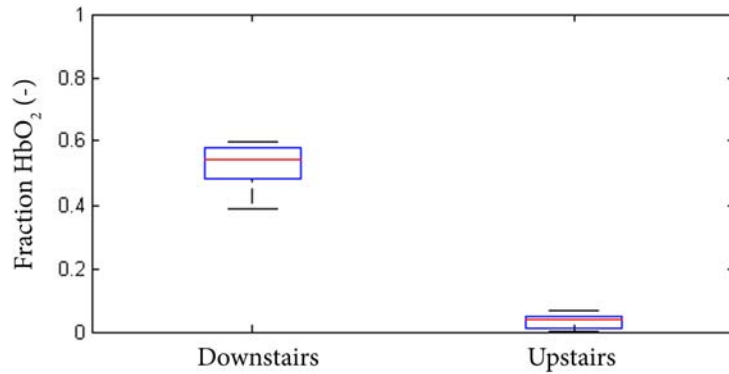


Figure 5.9. Box plots showing the measured HbO₂ fractions for blood stains downstairs and upstairs.

The average amount of HbO₂ for the blood stains downstairs is 0.52 (with a standard deviation of 0.08). The striped line in Figure 5.1 shows that this value corresponds with blood stains in the second phase (2-20 days). Using the second regression model described in formula 5.2, and formula 5.4 we calculated an age of 1.5 – 3.2 days, within a 95% confidence interval. This interval includes the moment a witness claimed to have heard the sound of gun shots. The fraction of HbO₂ found upstairs (average: 0.03, standard deviation: 0.03) does not correspond with these in the reference database at any moment in time, which suggests that the blood stains are very old. With a humidity and temperature comparable to the laboratory in which the reference blood stains were analysed (45 ± 5 % RH and 22.3 ± 0.5 °C respectively), this stage is not yet reached after 200 days. In a warmer atmosphere, reaction rates are faster and the amount of HbO₂ will decay faster⁵⁶. However, even in an environment of 40 degrees Celsius, the measured HbO₂ fraction was not reached after 20 days (unpublished results).

5.5. DISCUSSION

We demonstrated a light transport model which is able to correct for background absorptions (within limits), and therefore widely extends the

applicability of visible reflectance spectroscopy for blood stain age estimation in forensic practice. In a laboratory setup, we showed that the calculated fractions of haemoglobin derivatives were similar for blood stains on white, yellow and pink backgrounds. Finally, we successfully applied the blood stain age estimation technique in a criminal case and calculated 95% confidence intervals of the questioned age based on a statistical method described in this chapter.

The light transport model estimates the measured reflectance spectrum under the assumption that the blood stain is homogeneous and has a constant thickness. This is a simplified model, which will cause some deviations from the complex reflectance spectrum measured in reality. The described model incorporates the reflectance spectrum of the background in a non-linear way and varies the influence of background absorptions by varying the blood stain thickness. In theory, this model is a good estimation for all background colours. However, for green and blue backgrounds, the best fit deviated significantly from the measured reflectance spectrum. Optimization of the least squares fitting algorithm is needed to solve this problem. If the thickness of the blood stains can be measured, this reduces the amount of fit parameters, which may improve the fit quality. Until that time, the R^2 threshold serves as a quality check, to test which measurements can be successfully analysed.

The proposed statistical model uses three linear regression models to describe the data for the different phases in the aging process. These are simple models, which leave room for future improvement, but they describe the data sufficiently, as indicated by the high adjusted R^2 values. The boundaries of the three phases were chosen manually by observing the data, and correspond with the phases described by Bremmer et al⁵⁶. The first two phases have been attributed to fast oxidation of the α chains of haemoglobin and slow oxidation of the β chains. The change to the third phase may be related to the transition from an increase to a decrease of the amount of MetHb^{49, 107}. The optimal change points can be determined statistically in the future¹⁰⁸. How to deal with blood stains with an age around the boundaries of the models is a topic for further discussion.

In our model, we disregard the amounts of MetHb and HC for the age estimation of questioned blood stains, because of their dependence on the ambient relative humidity⁵⁶. If we would take these haemoglobin derivatives into account, a more accurate age estimation is expected, however the uncertainty and thus the confidence interval would be larger. The confidence intervals used are based on individual measurements of the reference database, instead of their averages. This procedure is conservative, but gives a good indication of the uncertainty. Confidence intervals may be decreased using an approach based on average measurements.

The resulting confidence intervals in casework are generally expected to be larger than intervals resulting from measurements performed in a laboratory setup. Variations in illumination intensity, blood stain thickness, background optical properties, environmental temperature and humidity may all cause differences in spectral response. These factors may also have caused the low fit quality of 8 blood stains analyzed in this case and the blood stains on blue and green backgrounds. Detailed knowledge about these influences is useful to create a list of requirements needed for practical applications to be successful, e.g. maximum and minimal stain thickness and blood stain sizes, background colours, etc. More research is scheduled to discover the limitations of the technique.

In the described case, the relative amount of HbO₂ in two groups of blood stains differed significantly. Under the assumption that the temperature upstairs was similar to downstairs, it was concluded that the blood stains upstairs were not created at the same time. The age interval estimated for the blood stains downstairs, 1.5 – 3.2 days old, was in agreement with tactical information (the reported sound of gun shots), and the estimated post mortem interval based on rectal temperature measurements. The blood stains found upstairs were much older. Combined with other tactical and technical evidence, these results indicated that the blood stains found upstairs were not created at the moment of the crime. DNA evidence showed that these stains all belonged to one of the victims, who lived in the residence.

The reported ages of blood stains should be interpreted with caution. Stains found on different locations may have aged under different

environmental circumstances. Humidity and temperature influence the speed of the chemical reactions within the blood stains⁵⁶. Hence, spectral variations are not necessarily caused by age differences, but can also be due to environmental differences. Prior knowledge about these circumstances is needed to correct for differences in chemical reaction rates. In the described case, a weed cultivation site was located in the attic. Although the blood stains were found on other floors, a higher temperature may have accelerated the aging process. However, even at a temperature of 40 degrees Celsius the amount of HbO₂ found upstairs was not yet reached after two weeks in our reference database⁵⁶, supporting the statement that the blood stains found upstairs were created at an earlier moment than the blood stains downstairs.

In the described case, it would have been interesting to know which person was shot first and what the time difference was between the shots. In a laboratory setup, the age of blood stains can be determined with an accuracy of 1 hour within the first day after bleeding⁶⁸. If our measurements would have been performed immediately after discovery of the crime scene, it may have been possible to indicate the sequence of different blood stain patterns created near the victims (different blood stains found downstairs). The chemical reactions taking place in the blood stains are rapid in the beginning, but slower in a later stage⁵⁶. As a result, the accuracy of age estimations decreases with the age of the blood stain. Thus, to culminate small age intervals, it is recommended to perform spectroscopic measurements as soon as possible.

If early measurements are not possible, stains may be collected from the scene and stored deep-frozen to slow down or even stop any further chemical reactions taking place before the analysis is performed. Ideally, stains are collected and frozen on their original background. Traditional collection of blood stains with moistened cotton swabs will alter their chemical composition, as the addition of water to a blood stain is known to induce the transition from HC back to MetHb¹⁰⁹. Further research is needed to find a collection procedure which does not influence the results of the age estimation.

As visible in Figure 5.7, the equipment used in this case was not dedicated for forensic practice. When used at the crime scene, equipment ideally is portable, wireless, easily decontaminated and user-friendly. Instead of

a fibre-optic probe spectroscopy setup, a hyperspectral imaging system may be used to perform measurements remotely, as in **Chapter 4**⁴⁹. An additional benefit of hyperspectral imaging is that the reflectance spectra of multiple blood stains can be recorded simultaneously, which makes the measurements more time-effective, while the spatial distribution of the stains in the scene is registered at the same time. Recent technological advances enable the development of wireless hyperspectral imaging systems which can easily be deployed at the crime scene.

In conclusion, we demonstrated a light transport model to for the age estimation of blood stains on coloured backgrounds, and a statistical model to calculate a 95% confidence interval. The practical applicability of the technique was demonstrated in a recent forensic case. When adopted in daily forensic practice, this innovative technique can add valuable information about the moment of a crime and the sequence of events.

6 - VISUALIZATION OF LATENT BLOOD STAINS USING VISIBLE REFLECTANCE HYPERSPECTRAL IMAGING AND CHEMOMETRICS

Accepted for publication by Journal of Forensic Sciences.

The detection of latent traces is an important aspect of crime scene investigations. Blood stains on black backgrounds can be visualized using chemiluminescence, which is invasive and requires a darkened room, or near infrared photography, for which investigators need to change filters manually to optimize contrast. We demonstrated the performance of visible reflectance hyperspectral imaging (400-720 nm) for this purpose. Several processing methods were evaluated: single wavelength bands, ratio images, Principal Component Analysis (PCA) and “SIMPLe-to-use Interactive Self-modeling Mixture Analysis” (SIMPLISMA). Using these methods, we were able to enhance the contrast between blood stains and 12 different fabrics. On black cotton, blood dilutions were visible with a minimal concentration of 25% of whole blood. The hyperspectral camera system used in this study is portable and wireless, which makes it suitable for crime scene use. The described technique is non-contact and non-destructive, so all traces are preserved for further analysis.

6.1. INTRODUCTION

The visualization of latent blood stains is of paramount importance for crime scene investigators. Because the human ability to visually detect traces is limited, various techniques are developed which enhance the contrast between blood stains and their backgrounds, using the intrinsic properties of blood stains or exogenous dyes. Several chemical reagents can be sprayed onto the blood stains to induce luminescence, e.g. luminol, bluestar or fluorescein¹¹⁰. Drawbacks of these methods are that a completely dark environment is needed to visualize the luminescence and that photographs have to be taken quickly. For the visualization of blood stains on dark backgrounds, the feasibility to use both analogue^{111, 112} and digital¹¹³ near infrared photography were successfully explored, both involving the use of several filters which have to be changed manually.

To overcome this problem, Schuler, Kish and Plese¹¹⁴ recently introduced near infrared hyperspectral imaging for the non-destructive detection of blood stains on dark backgrounds. Hyperspectral cameras automatically record the back scattered light of many narrow wavelength bands, resulting in a data set with monochrome images for each wavelength. They demonstrated that the contrast between blood stains and 3 black fabrics could be enhanced using hyperspectral imaging systems operating in the wavelength ranges from 650-1100 nm and from 960-1650 nm. We explored the performance of a visible reflectance hyperspectral imaging system operating in the wavelength range 400-720 nm to visualize blood stains on 12 different black fabrics. We developed a low-cost, portable and wireless systems, which can be transported to the crime scene to record large samples or even the entire crime scene.

Using hyperspectral imaging latent blood stains can be distinguished from their background based on spectral differences. Several processing methods can be used to increase the contrast between the blood stains and backgrounds. The easiest way to search for latent blood stains is by viewing all separate images individually or by selecting one wavelength based on prior knowledge of absorption spectra of the blood stain *and* its background. To

enhance spectral differences that are difficult to detect in individual images, a ratio of two wavelengths can be calculated. Ratio images may suppress the effect of variable illumination and topographic variations and may provide information not available in any of the single wavelengths. To make use of all subtle information present in the dataset, advanced chemometrical techniques can be used, e.g. Principal Component Analysis (PCA)¹¹⁵ or “SIMPLISMA-to-use Interactive Self-modeling Mixture Analysis” (SIMPLISMA)¹¹⁶. PCA converts the original wavelength bands into new variables, called principal components (PC), which are linear combinations of the original wavelength bands¹¹⁵. Each new PC will account for most of the variance in the observed wavelengths. Because blood stains and their backgrounds are spectrally different, it is expected that the first two PCs will emphasize the contrast. The SIMPLISMA algorithm searches pixels with a spectral contribution from one pure component, which are assumed to be present in the hyperspectral datacube¹¹⁶. Division of the hypercube by the pure spectra of the separate components gives the concentration profiles of these components. In a hyperspectral image showing a blood stain on a substrate, the concentration profiles of the first two pure components are expected to show the distribution of the blood and the substrate respectively. In this chapter, the above described processing methods are evaluated and the contrast in the resulting images is compared.

6.2. MATERIALS AND METHOD

6.2.a SAMPLES

For this study, three sample sets were created:

Fabrics) 12 different black fabrics with blood stains. The materials of the fabrics are listed in Table 6.1. All fabrics used were cut from second hand clothing, worn and washed regularly prior to application of the blood. The size of the samples was approximately 2 cm by 2 cm. On each fabric, one drop of blood was deposited directly from the fingertip.

Blood dilutions) A dilution series of freshly drawn blood stains in water, of which 1 ml was deposited on black cotton. Concentrations used were 100%, 50%, 25%, 12.5% and 0% of blood.

T-shirt) A cotton T-shirt with a spatter pattern of whole blood and several random blood dilutions.

All blood stains were left to dry and aged for one week prior to the hyperspectral imaging.

Table 6.1. List of materials of the 12 different fabrics.

Sample	Material	Sample	Material
1	100% polyester	7	90% polyamide, 10% elasthan
2	85% polyamide, 15% elasthan	8	65% polyester, 32% viscose, 3% elasthan
3	100% Merino wool	9	92% nylon, 8% elasthan
4	100% cotton	10	70% acryl, 30% wool
5	97% cotton, 3% lycra	11	100% polyester
6	100% nylon	12	55% polyester, 45% new wool

6.2.b HYPERSPECTRAL IMAGING

Hyperspectral images of all samples were recorded using a combination of a monochromatic CCD camera (Pixelfly vga; PCO; Kelheim, Germany), a 50 mm c-mount lens, and a liquid crystal tuneable filter (VariSpec VIS, 7 nanometre resolution; CRi; Woburn, USA) in the wavelength range from 400 to 720 nm, with a step size of 1 nm. The exposure time per wavelength was set to 40 ms, which resulted in a total scanning time of less than 15 seconds. All components are built into a wireless hyperspectral imaging system with a built-in acquisition board and computer (see Figure 6.1). Exposure time, focus, and wavelength range, were adjusted on the touch screen of the system. An in

house developed ring of white, blue and cyan LED's and an external halogen light source were used for illumination.



Figure 6.1. Custom made wireless hyperspectral imaging system, consisting of a liquid crystal tuneable filter, a CCD camera, a lens, a built-in acquisition board, computer, a battery, and a touch screen. A single wavelength band is shown on the live view of the camera.

Hyperspectral images are analogous to a stack of images, each acquired at a narrow spectral band. The resulting data set is a three-dimensional block of data, the so-called hypercube described in **Chapter 2**, with two spatial (x,y) dimensions and one wavelength (λ) dimension¹¹⁷. This hypercube provides images for each wavelength (λ_i) and a spectrum can be obtained from each individual pixel (x_i,y_i), as depicted in Figure 6.2.

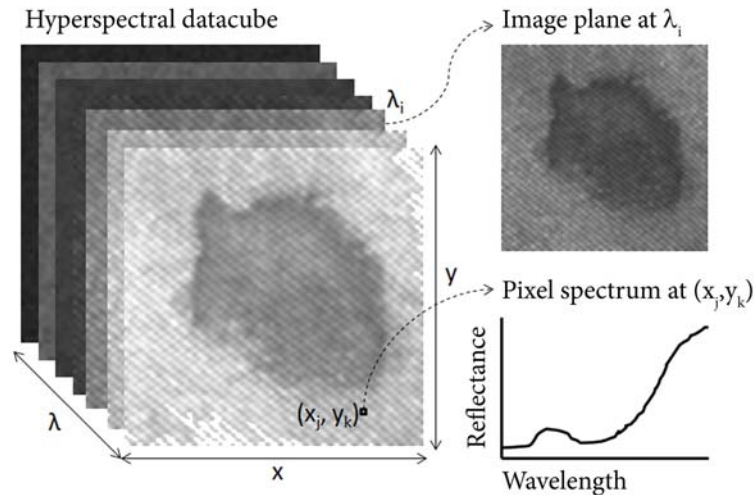


Figure 6.2. Hypercube of a blood stain on black fabric, with two spatial (x,y) and one wavelength (λ) dimension. From the hypercube an image plane is shown for one wavelength (λ_i) and a spectrum is obtained from one pixel (x_j,y_k).

6.2.c DATA ANALYSIS

Four different processing methods were used for the visualization of the blood stains on black fabrics and compared based on Fisher's ratio, a measure for the discriminating power between two groups¹¹⁸. To calculate Fisher's ratio, a region of interest containing the blood stain was selected manually. Less concentrated parts of the blood stain were included in this region. For each blood stain we compared four data analysis methods, based on the same regions of interest, as described below. The number of pixels used differed from stain to stain.

Band) A single wavelength band was chosen from the datacube. To visually find the wavelength with the highest contrast between the blood stain and the background, each wavelength can be viewed separately. However, as the amount of wavelengths is high in hyperspectral images (321 in our study) this method is time consuming. To reduce the amount of work and to increase the objectivity, we decided to use Fisher's ratio to find the optimal wavelength, which is only possible if the location of the blood stain is known a priori.

Ratio) A ratio image was calculated between two wavelength bands. When n is the total amount of wavelengths there are $(n^2-n)/2$ unique combinations of wavelengths, which leads to a substantial amount of possible ratios (51360 in our study). Again, Fisher's ratio was used to select the optimal combination of wavelengths to distinguish the blood stain from its background.

PCA) A scores image of one principle component (PC) was chosen. Although the number of PCs can maximally reach the number of wavelengths n (321 in this study), PCA is defined such that the first PC describes the highest possible variance in the data and each succeeding component in turn describes the highest variance possible. For a hyperspectral image of a blood stain and a background, the highest variance is expected to result from the different chemical compositions of the two components. As a consequence, the first PCs are expected to show this variance. Taking into account that inhomogeneous lighting conditions or textures can also cause some variance, we expect that the first 4 PCs are sufficient for the visualization of blood stains. Fisher's ratio was again used to select the optimal PC.

SIMPLISMA) A concentration distribution image of one pure component was chosen. This pure spectrum was based on Windig's discovery that the ratio of the standard deviation to the mean for the same variable correlates to the purity of the variable¹¹⁶. Because the goal was to create contrast between blood and the background, the algorithm was used to find 2 pure spectra and the corresponding concentration images. From these 2 images, the best one was chosen based on Fisher's ratio.

All results are depicted in grayscale images, with data stretching over the dynamic range. As a result of the different processing methods used, blood stains were sometimes shown as a dark stain on a light background, in other cases as a light stain on a dark background. For the ease of visual comparison, all images showing a light stain on a dark background were inverted. No further image processing or contrast enhancement was applied.

All data analysis was performed using custom-made scripts written in MATLAB (The Mathworks Inc., Natick, Massachusetts, USA). The SIMPLISMA algorithm was made available by Jaumot et al¹¹⁹.

6.3. RESULTS

Fabrics) White light photographs of all samples on the 12 different fabrics are shown in Figure 6.3. Although the blood stains are visible on some of the fabrics, the contrast is poor. Figure 6.3 also shows the results of hyperspectral imaging with the different processing methods. All these methods improved the contrast between the blood stains and the background.

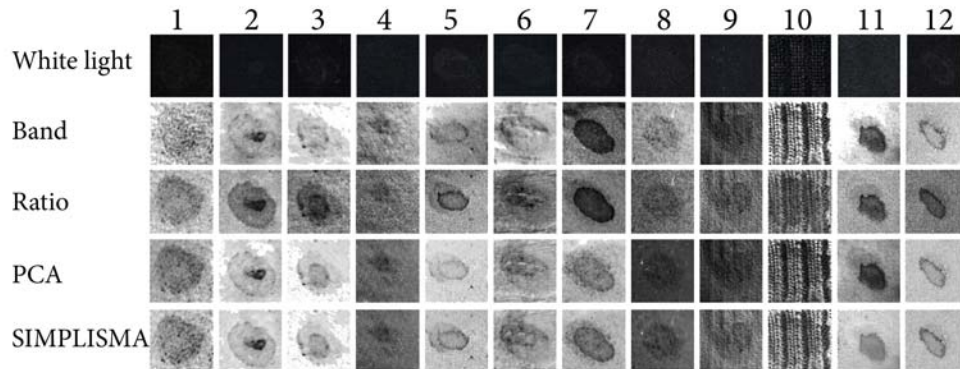


Figure 6.3. White light photographs of all samples on the 12 different fabrics and the results of the different hyperspectral imaging methods: band images, ratio images, PCA images and SIMPLISMA images.

Table 6.2. Fisher's ratios calculated for the different methods (band, ratio, PCA, SIMPLISMA) and the different fabrics (1-12). The highest value for each fabric is printed in bold script.

	1	2	3	4	5	6	7	8	9	10	11	12
Band	0.22	0.59	1.44	1.01	0.45	0.68	1.65	0.72	0.24	0.21	4.38	0.86
Ratio	2.49	2.68	1.91	0.47	1.67	1.02	8.03	0.39	0.36	0.30	5.05	2.31
PCA	2.76	0.95	1.74	0.81	1.38	1.28	2.79	0.47	0.23	0.17	3.73	1.65
SIMPLISMA	1.78	1.23	1.92	0.68	1.92	1.47	5.30	1.00	0.32	0.24	3.27	2.31

Table 6.2 lists Fisher's ratios for each method and each fabric, which is an objective measure to compare the contrast between the blood stains and the backgrounds. This shows that ratio images gave the best result for 6 fabrics,

SIMPLISMA for 5 fabrics and both single wavelength bands and PCA for 1 fabric.

Table 6.3 shows which wavelength, which combination of wavelengths, which principal component, or which concentration image gave the best result for the different methods respectively. The results show that for both the single wavelength band images and the ratio images the chosen wavelengths highly depend on the fabric. Even for similar materials (4-5, 2-7, and 1-11) the wavelengths are different, which implies that the dyes used for blackening are of influence. When PCA was used, PC 2 shows the best contrast in 9 cases, and PC 1 in the other 3 cases, which demonstrates that it is sufficient to use only 2 PC's. The same results were found when SIMPLISMA was used. In that case, we only calculated the concentration images of 2 pure spectra.

Table 6.3. Selected wavelength bands or components resulting in the highest Fisher ratios for the different methods (band, ratio, PCA, SIMPLISMA) and the different fabrics (1-12).

	1	2	3	4	5	6	7	8	9	10	11	12
Band	666	597	611	590	597	610	720	610	719	720	718	598
Ratio	678	646	416	424	665	634	674	411	574	607	662	663
	720	686	636	612	689	720	720	635	720	720	691	703
PCA	2	2	2	2	2	2	2	2	1	1	1	2
SIMPLISMA	2	2	2	2	2	2	2	2	1	1	1	2

Dilutions) Figure 6.4 shows white light photographs and the results of the different hyperspectral image analysis methods for all blood dilutions. Table 6.4 lists the corresponding Fisher ratios. Although the Fisher ratio increased with concentration, blood stains with a minimal concentration of 25% could be observed. For all these blood stains, SIMPLISMA had the best performance.

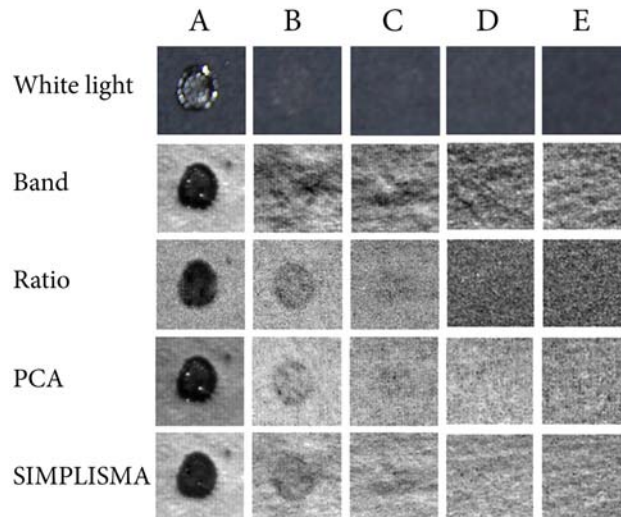


Figure 6.4. White light photographs of all blood dilutions (A: 100%, B: 50%, C: 25%, D: 12.5%, E: 0%) and the results of the different hyperspectral imaging methods: band images, ratio images, PCA images and SIMPLISMA images.

Table 6.4. Fisher ratios calculated for the different methods (band, ratio, PCA, SIMPLISMA) and the different blood dilutions (A-E). The highest value for each fabric is printed in bold script. Because no contrast was observed in dilution D and E, no Fisher ratio could be calculated.

	A	B	C	D	E
Band	12.21	0.26	0.05		
Ratio	8.11	0.85	0.10		
PCA	9.15	1.15	0.06		
SIMPLISMA	16.74	1.42	0.13		

T-shirt) A white light photograph of the black cotton T-shirt with diluted and pure blood stains is shown in Figure 6.5. Although several blood stains are visible, the contrast with the background is poor. Figure 6.5 demonstrates that this contrast can be enhanced using hyperspectral imaging and several processing methods. No Fisher ratios were calculated, because this requires selection of all blood stains. Optimal wavelengths for band and ratio images were chosen based on the results of the dilution series. Because both

PCA and SIMPLISMA will be disturbed when more than two components are present, prior to analysis the T-shirt was selected manually to separate it from the environment.

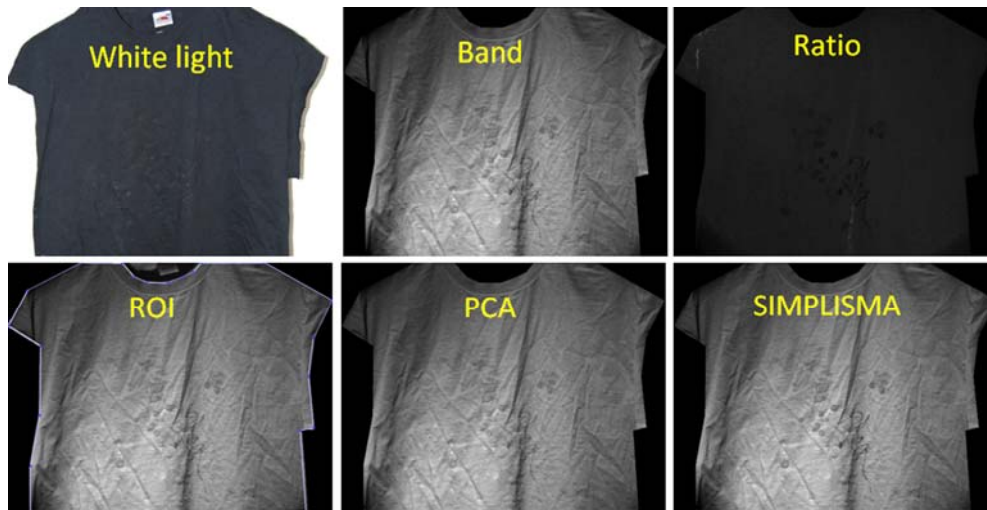


Figure 6.5. White light photograph of black cotton T-shirt with diluted and pure blood stains, the selected region of interest (ROI) and the resulting band, ratio, PCA and SIMPLISMA images. In the ratio image, the contrast was enhanced manually by adjusting the scale of the colour bar.

Visually, the resulting band, PCA and SIMPLISMA images are similar. The ratio image created with an automatic dynamic range showed several white pixels with an infinite pixel value, caused by black pixels in the original wavelength band through which was divided. Because these infinite pixel values influenced the automatic scaling of the greyscale values, the scale of the colourbar was manually adapted. After this manual scaling, a very high contrast between the blood stains and the T-shirt was observed (Figure 6.5). Most features caused by shadows and folds disappeared in this image.

6.4. DISCUSSION AND CONCLUSION

We demonstrated the capability of a visible reflectance hyperspectral imaging system (400-720 nm) to visualize blood stains on black backgrounds. Using this system, combined with several processing methods, we were able to enhance the contrast between blood stains and 12 different fabrics. On black cotton, blood dilutions were visible with a minimal concentration of 25%. The custom-made hyperspectral imaging system used in this study is portable and wireless, can be transported to the crime scene to record large samples or even the entire crime scene. Because this technique is non-contact and non-destructive, all traces are preserved for further analysis.

The four processing methods evaluated in this study all enhance the contrast between blood stains and black backgrounds compared to white light photography. Single wavelength bands are easily depicted in the live view of the camera, because no processing is needed. Using this live view, investigators can search for latent blood stains at the crime scene. The optimal wavelength depends on the spectral properties of the blood stains and the background. There may also be a variability between different stains on the same background, which was not tested in this study. Prior knowledge about the absorption properties can be used to choose a wavelength, or a full wavelength sweep can be viewed. Ratio images highly improve the contrast, as texture and lighting inhomogeneities are reduced. However, there are many possible combinations of wavelengths to create ratio images. To find the optimal combination, knowledge about the location of the blood stain is needed. PCA and SIMPLISMA are both unsupervised processing methods, which make more use of the spectral data. Although SIMPLISMA outperforms PCA, it is computationally intensive.

In their preliminary observations Schuler et al showed similar results using two hyperspectral imaging systems which perform in the near infrared wavelength range (650-1100 nm and 950-1650 nm). Although the absorption of blood is higher in the visible range than in the near infrared^{1, 19, 82}, on several backgrounds it may be impossible to find a contrast in the visible wavelength range, motivating the use of more expensive near infrared hyperspectral

imaging systems. Apart from blood stains, other latent traces may become visible using hyperspectral imaging and the processing methods described. It may be possible to discriminate blood stains from other substances based on their absorption properties, but this identification task is expected to be hampered by dark backgrounds, because of the dominant light absorption of the background. Instead of the visible wavelength range, near infrared wavelengths can be used for this task (**Chapter 7**).

In conclusion, visible hyperspectral imaging is useful for the visualization of blood stains on black backgrounds. Several processing methods enhance the contrast compared to white light photographs. To search for latent blood stains, a single wavelength band can be shown on the live view of the camera. Afterwards, ratio images, PCA or SIMPLISMA can be used to enhance the contrast.

7 - IDENTIFICATION AND AGE ESTIMATION OF BLOOD STAINS ON COLOURED BACKGROUNDS BY NEAR INFRARED SPECTROSCOPY

Forensic Science International 2012;220(1-3):239-44.

Non-destructive identification and subsequent age estimation of blood stains are significant steps in forensic casework. The latter can provide important information on the temporal aspects of a crime. As previously shown, visible spectroscopy of blood stains on white backgrounds can successfully be used for their identification and age estimation. The use of this technique however, is hampered by dark backgrounds. In the present study the feasibility to use near infrared (NIR) spectroscopy was evaluated for blood stain identification and age estimation on dark backgrounds. Using NIR reflectance spectroscopy, blood stains were distinguished from other substances with 100% sensitivity and 100% specificity. In addition, Partial Least Squares Regression analysis was applied to estimate the age of blood stains on coloured backgrounds. The age of blood stains up to 1 month old was estimated successfully with a root mean squared error of prediction of 8.9%. These findings are an important step toward the practical implementation of blood stain identification and age estimation in forensic casework, where a large variety of backgrounds can be encountered.

7.1. INTRODUCTION

Blood stains are important traces in many forensic investigations. After detection of a stain at the crime scene, a technique for blood stain identification is required to prove the presence of blood in the stain. Identified blood stains can subsequently be used for other purposes, like pattern reconstruction and DNA analysis. Most presumptive blood identification tests use chemicals which, in contact with blood, change colour⁷⁹, fluoresce¹²⁰ or luminesce¹²¹. However, these chemicals can lead to a loss of the blood stain patterns¹²¹, may interfere with subsequent tests, e.g. confirmative identification tests, species tests or DNA analysis¹²² and may be harmful for the investigators. There is a need for confirmatory, non-destructive methods which can be used to identify blood stains at the crime scene without the need of sampling and subsequent lengthy laboratory testing¹²³. In **Chapter 3** we⁶⁵ successfully applied reflectance spectroscopy for the non-destructive identification of blood stains. In the described study, blood stains were distinguished from other blood resembling substances (e.g. ketchup, red wine, lip gloss) deposited on white cotton. However, when blood stains are deposited on dark backgrounds, the identification of blood stains using visible reflectance spectroscopy is severely hampered by the absorption of visible light by the background. Because near infrared (NIR) light is absorbed less efficiently by many dark coloured substrates, NIR reflectance spectroscopy may solve this problem. Absorptions that occur in the NIR region of the electromagnetic spectrum (720-2500 nm) are due to the overtone and combination bands of molecular stretching and bending vibrations of the fundamental absorptions of –CH, –NH, and –OH groups^{124, 125}. As a result, NIR spectroscopy provides more information about the chemical structure of samples compared to visible spectroscopy, and is expected to be useful for identification purposes.

After a positive identification of blood stains, it is of interest to estimate the time of bleeding, which may help crime scene investigators to determine the temporal aspects of a crime. Several techniques, including high performance liquid chromatography¹²⁶, electron paramagnetic resonance^{89, 90}, atomic force microscopy¹²⁷ and RNA degradation measurements^{128, 129} have

been investigated for this purpose, as reviewed by Bremmer et al⁹⁴. However, none of these methods is yet implemented in forensic practice, and most require sample preparation and need to be performed in a laboratory. Just like identification, blood stain age estimation can be performed non-destructively using visible reflectance spectroscopy^{1, 68}. When blood exits the human body, oxyhaemoglobin auto-oxidizes into methaemoglobin, which in turn denatures into hemichrome¹. These reactions cause a colour change from red to brown. Visible (Vis) reflectance spectroscopy can be used to measure this colour change quantitatively, determine the chemical components and thereby estimate the age of blood stains (**Chapter 4,5**)¹. Botonjic-Sehic et al⁶⁶ explored the potential of using the NIR region for the age estimation of blood stains. They demonstrated that spectral changes in a broad wavelength band from 1460-1860 nm were useful to estimate the age of a blood stain on glass and on gauze.

In this study we investigated the use of NIR spectroscopy for the identification and age estimation of blood stains on coloured backgrounds. We therefore first inspected typical features in NIR reflectance spectra of aging blood stains and compared these qualitatively to literature spectra of different components of human blood. Next, we studied the sensitivity and specificity to distinguish blood from non-blood stains using NIR reflectance spectroscopy and subsequent analysis. Finally, we explored the use of NIR reflectance spectra to estimate the age of blood stains on coloured cotton backgrounds. For this task Partial Least Squares (PLS) Regression models were created. The accuracy of the age estimation models was evaluated.

7.2. MATERIALS AND METHOD

7.2.a SAMPLES

Pure blood

To characterize the spectral features of blood, initial measurements were performed on a single blood drop from a healthy male volunteer (volunteer #1) deposited directly onto a sample holder, without a substrate.

Samples on cotton

In forensic practice blood stains are always deposited on a substrate. Therefore, both blood and non blood samples were deposited on cotton backgrounds. To analyze the influence of coloured backgrounds, cotton with 5 different colours was used. This led to the following sample sets:

- Blood on white cotton) 3 blood stains, drawn from a healthy female volunteer (volunteer #2). Next to this, a plain cotton reference sample was created (see Figure 7.1). Reflectance spectra of these samples were measured repeatedly for 77 days (with varying frequencies of every 2 hours in the beginning up to monthly in the end, 54 measurements in total).
- Blood on coloured cotton) Blood from a healthy female volunteer (volunteer #3) was deposited on black, red, green and blue cotton (3 blood stains each). Next to this, plain cotton reference samples were created (see Figure 7.1). Reflectance spectra of these samples were measured repeatedly up to the age of 28 days (66 measurements in total).



Figure 7.1. Photographs of blood stains on white, black, red, green and blue cotton and corresponding plain reference samples (bottom row).

- Non blood on white cotton) 30 different samples of non-blood substances (specified in Figure 7.2). These samples were selected because they are likely to be false positives when using luminol (bleach) or visible spectroscopy (all other substances) for the detection of blood stains. Measurements on all non-blood substances were repeated after one week.



Figure 7.2. Photographs of non-blood samples containing: 1.tea, 2.coffee, 3.red wine, 4.red grape juice, 5.black currant soda ('cassis'), 6.coke, 7.cherry coke, 8.red berry juice, 9.tomato juice, 10.ketchup, 11.curry, 12.Tabasco, 13.ketjap manis, 14.Worstershire sauce, 15.soy sauce, 16.balsamic, 17.Maggi aroma, 18.red wine, 19.cherry marmalade, 20.forest fruit marmalade, 21.apple syrup, 22.chocolate sauce, 23.red cabbage, 24.red beet, 25.bleach, 26.lipstick, 27.lipstick, 28.lipstick, 29.red food colourant, 30.red food colourant.

7.2.b NIR SPECTROSCOPY

Pure blood

Using a Fourier transform near infrared spectrometer (Bruker, MPA-NIR-FT type), the NIR reflectance spectra (800-2778 nm) of the pure blood stain was measured repeatedly (every 5 min for the first 5 hours, thereafter hourly until the age of 4 days, 240 measurements in total).

Samples on cotton

Vis-NIR reflectance spectra of all samples on cotton and the reference substrates were measured using a FOSS NIR systems 6500 spectrophotometer (400-2500 nm). Samples had a diameter of approximately 3 cm, and were contained in glass covered sample holders. 32 scans from different positions on the sample were averaged to obtain an average spectrum. In between measurements, samples were stored in a laboratory at room temperature (≈ 22 °C).

7.2.c PRE-PROCESSING

All measured reflectance spectra were transformed to apparent absorbance spectra ($\log(1/R)$, where R is the reflectance). Next, all absorbance spectra of samples deposited on cotton were corrected for background absorption by subtracting the absorbance spectrum of the reference sample of the same colour. All data analysis was performed using custom-made scripts written in MATLAB (The Mathworks Inc., Natick, Massachusetts, USA).

7.3. DATA ANALYSIS

7.3.a BLOOD STAIN CHARACTERIZATION

To characterize the absorbance spectra of pure blood, the absorbance maxima were compared to reference absorption maxima (see Table 7.1) of the following blood components: oxyhaemoglobin, methaemoglobin, albumin, globulin, triglycerides, glucose, cholesterol, and urea. Reference spectra of fibrinogen were not found, as research is often done on serum, which does not contain fibrinogen. Other components, normally present in lower concentrations in blood, were not taken into account¹³⁰.

7.3.b WAVELENGTH SELECTION

When analyzing blood stains on cotton, the absorbance spectra are influenced by the background. Therefore we corrected these spectra for background absorptions. However, when the absorption of the background is high, the background dominates the spectra and spectral features of the blood stains become negligible. In these cases, the background correction is not optimal and blood stain identification and age estimation will be hampered. To analyze the influence of background absorptions on the corrected spectra, the absorbance spectra of the differently coloured reference backgrounds were compared and Pearson's correlation coefficient between the different backgrounds was calculated. Based on this, a wavelength region was selected in which the colour of the cotton apparently did not influence the spectra. This wavelength region was used for the subsequent identification and age estimation tasks.

7.3.c IDENTIFICATION

For the identification of blood stains on coloured cotton, we used a comparison library and a test set. The comparison library consisted of 3 absorbance spectra of blood stains on white cotton with an age of 1 day, 1 week and 1 month. All other absorbance spectra of blood stains on white, black, red, green and blue cotton (315 in total) formed the test set. Of all spectra, the wavelength region determined above was selected. Spectra of the blood stains from the test set were compared to the library using the coefficient of determination (R^2). R^2 values were calculated between all spectra from the library and the test set. For each sample from the test set, the maximum R^2 value was plotted in a box plot. Spectra of all blood stains were expected to be similar to the spectra from the library, which means the R^2 values were expected to approach 1.

Similarly, R^2 values were calculated between all spectra from the library and the non blood samples on white cotton. Again, the maximum R^2 value was plotted in a box plot. For these non blood samples, lower values were

expected. If all R^2 values for non blood samples were lower than the R^2 values for blood samples, blood stains could be identified based on the coefficient of determination.

7.3.d AGE ESTIMATION

To estimate the age of blood stains on coloured backgrounds PLS regression analysis was applied, using the wavelength region selected above. PLS is a useful statistical tool for the analysis of spectroscopic data, as it can handle datasets with more variables than observations, and the data may contain highly correlated predictor variables¹³¹. PLS makes linear combinations of the original predictor variables to construct new predictor variables, which are the most relevant for estimating the age.

A PLS model was created for each coloured background. Each time, the data was split into a training set and an independent test set. The training set consisted of the absorbance spectra of blood stains on four colours, not including the questioned colour. The test set consisted of absorbance spectra of blood stains on the background colour in question, and was used to predict the ages of blood stains. To evaluate the performance of these predictions, the coefficient of determination R^2 and the root mean squared error of prediction (RMSEP) were calculated for each background.

7.4. RESULTS

7.4.a BLOOD STAIN CHARACTERIZATION

Fourier transform NIR spectroscopy on a pure blood stain showed the temporal spectral changes in the first days of aging. In the first minutes, the spectrum was dominated by water absorption peaks at 1454 and 1940 nm, indicated by the blue lines in Figure 7.3.

After drying (in air at room temperature, for approximately 10 min), several peaks appeared which have been reported in literature as absorption peaks of haemoglobin, albumin, and globulin (see Figure 7.3 and Table 7.1). The slope of the spectrum near the peaks at 1690 and 1740 nm changed in

time. These peaks are also reported in spectra of glucose, but other glucose absorption peaks (around 2120 and 2260 nm)¹³²⁻¹³⁴ were not visible in the blood spectra. Absorption peaks of cholesterol (around 1472, 1718, 1750, 2076, and 2310 nm)^{134, 135}, urea (around 2200 nm)^{134, 136} and triglyceride (around 1725 and 2130 nm)¹³⁷ were not visible.

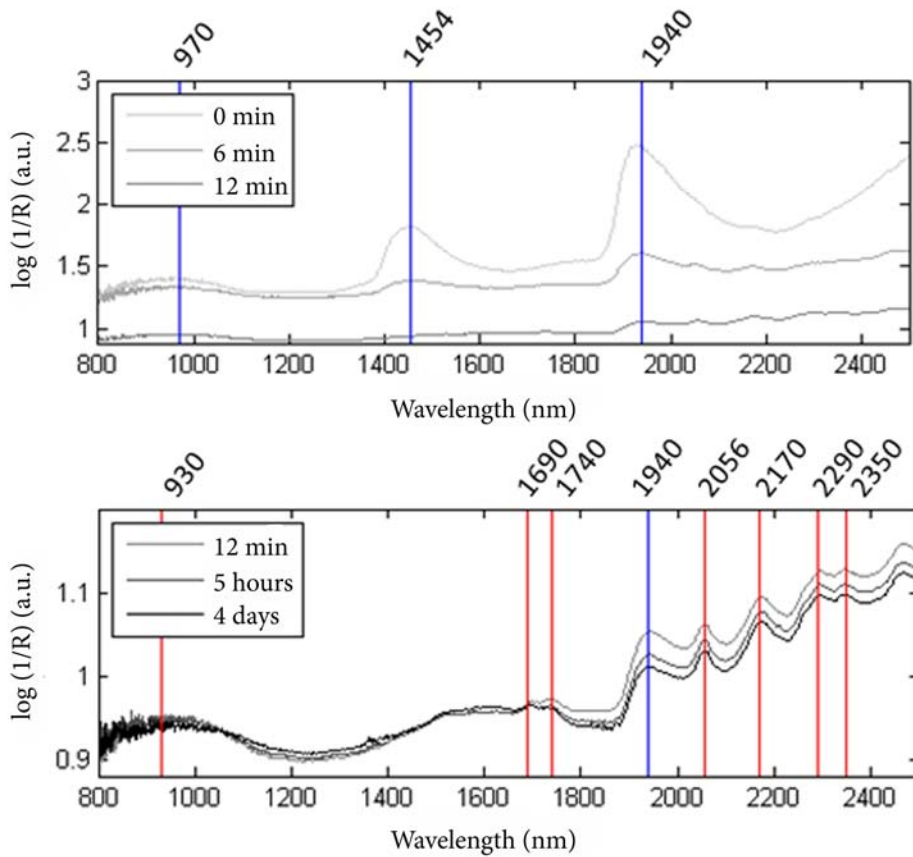


Figure 7.3. Log (1/R) spectra of a wet blood stain of 0, 6 and 12 min old (top) and spectra of the same blood stain after drying with an age of 12 min, 5 hours and 4 days (bottom). Units are arbitrary (a.u.). Lines in the figure show the position of absorption peaks listed in Table 7.1, blue lines referring to water peaks, red lines to peaks from other components present in blood.

Table 7.1. List of absorption peaks of several blood components as reported in literature, which were observed in the spectra in Figure 7.3. Positions of these peaks are depicted in Figure 7.3. Possible chemical origins of the peaks are mentioned, next to the bonds found in the references listed.

Wavelength (nm)	Component	Bond	References
930	Oxyhaemoglobin	Third overtone of –CH and –CH ₂ stretching vibrations	138, 139
970	Water	Combination of H-O-H symmetric and asymmetric stretching vibrations	124, 140, 141
1454	Water	Combination of H-O-H symmetric and asymmetric stretching vibrations	124, 138, 140, 141
1690	Haemoglobin, Albumin, Globulin	First overtone of –CH stretching vibration	132, 133, 136, 138, 142, 143, 143, 143-145
1740	Haemoglobin, Albumin, Globulin	First overtone of band at 3477 nm	132, 133, 136, 138, 142, 143, 143, 143-145
1940	Water	Combination of H-O-H bending and asymmetric stretching vibrations	124, 138, 140-142
2056	Haemoglobin, Albumin, Globulin	Combination of amide A and amide II or another combination	125, 133, 138, 142-144
2170	Haemoglobin, Albumin, Globulin	Combination of amide B and amide II or overtone of amide II	125, 133, 138, 142-144
2290	Haemoglobin, Albumin, Globulin	–CH stretching and deformation combinations	125, 133, 138, 142-144
2350	Haemoglobin, Albumin, Globulin	–CH stretching and deformation combinations	125, 133, 138, 142-144

7.4.b WAVELENGTH SELECTION

Absorbance spectra of the differently coloured cotton reference samples are shown in Figure 7.4. This figure shows that coloured cotton backgrounds absorbed highly in the visible region, whereas white cotton absorbed almost no light in this region. For wavelengths over 1150 nm, however, the absorbance spectra of different colours almost overlapped, showing typical features of cotton¹⁴⁶, which was confirmed by a correlation analysis. Pearson's correlation coefficient between the different background spectra from 1150 -2500 nm exceeded 0.999. Therefore, this region was selected for subsequent analyses.

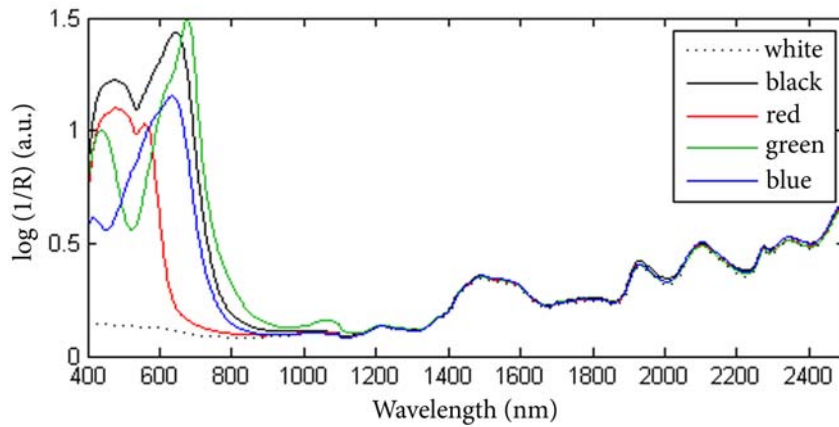


Figure 7.4. Log (1/R) spectra of white, black, red, green and blue cotton backgrounds. This shows that white cotton absorbed almost no light in the visible region, while coloured backgrounds absorbed highly in this region. For wavelengths larger than 1150 nm however, the spectra of different colours almost overlapped.

7.4.c IDENTIFICATION

Example absorbance spectra of blood and non blood spectra on white cotton are shown in Figure 7.5.

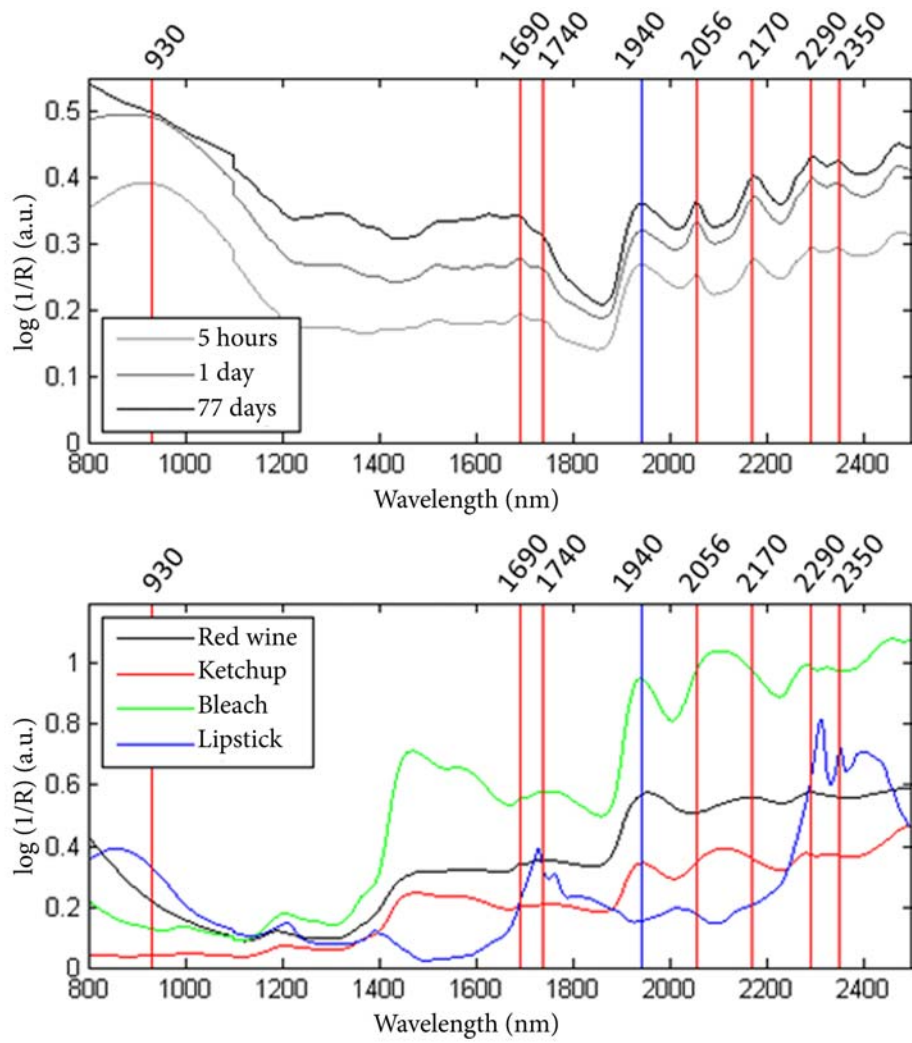


Figure 7.5. Apart from the water peak at 1940 nm, the spectra of non blood stains (lower panel of Figure 7.5) clearly differed from the blood spectra.

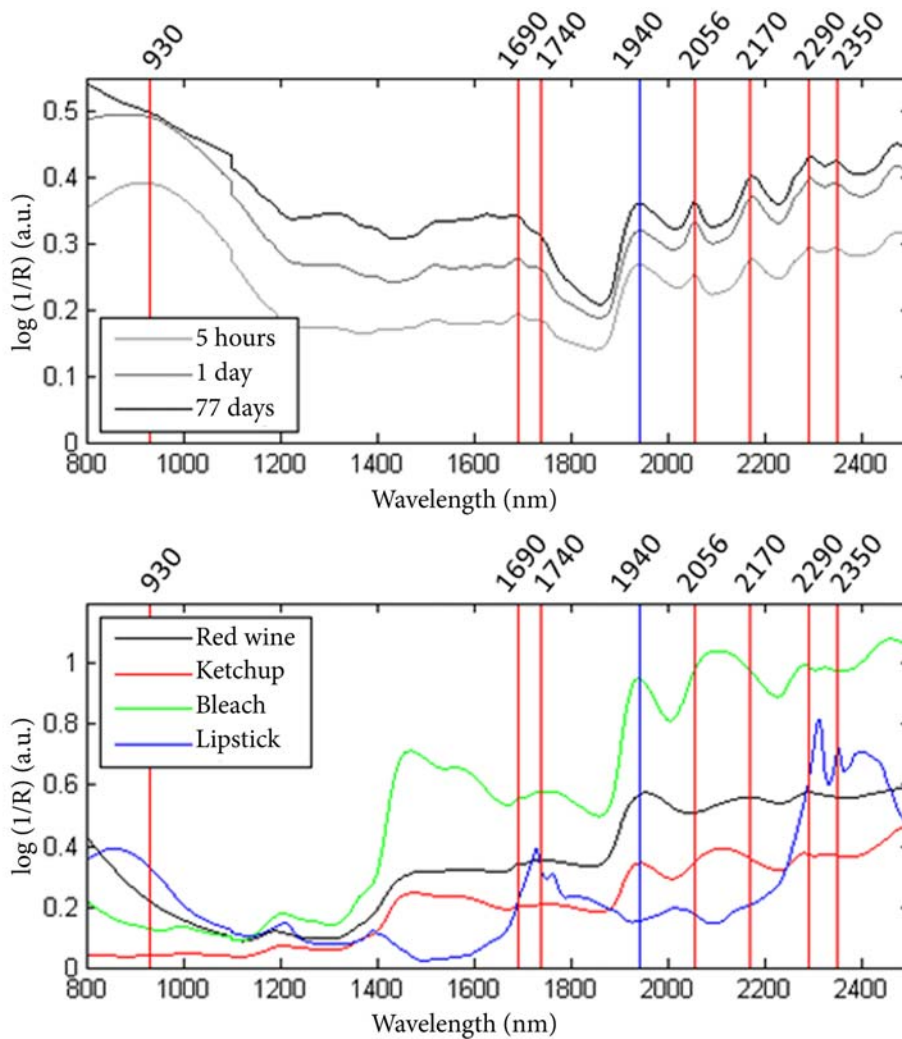


Figure 7.5. Background corrected $\log(1/R)$ spectra of dry blood stains on cotton of 5 hours, 1 day and 77 days old (top) and of 2 days old samples of red wine, ketchup, bleach and lipstick (bottom). Vertical lines in the figure show the position of absorption peaks listed in Table 7.1.

R^2 values between the absorbance spectra of blood stains in the library and spectra from other blood stains on the one hand and spectra from non blood samples on the other hand are depicted by the box plots of Figure 7.6.

This figure shows that a threshold could be chosen which separates all blood stains from all non blood samples, e.g. if a threshold of $R^2=0.8$ was used to identify blood stains, this resulted in 0 false positives and 0 false negatives. This means blood stains could be identified with a sensitivity of 100% and a specificity of 100%.

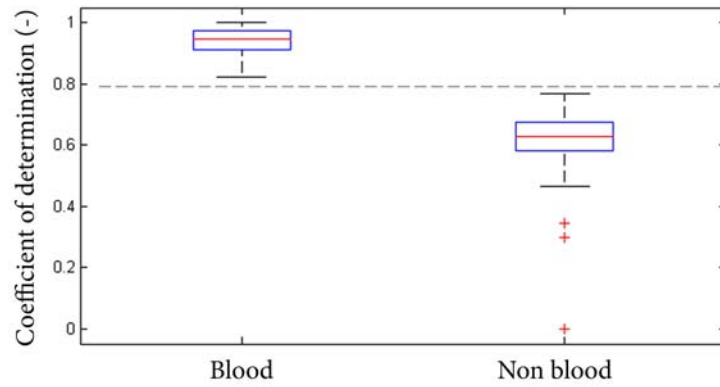


Figure 7.6. Box plots showing the coefficients of determination (R^2) between blood stain absorbance spectra from the library and all other blood stain absorbance spectra and non blood absorbance spectra. At a threshold of $R^2=0.8$ (dashed line) all R^2 values from blood stains can be distinguished from these from non blood stains.

7.4.d AGE ESTIMATION

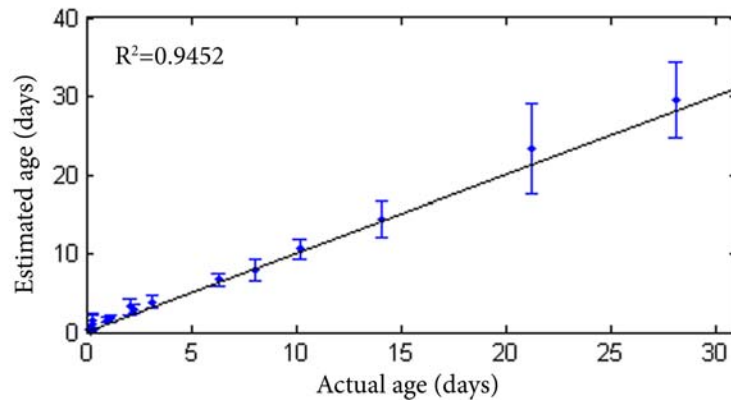


Figure 7.7. Results of the age estimation of blood stains on black cotton using a PLS model in which a part of the NIR region was used (1150-2500 nm). Dots represent average measurements of three blood stains, whiskers depict the standard deviation. The line of unity is plotted for comparison ($R^2 = 0.9452$).

To estimate the age of blood stains on coloured backgrounds, a PLS model was created for each colour, which was trained with absorbance spectra of blood stains on all other backgrounds. Estimated ages of blood stains on black cotton were plotted in Figure 7.7. This figure shows that the accuracy of the estimation decreases with age, which is shown by the larger error bars for older blood stains. Results for the other colours were similar. For each colour, the coefficient of determination R^2 between actual ages and estimated ages and the root mean squared error of prediction (RMSEP) were calculated (see Table 7.2). The RMSEP values are relative errors, the absolute errors increase with age.

Table 7.2. Results of the age estimation task for blood stains on different cotton backgrounds. For each test and training set, the resulting R^2 and RMSEP are given.

Training set	Test set	R^2	RMSEP
white, red, green, blue	black	0.9452	8.9%
white, green, blue, black	red	0.9679	6.8%
white, red, blue, black	green	0.9607	8.5%
white, red, green, black	blue	0.9749	9.1%

7.5. DISCUSSION

In this study, we identified NIR spectral features of blood stains which can be used for blood stain identification and age estimation, even when blood is deposited on coloured backgrounds. Using NIR reflectance spectroscopy blood stains can be distinguished from other substances with a sensitivity of 100% and a specificity of 100%, and their ages can be estimated non destructively.

7.5.a BLOOD STAIN CHARACTERIZATION

NIR reflectance measurements on blood stains show that the spectra are dominated by decreasing water absorption peaks in the beginning of the aging process. After drying, absorption peaks from several other components of human blood, e.g. haemoglobin, albumin, globulin are observed. Because NIR absorption bands are characteristically weak, highly overlapping, and very broad¹²⁵, identification of the contributions of different components to the spectrum of whole blood is difficult. The components and bonds mentioned in Table 7.1 are therefore just indicative. Other techniques, e.g. Raman spectroscopy, may be useful for the exact identification of all components. Using Raman spectroscopy, Boyd et al identified scattering peaks characteristic of haemoglobin and fibrin¹⁰³. Identification of more components present in blood could provide interesting information about the chemical processes involved in the aging of blood stains.

7.5.b IDENTIFICATION

In the first 77 days of aging, we found that the NIR absorbance spectra of blood stains correlate highly, and are thus useful for the identification of blood stains. By analyzing the similarity with a library of 3 blood stains of different ages, NIR absorbance spectra of all blood stains were distinguished from a set of other substances. Apparently, the similarity of the spectra of blood stains was high compared to the similarity between blood and our selection of non blood samples. This limited non blood sample set was chosen such that it

contained substances which are likely to be false positives when luminol or visible spectroscopy is used for the identification of blood stains. Other substances with absorption properties resembling blood stains in the NIR wavelength range may exist (e.g. substances containing proteins). Adding other samples to the set may induce false positives and thus reduce the specificity. Regarding the sensitivity, it is unknown if we will be able to identify blood stains older than 77 days, diluted blood stains, or blood from smokers or people suffering from certain diseases.

Compared to chemical blood identification tests, e.g. luminol¹²¹, the main advantage of spectroscopy based techniques is their non-destructiveness. Therefore, Raman spectroscopy^{74, 81, 84, 103, 147} and visible spectroscopy (**Chapter 3**)⁶⁵ have been examined recently for the purpose of blood identification. We now added NIR spectroscopy to this range of techniques. All spectroscopic techniques are hampered by certain backgrounds, which can be encountered in forensic practice. While Raman spectroscopy is difficult on strongly fluorescing backgrounds, like fabrics, visible spectroscopy is hindered by coloured backgrounds. We demonstrated that NIR spectroscopy can be complementary to Raman and visible spectroscopy, as we successfully identified blood stains on coloured fabrics. It is expected that this method will be successful on many other backgrounds. Only materials which highly absorb light of many NIR wavelengths are expected to complicate the identification task. Similarly, water absorption peaks complicate the identification of wet blood stains using NIR spectroscopy.

7.5.c AGE ESTIMATION

After a successful identification, the ages of blood stains on coloured backgrounds were estimated using NIR spectroscopy. The RMSE of prediction of the age of blood stains on black cotton up to one month old was 8.9%. We observed a better accuracy for younger than older blood stains, which can be explained because chemical and thus spectral changes are faster in the beginning of the aging process. These results demonstrate that NIR spectroscopy is suitable for short term age estimation, as previously shown by

Botonjic-Sehic et al⁶⁶. While Botonjic-Sehic et al calculated the areas under a small part of the spectra, we used a large wavelength region to estimate the age of blood stains with PLS regression. In addition, we demonstrated the applicability of this technique on coloured backgrounds, where age estimation using visible spectroscopy is hampered¹. As the sample set used for training the PLS model did not include the background colour of the test set, this method is expected to be successful for other colours not included in our sample sets.

Other methods for age estimation, e.g. high performance liquid chromatography, electron paramagnetic resonance, atomic force microscopy and RNA degradation measurements are more invasive and can only be performed in the laboratory. Although in this study a laboratory setup was used, with two large spectrometers, recent developments in hyperspectral imaging technology, i.e. the combination of spectroscopy and conventional imaging, offer potential for crime scene investigations. The development of portable equipment enables the analysis of an unknown stain at the crime scene without waiting for results from the laboratory.

Before NIR spectroscopy for blood stain age estimation can be applied in practice, key steps in the research process are refining and validating the data to meet the needs of the legal and scientific communities. For example, more research is needed on the effect of environmental conditions. As the aging of blood stains is influenced by factors like temperature, humidity and lighting conditions⁵⁶, the effect on the NIR spectra should be studied.

7.5.d CONCLUSION

NIR spectroscopy can be employed for the non-destructive identification and age estimation of blood stains on coloured backgrounds. When introduced in forensic casework, the described method can provide investigators with important information; it can give an indication of when a crime was committed, or it can help investigators to determine if a certain stain is relevant to the case.

7.6. ACKNOWLEDGEMENTS

We would like to acknowledge RIKILT Institute of Food Safety, Wageningen University and Research centre for the use of their facilities and assistance in the NIR spectroscopy measurements. We thank Mr. Rob Frankhuizen for sharing his experience in the analysis of near infrared spectra. Additionally, we appreciate the enthusiasm of the volunteers and the important input of Mr. Jan Winder from Abbott Healthcare Products, who kindly assisted us with the initial measurements. An application of the results of this research is being developed in the project CSI the Hague, within the *Pieken in de Delta* program by the NL Agency of the Dutch Ministry of Economic Affairs, Agriculture and Innovation (project number PID082036).

8 - INFRARED IMAGING OF THE CRIME SCENE: POSSIBILITIES AND PITFALLS

Journal of Forensic Science 2013; Sep;58(5):1156-62

All objects radiate an amount of infrared energy invisible to the human eye, which can be converted into visible images by infrared cameras, visualizing differences in temperature and/or emissivity of objects. As a result of improvements in technology and a decrease in costs infrared imaging is an emerging technique for law enforcement and forensic investigators. The rapid, non-destructive and non-contact features of infrared imaging indicate its suitability for a wide range of forensic applications, which can be divided into two approaches; passive and active infrared imaging. The passive approach, referring to infrared imaging without using an external energy source, is useful for non-contact radiation measurements, e.g. for the estimation of the time of death, which is currently often based on invasive rectal temperature measurements. Passive infrared imaging of objects at the crime scene can provide new investigative leads, e.g. an indication of recent human contact or the time since a device was used. Active infrared imaging requires external heating or cooling of the target prior to imaging. Using this approach, contrast can be visualized between traces and their surroundings due to differences in thermal response, e.g. blood stains on red carpet. This chapter provides an overview of the principles and instrumentation involved in infrared imaging. Difficulties concerning the image interpretation due to different radiation sources and different emissivity values within a scene are addressed. Finally, reported forensic applications are reviewed and supported by practical illustrations.

8.1. INTRODUCTION

Infrared cameras, also known as thermal cameras, convert invisible infrared radiation into visible images. This technique was originally developed for military use but has since found application in such diverse fields as medicine¹⁴⁸, agriculture and the food industry^{149, 150}. As a result of improvements in technology and a decrease in costs infrared imaging is an emerging technique for law enforcement and forensic investigators. Previous work showed that infrared imaging of crime scenes has serious potential for aiding forensic case work¹⁵¹⁻¹⁵⁴. It is a non-destructive technique, which can reveal information invisible to the naked eye.

Infrared imaging is suitable for a wide range of forensic applications, and can be divided into two approaches; passive and active infrared imaging. The passive approach, referring to infrared imaging without using an external energy source, is useful for non-contact radiation measurements. As all objects radiate an amount of infrared energy, increasing with temperature, the radiation detected by infrared cameras can be used to measure temperatures and visualize temperature differences. However, the amount of infrared radiation emitted by an object is also influenced by the emissivity value, which should be taken into account when temperatures or temperature differences are measured. An interesting forensic application of passive infrared imaging is the estimation of the post mortem time interval, which is currently often based on invasive rectal temperature measurements. Using passive infrared imaging, a post mortem body temperature can be recorded non-invasively, without the risk of contamination¹⁵¹. Additionally, passive infrared imaging of objects at the crime scene can provide new investigative leads, e.g. an indication of recent human contact or the time since a device was used¹⁵².

Active infrared imaging requires external heating or cooling of the target prior to imaging. Using this approach, surface inhomogeneities can be visualized, due to differences in thermal response. When heated with an external source, e.g. blood traces on similarly coloured backgrounds and invisible to the human eye may be highlighted on infrared images. The external

heat source can be part of the active thermal imaging system, but may also be a human body, a domestic heating or an air-conditioning system.

External heat sources also complicate the interpretation of infrared images of a crime scene, as the image of a target object is influenced both by the surrounding objects, and by the presence of the investigators who emit infrared radiation. Infrared radiation that enters the camera lens is a combination of emitted, transmitted and reflected radiation, and comes from three different sources: the target object, its surroundings, and the atmosphere. To guarantee a correct interpretation of infrared images, investigators should be trained and educated, and standardized protocols for image capture and analysis are needed.

In this chapter we describe the possibilities and pitfalls of thermal imaging for crime scene investigation. Although this topic is scarcely covered in forensic literature, we review the existing literature and elaborate on some of the proposed applications using practical illustrations. While infrared imaging can also be useful in the forensic laboratory^{155, 156} and for surveillance purposes¹⁵⁷, this chapter is confined to crime scene purposes only. Next to a theoretical background, recent advances in infrared imaging technology are described, which reduce the size and costs of the equipment and thus enable future applications at the crime scene.

8.2. THEORETICAL BACKGROUND

8.2.a INFRARED EMISSION

All objects with a temperature above the absolute zero emit infrared radiation. The amount of energy emitted by an object increases with temperature, as described by Stefan-Boltzmann's law:

$$W = \sigma \epsilon T^4,$$

where W is the total amount of energy emitted by an object per square meter (Wm^{-2}), σ is Stefan-Boltzmann's constant ($5.67 \times 10^{-8} \text{ Wm}^{-2}\text{K}^{-4}$), ϵ is the

emissivity of the object and T its temperature (K). This relation between emitted energy and temperature is the basis of infrared imaging. It shows that the temperature of an object can be determined by measuring the radiated energy if the emissivity of the object is known, which is defined as the energy emitted by an object relative to the energy emitted by a blackbody at the same temperature.

A blackbody is a theoretical object with an emissivity of 1. In practice, the emissivity of an object can vary from 0 to 1, and depends on temperature, wavelength, material and the surface texture of an object. Objects with glossy surfaces have a lower emissivity than objects with matt surfaces, e.g. aluminum foil has an emissivity of approximately 0.1, water and human skin of 0.98¹⁵⁸⁻¹⁶⁰. Emissivity values for common materials and surface characteristics can be looked-up in tables or estimated experimentally, e.g. by comparing infrared images of an object at two distinct known temperatures¹⁶¹. Although a perfect blackbody absorbs all infrared radiation, all real objects react to incident radiation from their surroundings by absorbing, reflecting and transmitting a portion of it. The sum of the object's incident energy absorbance (α), reflectance (ρ), and transmittance (τ) equals one:

$$\alpha + \rho + \tau = 1.$$

At thermal equilibrium, the amount of absorbance will equal the amount of emission (Kirchhoff's law):

$$\alpha = \varepsilon. \tag{8.1}$$

Combining these equations shows that the emissivity of an object can also be estimated by measuring the reflectance and transmittance at thermal equilibrium and using the following equation¹⁶²:

$$\varepsilon = 1 - \rho - \tau.$$

8.2.b INFRARED IMAGING SYSTEMS

Infrared imaging systems detect infrared radiation and convert this to an image, similar to a common camera that forms an image using visible light. A typical infrared imaging system comprises an optical system, an infrared detector, a signal processing unit and an image acquisition system. Many characteristics of infrared radiation are similar to visible light; infrared radiation can be focused, refracted, reflected and transmitted. However, infrared cameras cannot use regular glass lenses, as glass will reflect infrared radiation rather than allowing the radiation to pass through the lenses. Commonly used materials for infrared lenses and their respective transmission windows are Germanium (Ge, 2-11 μm), fused Silica (IR grade SiO_2 , 0.2-4 μm), Zinc Selenide (ZnSe , 0.5-11 μm) and Zinc Sulfide (ZnS , 3-10 μm).

These lenses are used to focus the infrared radiation onto a focal plane array of detectors, which in turn convert the radiant energy into electrical signals proportional to the amount of radiation. Two types of detectors are known¹⁶³: thermal detectors and photon detectors. In classical photon detectors (e.g. HgCdTe (0.8-25 μm), InGaAs (0.7-2.6 μm)), photons are absorbed and generate free carriers which produce a current, voltage or resistance change of the detector. Photon detectors are highly sensitive, but require cooling, which implies a significant increase in cost, weight and size. In thermal detectors (e.g. microbolometers), infrared radiation causes a temperature rise of a thermally isolated detector element, which is a measure of the amount of radiation. These detectors do not require cooling, but are in general less sensitive than photon detectors. However, recent technological advances enable higher performance of uncooled thermal detectors, as well as low power lightweight detectors, proficient for helmet mounted systems, robotic systems and micro-air vehicles¹⁶⁴.

When selecting an infrared imaging system, an important aspect is the operating wavelength range. Most infrared cameras operate in the wavelength range from 3 to 5 μm or from 8 to 12 μm , because the absorption of the atmosphere is minimal in these windows (Figure 8.1). The required

temperature range is an important selection criterion, as the emitted wavelengths are temperature dependent, a relation described by Planck's law:

$$B(T) = \frac{2hc^2}{\lambda^5} \left(e^{\frac{hc}{\lambda k_B T}} - 1 \right)^{-1}, \quad (8.2)$$

where B is the spectral radiation, T is the absolute temperature of the black body, k_B is the Boltzmann constant ($1.3806488(13) \times 10^{-23} \text{ JK}^{-1}$), h is Planck's constant ($6.62606957(29) \times 10^{-34} \text{ Js}$), and c is the speed of light ($2.99792458 \times 10^8 \text{ ms}^{-1}$).

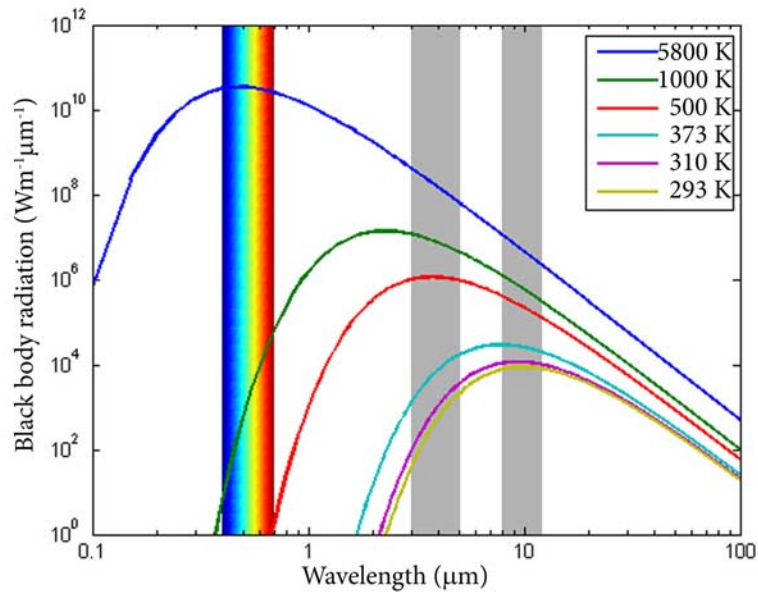


Figure 8.1. Wavelength dependent radiation emitted by a perfect black body at different temperatures, calculated using Planck's law (formula 8.2). The visible wavelength range is depicted by the coloured bars. Grey bars illustrate the atmospheric infrared transmission windows in which most cameras operate.

The resulting radiation for a blackbody at several temperatures is depicted in Figure 8.1, which shows that the wavelength of the emission peak is lower for hot objects. The peak wavelength (λ_{\max} (μm)) can be calculated using

$$\lambda_{\max} = b / T,$$

in which b is Wien's displacement constant, equal to 2.89×10^{-3} mK, and T the absolute temperature (K). This formula shows that the sun, with a temperature of approximately 5800 K, has a peak emission around 500 nm, which lies in the visible wavelength range. Objects at room temperature and human body temperature emit peak radiation around 10 μm , in the far infrared.

8.2.c IMAGE INTERPRETATION

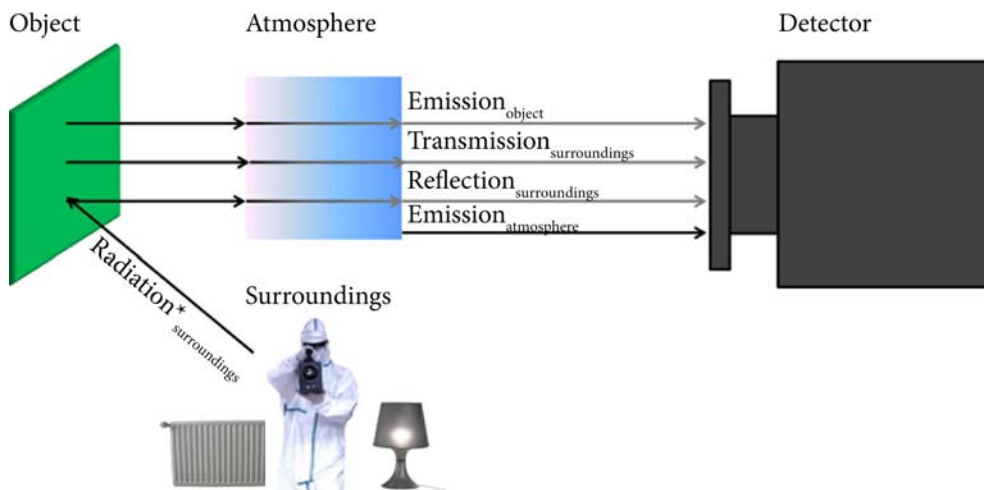


Figure 8.2. Schematic showing the contributions of the target object, its surroundings, and the atmosphere to the total radiation detected by an infrared camera.

An infrared camera converts infrared radiation to an image, displaying variations across an object or a scene. Interpreting these infrared images is not straightforward, as the camera receives radiation emitted from the target object, plus radiation from its surroundings that is transmitted through or reflected by the object (Figure 8.2). All these radiation components become

attenuated when they pass through the atmosphere. Since the atmosphere absorbs part of the radiation, it will also emit some itself (Kirchhoff's law, formula 8.1). Consequently, the radiation that impinges on the camera lens comes from three different types of sources: the target object, its surroundings, and the atmosphere. Differentiating between emitted, transmitted and reflected radiation is not possible (Figure 8.3), which is a probable cause of misinterpretation.

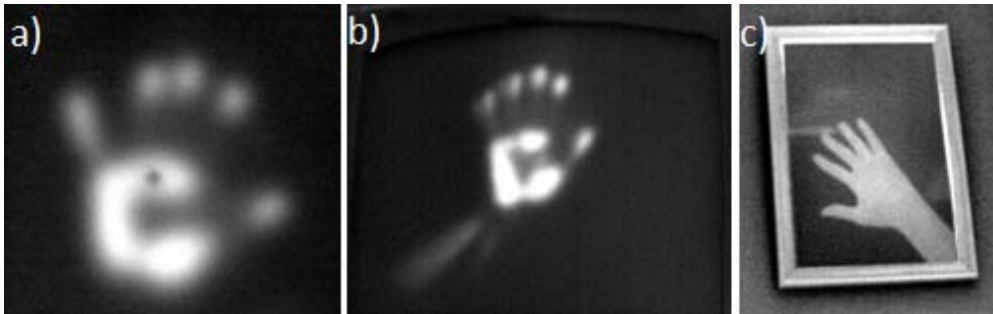


Figure 8.3. Infrared images depicting: a) Emitted radiation of body heat left by a hand pressed shortly against the wall, prior to recording the image. b) Transmitted radiation of the body heat of a hand through the door of a closet. c) Reflected radiation of body heat, reflected by the picture frame.

To calculate the temperature of the target object, infrared camera software requires input for the emissivity of the object, the atmospheric transmittance, the object distance, atmospheric temperature, and ambient temperature. Consequently, for images showing objects with different emissivities the input parameters should be adjusted for each material in order to compare the temperature of different objects. Thus, false-colour infrared images and temperature scale bars usually provided by infrared imaging software must be interpreted with caution (Figure 8.4).

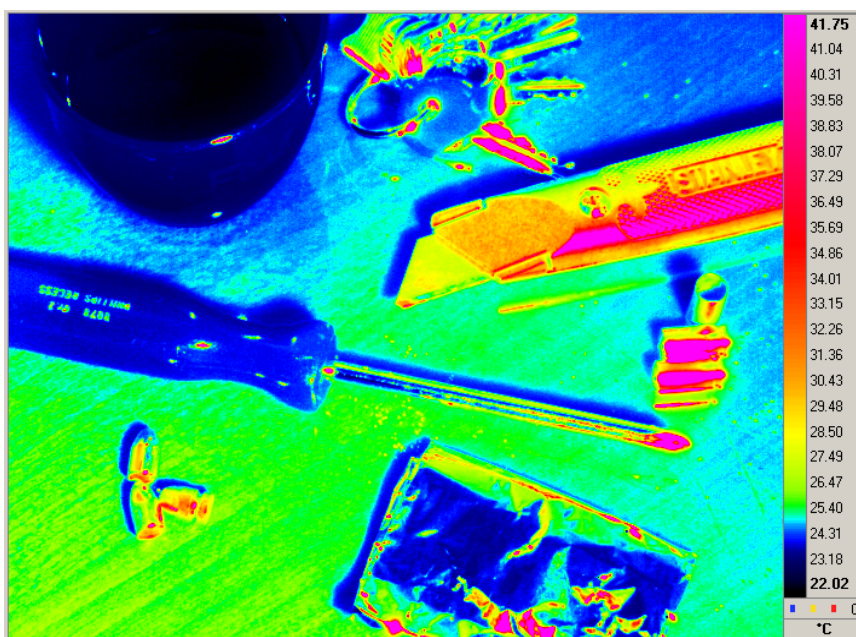


Figure 8.4. False-colour infrared image of a cup of water, keys, a knife, a screw-driver, bullets, bullet cases and aluminum foil on a table. All objects have room temperature. The scale bar on the right is based on an emissivity value of 0.98, and thus only shows the right temperature for the water (room temperature) in this scene.

To guarantee a correct interpretation of infrared images, investigators should be trained and educated, and standardized protocols for image capture and analysis are needed. Measurements of objects with low temperatures or low emissivities are most critical, since the relative contribution of external radiation is high in those cases.

8.3. APPLICATIONS

Several applications of infrared imaging for crime scene investigation have been proposed in conference proceedings^{152, 165} and scientific journals^{151, 153, 154}. In this section we elaborate on the theoretical background of possible applications, illustrated with some practical examples. Difference is made between applications using passive and active infrared imaging. Passive

infrared imaging can be used to investigate heat traces, which cause contrast because of temperature differences. Active infrared imaging can be used to visualize differences in thermal response, by using an external heat source.

8.3.a PASSIVE INFRARED IMAGING

Because the human body temperature is usually higher than the environmental temperature, people leave heat traces invisible to the human eye, which can be observed with an infrared camera. Consequently, infrared imaging can give insight in the recent presence of people and recently handled objects. As it is frequently possible to obtain DNA from an individual who has simply touched an object¹⁶⁶, this is highly important information supporting crime scene investigators in their search for trace evidence. Additionally, information about the presence of people and recent activities is useful for crime reconstruction purposes and for the verification of statements.

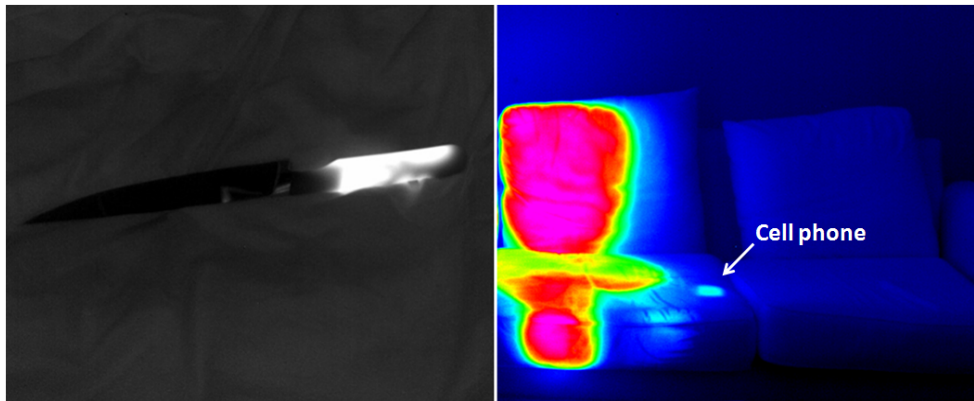


Figure 8.5. Heat traces of human contact with a knife (left) and a couch (right), visualized in greyscale and false colours respectively. Additionally, a heat trace of a cell phone is visible on the couch.

Figure 8.5 shows two examples of human heat traces visualized by an infrared camera, indicating the handle of the knife and one side of the couch were recently touched. As described above, these images should be interpreted with caution, but can give valuable qualitative information. In case contrast changes

are observed in time, this indicates the contrast will be due to temperature differences instead of emissivity differences. The time traces stay visible depends on the temperature difference, the material properties and the environmental conditions, e.g. the heat on the knife was visible for a few minutes, the heat on the sofa for an hour.

Apart from the human heat trace, Figure 8.5 shows the heat trace of a cell phone. Van Iersel et al showed the visibility of heat traces from cups of fluid and electronic devices, e.g. a computer screen¹⁵². These traces may also provide information useful for reconstruction purposes. Heat traces may lead to an indication of the time since an object was used. For instance, if the barrel of a gun is still warm, experiments can be performed to measure a cooling curve specific for the gun after firing in similar environmental circumstances. By comparing the cooling curve with the heat measured at the crime scene, the time since firing can be estimated.

The post mortem cooling curve of a body can also be recorded by infrared imaging^{151, 154, 165}. Currently, the Henssge nomogram is the gold standard for the estimation of the post mortem interval; the time since the death of a person. Henssge's nomogram is based on empirical data of human body cooling and requires the ambient temperature, the rectal temperature, the weight of the body and a clothing parameter to be able to lookup the estimated post mortem interval¹⁶⁷. Rectal temperature measurements are not favorable in a forensic setting because of the high risk of contamination and possible loss of traces of sexual assault. Since infrared imaging is non-invasive it is highly profitable to explore the possibilities of this technique for post mortem temperature measurements.

However, as infrared imaging systems measure the skin temperature instead of the core temperature, new models are required to determine the post mortem interval based on skin temperatures. Before application in forensic practice, new models need a thorough validation. Several promising studies have been performed on the post mortem cooling of the human head^{151, 168}. Figure 8.6 shows an infrared image of a body and the postmortem cooling curve. Based on such measurements, a model for postmortem skin cooling can be developed. Mall et al¹⁶⁸ stated that changes in ambient temperatures highly

influence the skin temperature, and thus need to be taken into account in a model for postmortem skin cooling. This is confirmed by the cooling curve in Figure 8.6, where fluctuations in the ambient temperature, caused by the cooling system, are clearly visible in the temperature measurements. A disadvantage of using infrared imaging for post mortem interval estimation is that the temperature of the skin decreases more quickly to the environmental temperature than the core of the body. A benefit is the high emissivity value of the human skin (0.98), which implies that reflections of surrounding heat sources are minimal. However, the skin is not always directly visible. Measurements on clothing are possible, but this severely complicates the interpretation.

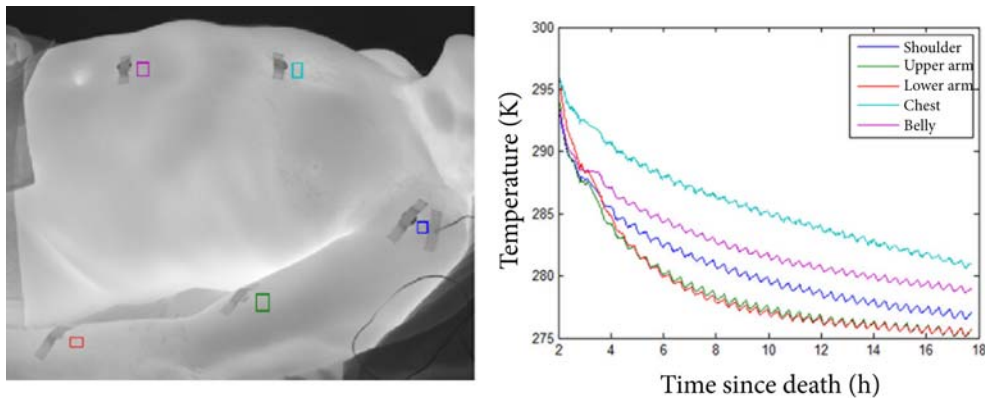


Figure 8.6. Infrared image of a body (left) and the cooling curves of regions of interest (indicated by the rectangles) on the shoulder, upper arm, lower arm, chest and belly (right).

Infrared imaging of a human body may lead to additional information relevant to forensic medical examiners, as reviewed by Ammer¹⁵⁴. Blunt traumas without skin damage may be detected using infrared imaging, due to an inhomogeneous temperature distribution. Similarly, hematomas due to strangulation may become visible using infrared imaging, which helps investigators in their search for crime-related DNA traces.

Apart from heat traces, wet traces are also easily visualized using infrared imaging. Figure 8.7 demonstrates an infrared image of a wet blood

stain hardly visible to the human eye. The infrared image shows high contrast between the wet blood stain and its background. This may be due to evaporation, which causes cooling of the blood stain, combined with the high absorption of infrared radiation by water. Regardless the physical explanation, it is clear that infrared imaging can be used to visualize fluids. After drying, in general less contrast is observed between stains and their backgrounds. In these cases, active infrared imaging can be applied, which is described below.

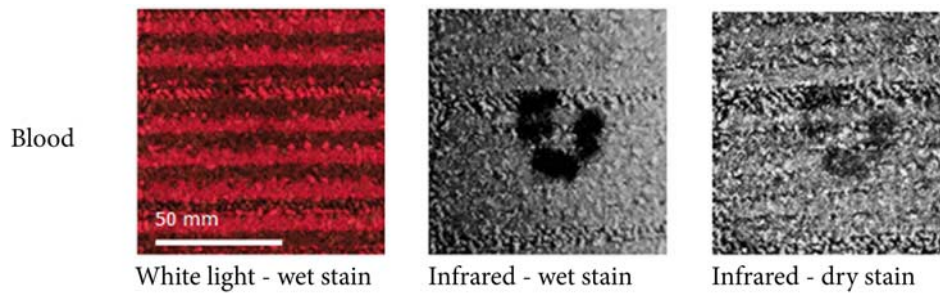


Figure 8.7. Photograph taken with white light (left) and infrared images of blood stains on carpet. The first infrared image (middle) was created passively while the stain was wet. The second infrared image (right) was created actively after drying. More contrast is observed for the wet stain. This may be due to evaporation, which causes cooling of the blood stain, combined with the high absorption of infrared radiation by water.

8.3.b ACTIVE INFRARED IMAGING

Even traces in thermal equilibrium with the environment can be visualized using infrared imaging, if the thermal response is different from its surroundings. The thermal response of a material is influenced by many physical properties including the conductivity, diffusivity, specific heat and radiative properties (emissivity, absorbance, reflectance and transmission). Inhomogeneities in the thermal response become evident when an external source causes a temperature change. This external source can be part of the active infrared imaging system, but may also be a human body, a normal building heating or an air-conditioning system (Figure 8.2)¹⁶⁵. By recording the

heating and cooling process of an object, inhomogeneities can be visualized (Figure 8.8).

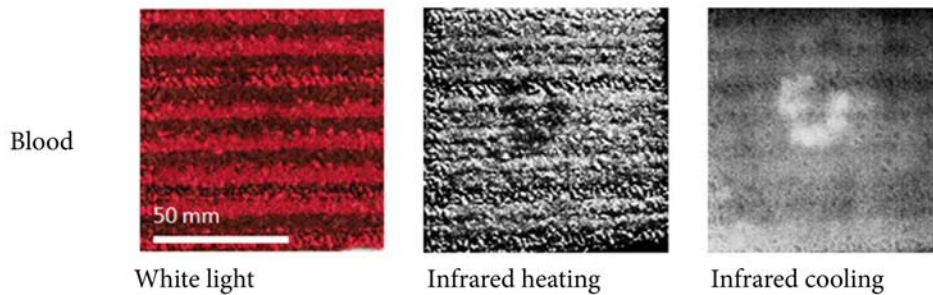


Figure 8.8. Photograph taken with white light (left) and infrared images of blood stains on carpet. The first infrared image (middle) is created using an external heat source. Contrast is observed because more heat is absorbed by the blood stain than by the background, which makes it appear darker. The second infrared image (right) is created after removal of the external heat source. In this case, contrast is observed because the absorbed heat is reemitted by the blood stain, which makes it appear brighter.

Based on this principle, drag traces may be visible long after thermal equilibrium is reached, because of an abraded surface, which causes a different heat flow^{152, 154, 165}. Another application is the visualization of body fluids. Brooke et al used active infrared imaging for the detection of blood on a dark, acrylic fabric¹⁵³. They reported contrast differences between the clean fabric and the fabric stained with blood diluted as low as 1:100. Additionally, they were able to discriminate between a blood stain and four common interfering agents (bleach, rust, cherry soda, and coffee) to other blood detection methods.

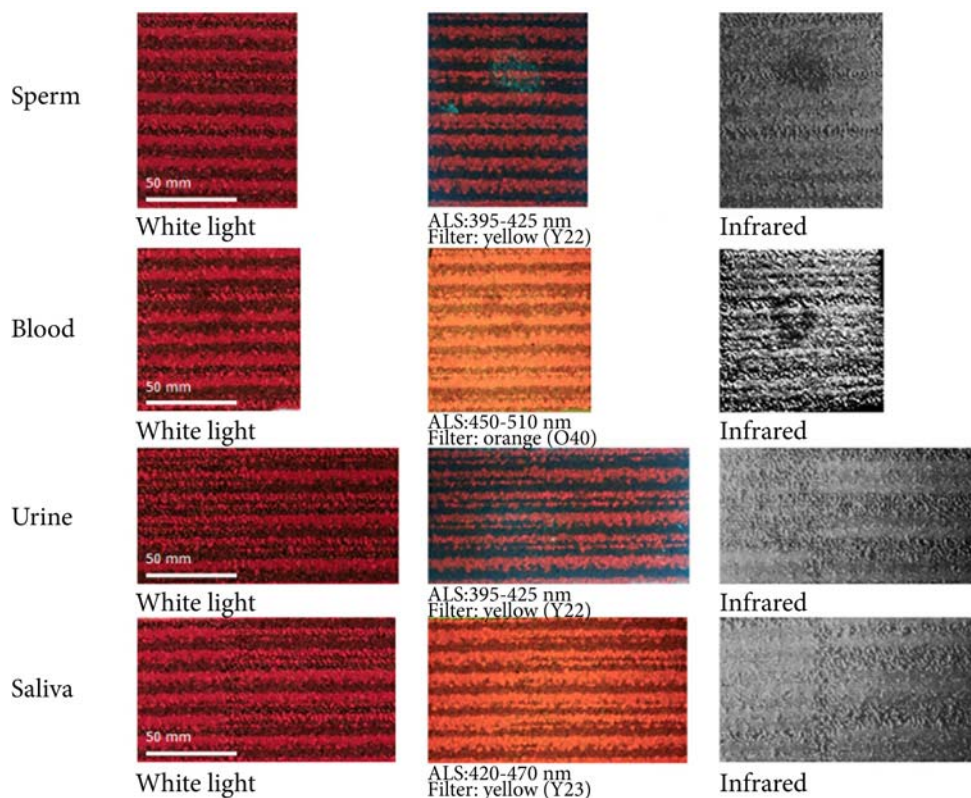


Figure 8.9. Photographs taken with white light (left) and alternative light sources (middle) and infrared images (right) of sperm, blood, urine, and saliva on floor tiles. Infrared images are created using an external heat source.

To explore the value of infrared imaging for the detection of body fluids, we compared the results with photographs taken using alternative light sources and filters. Sperm, blood, urine, and saliva stains were deposited on red/brown floor tiles and photographed using white light and a combination of alternative light sources and filters. The best results are shown in Figure 8.9, next to the infrared images of the floor tiles. This figure demonstrates that urine and sperm are highly fluorescent, which make them ideal candidates for visualization with alternative light sources. However, infrared imaging of sperm also revealed contrast on this background, in contrast to the urine stains, which could not be visualized using infrared imaging. On the other hand, blood stains

hardly visible to the naked eye became evident using active infrared imaging, while alternative light sources did not generate much contrast between the stain and its background. Saliva stains were not visible using either method. Success or failure of both methods highly depends on the background; the use of alternative light sources is hampered by highly absorbing (dark) backgrounds, infrared imaging is more difficult when stains are deposited on inhomogeneous structures or when there is a lack of thermal contrast.

8.4. DISCUSSION AND CONCLUSION

Infrared imaging of crime scenes has serious potential for aiding forensic case work. It is a non-destructive technique, which can reveal information invisible to the naked eye. Both temperature differences and differences in thermal material properties can induce contrast in infrared images. The use of passive or active infrared imaging at the crime scene can provide both investigative leads and evidence in court (provided the used technique is properly validated and accepted). Applications described range from the estimation of the post mortem interval to the visualization of blood traces on dark backgrounds.

We demonstrated the post mortem cooling curves of several parts of the human body (Figure 8.6). These curves were measured non-invasively using passive infrared imaging, which minimizes the risk of contamination and possible loss of traces of sexual assault. After a thorough validation and development of an appropriate mathematical model, this technique may be able to replace the current standard: Henssge's nomogram, an empirical model based on core body temperature measurements. Apart from measuring post mortem temperatures, infrared imaging can be used to detect heat traces caused by human contact (Figure 8.5). These traces indicating human presence or the recent use of objects can help investigators in their search for DNA or other relevant crime-related traces in those cases the incident recently happened.

The amount of time it takes until thermal equilibrium is reached depends on the temperature difference and the object properties; while a human heat trace on a knife may only be visible for a few minutes, a human

body can stay warmer than the ambient temperature for more than 24 hours after death. Consequently, heat traces are only temporarily available, and therefore crime scene investigators are advised to start the crime scene survey with infrared imaging. However, to preserve heat traces only shortly visible, it may be possible to provide first responders with a helmet mounted infrared camera (preferably combined with a normal video camera), as currently already available for firefighters. Infrared camera systems used for forensic purposes are ideally wireless, portable, waterproof, and sealed (to avoid contamination). Due to recent developments infrared imaging becomes more sensitive, user-friendly and cost effective. Consequently, an increased adoption of this technology by forensic investigators is highly likely.

When used actively, i.e. with an external heat source, infrared imaging can be used for the detection of traces not or hardly visible to the naked eye. We compared images of several body fluids on carpet created using alternative light sources (ALS, the current standard) with the corresponding infrared images (Figure 8.9). This comparison demonstrated that the success rate of both ALS and infrared cameras highly depends on the type of trace and its background. The well known expression “Absence of evidence is not evidence of absence” is certainly in place. Viewed from the perspective of a forensic investigator at the crime scene all information gained with different techniques used on the crime scene can be useful, provided they are correctly interpreted. Due to the fact that no single technique is capable to detect and identify all types of traces at the crime scene without the need of further confirmation, we can combine different techniques to search for all kinds of traces. To conserve traces for further analysis, non-destructive techniques are preferable.

In conclusion, we showed several potential applications of infrared imaging for crime scene analysis. Many of the applications discussed are still at an experimental stage. Initial experiments for the estimation of the time of death using infrared imaging are promising. Additionally, as it can help in the search for crime related traces, infrared imaging can be a good addition to the resources of the crime scene investigator. However, before infrared imaging can be used as evidence in the courtroom, several (key) steps have to be taken; are refining and validation of the technique to meet the needs of the legal and

scientific communities. Prior to that, infrared images may be used indicatively to lead the further investigation. When introduced in forensic casework, infrared imaging can help investigators detecting, visualizing and identifying useful evidence non-destructively.

8.5. ACKNOWLEDGEMENTS

The practical applicability of infrared imaging at the crime scene was tested using the facilities generated by the project CSI the Hague, within the Pieken in de Delta program by the NL Agency of the Dutch Ministry of Economic Affairs, Agriculture and Innovation (project number PID082036). The authors like to thank Bibianne Geerts for performing measurements on human body cooling.

9 - DISCUSSION

This chapter reflects on the contents of this thesis. It summarizes the proposed spectroscopic techniques for the detection, identification and age estimation of blood stains. We discuss the physical light-transport model used to analyse reflectance spectra of blood stains, and compare it with a statistical and empirical method described in literature. The main advantage of a physical approach is the ability to correct for background interferences, which is important in forensic applications, due to the wide range of substrates possibly encountered at crime scenes. We describe several complimentary techniques, which may be combined to gather a maximum amount of information from a sample. To conclude, several practical challenges are discussed, which need to be addressed before the described methods for the analysis of blood stains can routinely be used in criminal investigations.

9.1. INTRODUCTION

Blood stains are often encountered in crime scene investigations and can provide investigators with interesting information regarding the donor of the blood stain (using DNA analysis) or the activities needed to create the stain (by bloodstain pattern analysis). To be able to analyse blood stains however, they first need to be detected. Next, the nature of the stain must be identified to distinguish blood from other substances. Furthermore, blood stains would be even more informative if their age could be measured. This brings us to the three main challenges addressed in this thesis:

1. the detection of latent blood stains;
2. the identification of blood stains;
3. the age estimation of blood stains.

Our aim was to develop methods to tackle the above described challenges for the analysis of blood stains, which can be applied at the crime scene, so traces can be judged and interpreted in the original context, without the need to wait for results from a remote laboratory. Techniques used for crime scene investigations ideally are non-destructive, portable and require no sample treatment. Several optical spectroscopic techniques fulfil these requirements and were explored in this thesis. Because traces are generally not found on ideal backgrounds used in laboratories, but many different backgrounds can be encountered at the crime scene, we address the problem of background interference and suggest a correction method.

9.2. DETECTION OF BLOOD STAINS

To detect blood stains on black backgrounds crime scene investigators conventionally use chemicals which react with amino acids, proteins, or heme, and induce chemiluminescence or fluorescence in contact with blood. These methods are invasive and require a darkened room for the detection. We explored two non-destructive optical techniques for this purpose: visible hyperspectral imaging and mid infrared imaging.

9.2.a VISIBLE HYPERSPECTRAL IMAGING

Hyperspectral imaging is a promising technique for the detection of latent blood stains. As described in **Chapter 1**, hyperspectral imaging combines spectroscopy with digital imaging and can be used for the non-destructive detection and chemical analysis of forensic traces, e.g. fingerprints. In **Chapter 6**, we demonstrated that visible hyperspectral imaging can be valuable for the detection of latent blood stains on black fabrics. Using this technique combined with data processing methods we successfully enhanced the contrast between blood stains and their backgrounds compared to white light photography.

9.2.b MID INFRARED IMAGING

Another non-destructive technique, which can reveal information invisible to the naked eye is mid infrared imaging, as described in **Chapter 8**. Both temperature differences and differences in thermal material properties can induce contrast in mid infrared images. Apart from measuring post mortem temperatures and the detection of heat traces caused by human contact at the crime scene, mid infrared imaging was used to detect latent blood stains. Blood stains hardly visible to the naked eye became evident using mid infrared imaging, while conventional photography combined with forensic light sources did not generate much contrast between the stain and its background.

9.3. BLOOD STAIN IDENTIFICATION

Most chemical methods used to detect latent blood stains can also be used for identification purposes. Two commonly used tests are tetrabase⁷⁵ and Kastle-Meyer, which employ peroxidase activity of haemoglobin molecules, causing a colour change. Again, the main disadvantage of these techniques is their invasiveness. We used near infrared and visible spectroscopy and hyperspectral imaging to identify blood and distinguish it from other substances.

9.3.a VISIBLE SPECTROSCOPY AND HYPERSPECTRAL IMAGING

In **Chapter 3** we demonstrated that blood stains can be identified based on their visible reflectance spectra, by deducing the presence of haemoglobin and its oxidation products oxyhaemoglobin, methaemoglobin, and hemichrome. We started using a spectroscopy setup in the laboratory and moved on to hyperspectral imaging in a simulated crime scene. Using hyperspectral imaging for the analysis of blood stains has several advantages compared to conventional spectroscopy. First of all, reflectance spectra of many blood stains can be measured in one scan, which makes the analysis of a complete crime scene far less time-consuming. Additional information is acquired, because the spatial information of the blood stain distribution is recorded simultaneously, showing the location and context of each stain and thus reducing the amount of documentation needed. Being able to view the spectral and spatial information side by side may also improve bloodstain pattern analysis, by enabling to group stains from individual events based on their age.

9.3.b NEAR INFRARED SPECTROSCOPY

When the absorption of visible light is dominated by the background, we recommend to move beyond the visible wavelength range for the identification of blood stains. In **Chapter 7** we showed that blood stains can be identified using near infrared (NIR) spectroscopy, even on black backgrounds. NIR spectra of blood stains show absorption peaks characteristic for several components of human blood, e.g. haemoglobin, albumin, globulin. Based on these peaks, blood stains can be distinguished from other samples visually mimicking blood.

9.4. BLOOD STAIN AGE ESTIMATION

In many criminal investigations there is a lack of temporal information. Only few techniques are routinely used in forensic investigations, e.g. determination of the time of death¹⁶⁹. Because of the importance to situate events in time, age estimation techniques are one of the holy grails in forensic science. In this

thesis, we described how blood stains can be dated using visible and NIR spectroscopy and hyperspectral imaging.

9.4.a VISIBLE SPECTROSCOPY AND HYPERSPECTRAL IMAGING

In **Chapter 4** we described how the age of blood stains on white backgrounds can be estimated by the analysis of their visible reflectance spectra, which can either be measured using spectroscopy or hyperspectral imaging. From these spectra, we not only derived the presence of the haemoglobin derivatives used for identification purposes, but were able to deduce their relative concentrations. This way we gained insight in the chemical reactions taking place in the blood stains. By comparison with a reference dataset, the measured concentrations were used to estimate the age of a questioned blood stain.

In **Chapter 5** we adapted the light transport model used to be able to correct for background absorptions and demonstrated the applicability of this technique for blood stain age estimation in casework. In a recent case we estimated the age of blood stains using reflectance spectroscopy. A statistical approach was introduced to calculate an age interval. At the scene of a presumed double homicide followed by suicide, we analyzed blood stains on several backgrounds at two distinct locations: downstairs where the victims were found, and upstairs. The results indicated that the group of blood stains found upstairs was older than the blood stains found in the vicinity of the bodies downstairs, suggesting that the blood stains found upstairs were not related to the crime. DNA evidence showed that the blood stains upstairs all belonged to one of the victims, who lived in the residence. The time interval estimated for the creation of the blood stains downstairs included the moment gun shots were heard by a witness. Combined with other evidence, the gathered information could lead to a better reconstruction of the timeline of events.

9.4.b NEAR INFRARED SPECTROSCOPY

In **Chapter 7** we successfully explored NIR spectroscopy for the age estimation of blood stains on dark backgrounds. While visible spectroscopy provides information about chromophores, NIR spectroscopy gives insight in molecular vibrations induced by the interaction with light. As a result, NIR spectroscopy gives more insight in the chemical structure of samples compared to visible spectroscopy. However, while only a few clearly distinguishable chromophores, i.e. the haemoglobin derivatives, absorb visible light, it is less clear which components present in blood stains contribute to the absorption of NIR light, because the molecular vibrations are not specific for one certain molecule. The large number of possibly absorbing components, among which haemoglobin, albumin, and globulin, complicated the analysis and compelled us to use a different approach for the data analysis. We chose Partial Least Squares (PLS) regression for the age estimation task. PLS is a useful statistical tool for the analysis of spectroscopic data, as it can handle datasets with more variables than measurements, and the data may contain highly correlated predictor variables¹³¹. PLS makes linear combinations of the original predictor variables to construct new variables, which are the most relevant for estimating the age. We built a PLS model using a training set of blood stains on black cotton and tested it on blood stains on red, green and blue cotton. The results demonstrated that we were able to estimate the age of blood stains independent of the background colour. Different background materials however may introduce new absorption peaks, which can disturb the age estimation task, demanding a new training set.

9.5. SPECTRAL PRE-PROCESSING

When moving a laboratory technique to the crime scene, the measurement setup is typically less controlled, e.g. the distance from different samples to the detector may vary. To reduce spectral variability caused by these variations in the measurement geometry, we needed advanced pre-processing of the data. By using the standard normal variate correction algorithm, we were able to

correct for spectral differences which were due to physical variability such as illumination intensity differences rather than chemical variability, as shown in Figure 9. The introduction of this correction algorithm was an important step needed for the practical applicability of the technique. Without this correction, blood stains of the same age show big spectral differences, e.g. the offset, which makes it difficult to distinguish blood stains of different ages. After correcting the spectra, the physical differences between blood stains of the same age disappear and the chemical differences between blood stains of different ages remain clearly distinguishable. Several other pre-processing techniques have been explored, e.g. multiplicative scatter correction, derivation, and smoothing (see **Chapter 2** for a description of these techniques), but have not proven their added value. The main risk when using such techniques is the loss of informative peaks and the creation of artefacts.

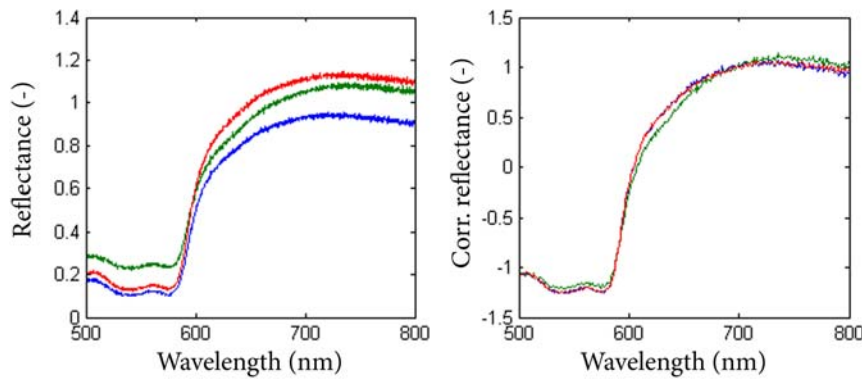


Figure 9.1. Reflectance spectra of blood stains without correction (left) and with standard normal variate correction (right). After correction the spectra of blood stains with the same age overlap (red and blue lines, 2 hours old) and are clearly separated from a spectrum of a blood stain with a different age (green line, 3 hours old).

9.6. DATA ANALYSIS

After pre-processing of the data, the main challenge was to extract the chemical changes from the reflectance spectra and relate them to the age of blood stains. We used a physical approach to gain insight in the concentration

of oxyhaemoglobin, methaemoglobin and hemichrome present in blood stains, which in turn can be used to estimate the age. Other research groups used a statistical or an empirical approach to analyse similar data, on which we elaborate below.

9.6.a PHYSICAL APPROACH

Although the changing absorption properties are clearly notable in the corrected reflectance spectra of blood stains, more factors influence the shape of the spectra. The difference between emitted and detected light not only results from light absorption, but photons are moreover lost by other interactions with a blood stain, e.g. scattering, transmission and specular reflections. The blood stain substrate complicates the situation even more, by likewise reflecting, transmitting, scattering and absorbing light.

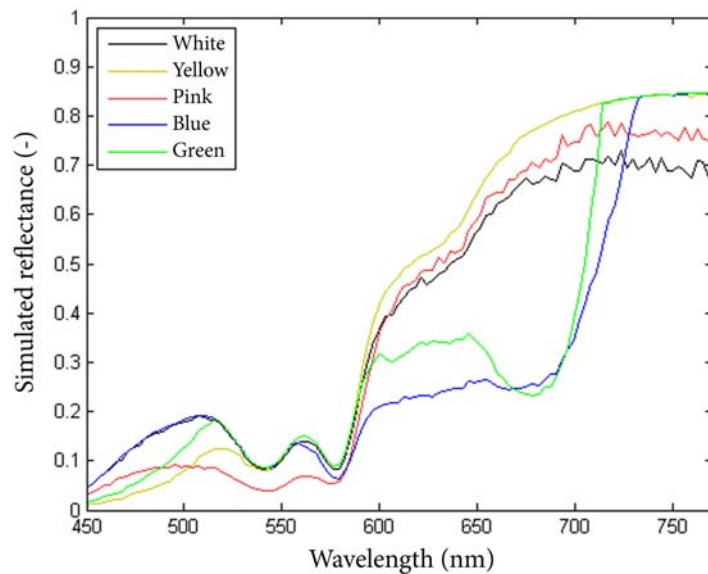


Figure 9.2. Simulated reflectance spectra for blood stains of 30 μm on white, yellow, pink, blue and green backgrounds.

To demonstrate the effect of the background colour on the reflectance spectra we simulated a two-layered sample, consisting of a layer of blood and a background layer using the Monte Carlo technique¹⁷⁰ (Figure 9.2). Reflectance spectra of blood stains with green and blue backgrounds show dips around 680 nm, whereas spectra of yellow and pink backgrounds mainly deviate from the white background in the short wavelength region. These background interferences have to be taken into account to deduce solely the contribution of absorption by the blood stain, from which the chemical composition of the blood stain can be deduced.

The complex interaction of the incoming light with a blood stain and its background can be approximated using a two flux model, in which an upward and downward flux of light are transported. This model leads to a system of differential equations, which can be solved analytically to give a relationship between the reflectance and the absorption and scattering properties of a sample, as described in **Chapter 5**:

$$R = \frac{1 - R_b \cdot (a - b \cdot \coth(bST))}{a - R_b + b \cdot \coth(bST)}, \text{ with } a = \frac{S + K}{S} \text{ and } b = \sqrt{a^2 - 1}, \quad (9.1)$$

where R is the reflectance, R_b the reflectance of the background, S is a scattering coefficient, K an absorption coefficient and T is the blood stain thickness⁸⁶. As a first approximation, the presence of a background was disregarded in **Chapter 4**, by assuming a blood layer of infinite thickness interacting with the incoming light, which reduces the formula:

$$R = 1 - \frac{K}{S} \left(\sqrt{1 + \frac{2S}{K}} - 1 \right). \quad (9.2)$$

By fitting this equation with the measured reflectance spectra, we successfully calculated the haemoglobin derivative fractions for blood stains on white cotton. In **Chapter 5** we extended this method, by taking the contribution of the background into account, as described in equation 9.1. In theory, this

method works for each background, as the reflectance of the clean background can be measured and incorporated in the model.

9.6.b STATISTICAL APPROACH

Recently, more research groups have studied the use of hyperspectral imaging either for blood stain identification or age estimation purposes. While the data acquisition methods of these groups were similar, the main difference lies in the approach of the data analysis. Li et al proposed a statistical method for blood stain identification and age estimation based on linear discriminant analysis (LDA)^{67, 68}. LDA is a multivariate classification algorithm Li et al used to separate a class of blood stains from other stains (the identification task) and to categorize the blood stains in predefined age classes (the age estimation task). Using a training set, the LDA algorithm selects wavelengths with a minimal within class variability and a maximum between class variability, whereupon a linear combination of these wavelengths is used for classification. For this approach to be successful, it is important that the training set used is representative for the questioned blood stain. In forensic practice, if blood stains are found on other backgrounds or in other environmental circumstances, a new training set is thus required, representative for the situation at the crime scene.

9.6.c EMPIRICAL APPROACH

Apart from the physical and statistical approaches described above, reflectance spectra can be analysed using an empirical approach. In an attempt to develop a method for the identification of blood stains applicable for many different backgrounds, Janchaysang et al acquired several empirical criteria for the detection and identification of blood stains based on their reflectance spectra or mathematical transformations of these spectra, e.g. the absorbance at a certain wavelength should not exceed a certain threshold¹⁷¹. Each questioned stain was tested upon all criteria using Boolean logic, and was excluded or included accordingly. Although criteria were selected based on empirically

collected data from blood stains on a variety of substrates, it remains difficult to extrapolate this method to the infinite amount of backgrounds possibly encountered at the crime scene.

9.7. MULTIDISCIPLINARY APPROACH

As demonstrated in this thesis, one of the main challenges when performing spectral measurements at the crime scene is how to correct for background interferences. These interferences are a general problem encountered in forensic applications, where traces are typically not found on ideal neutrally reflecting backgrounds used in laboratories, but all possible backgrounds can be encountered (e.g. different materials, porous, non-porous, coloured, patterned, etc.). Although all spectroscopic techniques are hampered by certain backgrounds, different techniques can be complementary. Therefore, a multidisciplinary approach is advised in which several techniques are combined to optimize the results for each specific background.

We introduced a method to correct for coloured backgrounds which cause interference in visible reflectance spectra (**Chapter 5**). On dark backgrounds however, light absorption of the background is dominant and hampers the use of visible reflectance spectroscopy or hyperspectral imaging for the identification and age estimation of blood stains. NIR spectroscopy can be used instead (**Chapter 6**), but is on its turn hampered by dominating water absorptions when blood stains are wet.

9.7.a OTHER SPECTROSCOPIC TECHNIQUES

Apart from the techniques explored in this thesis, several other non-destructive spectroscopic techniques may provide information useful for the analysis of blood stains. Raman spectroscopy is a vibrational technique complementary to NIR spectroscopy. Raman spectra generally have sharper and better resolved peaks than NIR spectra, and can provide more chemical information of unknown samples. Recently, several research groups have studied the use of Raman for the identification of blood stains^{84, 103, 147}. It was demonstrated that

blood stains can be identified based on their Raman spectra, and that human blood can be distinguished from blood from other species¹⁰⁴. Because quantitative information about haemoglobin derivatives can be derived from Raman spectra, it may also be possible to use them for age estimation of blood stains in the future^{172, 173}. However, Raman spectroscopy is complicated by strongly fluorescing backgrounds, like fabrics¹⁰⁵. Furthermore, Raman spectra can be very complex and can contain broad and superimposed bands, especially for biological samples, which often include spectral features of multiple constituents: proteins, lipids, DNA, RNA, individual amino acids, biological chromophores (haemoglobin), and other metabolites¹⁴⁷. The extraction of useful information requires advanced data analysis.

Even more chemical information about blood stains can be obtained by means of the mid infrared (mid IR) wavelength region. In **Chapter 8** we used Mid IR imaging for the detection of blood stains. It would be interesting to extend this to Mid IR hyperspectral imaging or spectroscopy. Mid IR reflectance spectroscopy provides information about fundamental molecular vibrations, of which overtones and combination bands are visible in the NIR region^{138, 142}. Although no forensic applications of mid IR spectroscopy for the analysis of blood stains are described, it may be worthwhile to explore. On the other side of the electromagnetic spectrum, with wavelengths shorter than the visible region, ultraviolet (UV) spectra may provide useful information as well. Using UV-Vis spectroscopy Hanson and Ballantyne revealed a blue shift in the so-called Soret band of haemoglobin. The peak of this band starts at 412 nm in fresh blood stains and shifts to shorter wavelengths as the age of the stain increases¹⁷⁴. Because of its high absorption intensity, using the Soret band is expected to be highly effective for the identification and age estimation of blood stains. Further research in this wavelength range is recommended. If we move to even shorter wavelengths, we arrive in the region of X-ray radiation. Trombka et al explored the use of X-ray fluorescence (XRF) for the identification of blood stains¹⁷⁵. XRF is an analytical method which can identify the elemental composition of a sample. Trombka et al showed that XRF allows the identification of blood by the detection of iron present in the haemoglobin molecule. To test the practical value of this technique, the specificity and

sensitivity of this technique must be studied. Also, possible background interferences are yet unknown.

9.7.b OTHER TECHNIQUES

Apart from the optical spectroscopic methods described above, other methods for age estimation have been explored in the past, as reviewed by Bremmer et al, e.g. high performance liquid chromatography, electron paramagnetic resonance, atomic force microscopy and RNA degradation measurements⁹⁴. These methods are more invasive and can only be performed in the laboratory.

Recently, Gas Chromatography- Mass Spectrometry (GC-MS) has been explored to study the composition and degradation of fingerprints¹⁷⁶. Similarly, MS has the potential to become an important tool for the age estimation of blood stains, due to its simplicity, sensitivity and effectiveness in separating and identifying chemical components. Portable GC-MS systems enable the application of mass spectrometry in non-laboratory environments, but they still require extensive sample preparation due to the constraints of chromatography, thus increasing total analysis time. Ambient MS techniques have greatly simplified and increased the speed of MS analysis, and can be performed directly on samples, including complex matrices such as biological fluids in their natural environment¹⁷⁷. One of the simplest ambient MS methods reported is paper spray MS, which generates ions by applying a high voltage to a paper triangle wetted with a small volume of a solution. Samples can be transferred from surfaces using the paper as a swab. Paper spray MS has proven to be highly useful for drug monitoring from whole blood spots¹⁷⁸. The applicability of this relatively new technique in forensic casework however, remains largely uninvestigated.

The well-known expression “Absence of evidence is not evidence of absence” can be used to demonstrate the limitations of forensic techniques. No single technique is capable to detect and identify all types of traces at the crime scene without the need of further confirmation. By combining several (spectroscopic) techniques and selecting the optimal technique for each background, the applicability of methods for detection, identification and age

estimation of blood stains in forensic practice can be extended. All information gained with different techniques can be useful for a crime scene investigator, provided they are correctly interpreted. To determine which technique is favourable in certain circumstances, it is important to study the boundaries of each technique.

9.8. TOWARDS IMPLEMENTATION

Before the new method for age estimation of blood stains described in **Chapter 5** can be applied in standard forensic practice, key steps in the research process are refining and validating the data to meet the needs of the legal and scientific communities. It is important to explore the boundaries of the technique and to describe the limitations, e.g. minimal blood stain size, minimal and maximum blood stain thickness, and requirements of the background colour, porosity etc. Furthermore, the effect of different aging circumstances should be known.

9.8.a ENVIRONMENTAL INFLUENCES

The described approach of splitting the spectra into the different chemical components (**Chapter 4, 5**) has the advantage that the influence of temperature, humidity or other environmental circumstances can be studied. As described by Bremmer et al, the temperature increases the speed of the chemical reactions in a blood stain, whereas humidity only influences the denaturation of methaemoglobin into hemichrome⁵⁶. The influence of environmental factors at the crime scene will make precise estimation of the absolute age of blood stains challenging. If the environmental factors can be reconstructed we are able to study the kinetics of the haemoglobin derivatives, which can be used to estimate the absolute ages of blood stains, as shown in the case example in **Chapter 5**. Additionally, even in unknown circumstances, we demonstrated the possibility to determine the relative age of different blood stains, under the assumption that they were exposed to similar environmental conditions. Because the fraction of HbO₂ decreases in time, this fraction can be

used to determine the order of formation of different blood stains, as demonstrated by the analysis of the simulated crime scene in **Chapter 4**.

9.8.b HUMAN VARIABILITY

Apart from the environmental circumstances, more research is needed to gain knowledge about the biological variability between and within humans. In a prior study of Bremmer et al¹, no significant differences were found between or within donors. Because we analysed blood of healthy non-smoking volunteers who usually have only a small percentage (<4%) of carboxyhaemoglobin⁹⁹, the possible presence of this haemoglobin derivative was not taken into account in this thesis. The increased level of carboxyhaemoglobin expected for smokers, people suffering from sickle cell disease, fire victims or in cases of fatal carbon monoxide poisoning, may influence the results in forensic practice¹⁰⁰⁻¹⁰². However, because our model does not include the absorption properties of carboxyhaemoglobin, we expect a bad correlation between the measured reflectance spectrum and the theoretical fit. By embedding a threshold for this correlation as a quality check for the fit (**Chapter 4, 5**), results will be inconclusive in these cases, rather than giving a wrong age estimation.

9.8.c BLOOD STAIN THICKNESS

Another source of spectral variation is the blood stain thickness. Monte Carlo simulations of reflectance spectra of blood stains with various thicknesses on a white background are shown in Figure 9.3. As expected, this figure shows that the overall reflectance is higher for thinner blood stains. For thicker blood stains, the characteristic absorption features of oxyhaemoglobin (dips at 540 and 576 nm) and methaemoglobin (dip at 630 nm) are less pronounced⁸². The influence of the blood stain thickness on the identification (**Chapter 3**) and age estimation (**Chapter 4, 5**) tasks should be studied to gain insight in the limitations of the technique. Thick blood stains are expected to complicate the

analysis due to their high absorption and thus low signal to noise ratios, whereas thin blood stains will be greatly influenced by the background.

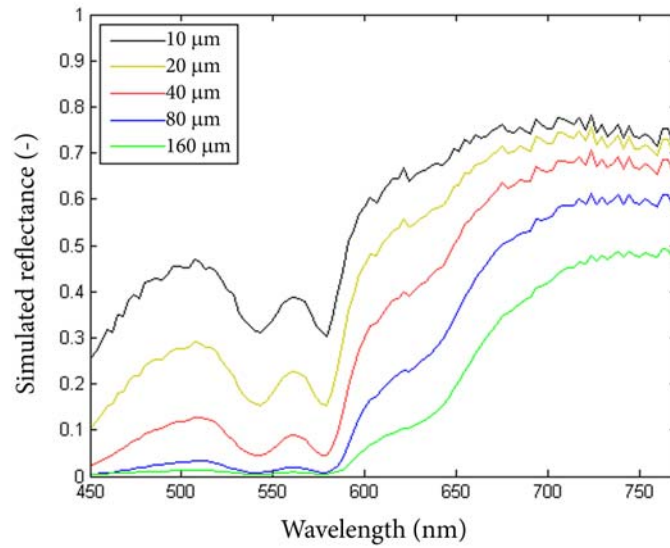


Figure 9.3. Simulated reflectance spectra for blood stains of 10, 20, 40, 80 and 160 μm on a white background.

9.8.d COLLECTION OF BLOOD STAINS

In case the background interference is too dominant to correct for, no matter which technique is used, blood stains can be extracted from the background to be applied on an ideal non-interfering background (e.g. white cotton when visible spectroscopy is used). This practical approach enables investigators to bring a blood stain to the laboratory for further analysis. The challenge in this case, however, lies in the fact that the chemical composition of the blood stain may not be changed while transferring it to another background. Traditional collection of blood stains with moistened cotton swabs will alter their chemical composition, as the addition of water to a blood stain is known to induce the transition from hemichrome back to methaemoglobin¹⁰⁹. Further research is needed to invent a collection procedure which does not influence the results of the age estimation task. When successful, stains may be collected from the

scene and stored deep-frozen to slow down or even stop any further chemical reactions taking place before the analysis is performed. In that case however, the method is no longer non-destructive.

9.8.e ACCURACY

In forensic practice, many factors contribute to spectral differences which increase the calculated confidence intervals for age estimations, e.g. detector noise, biological variations in blood stains, environmental differences, etcetera. Additionally, there will be errors in the estimated haemoglobin derivative concentrations due to imperfect corrections for blood stain thickness, and background optical properties. To culminate small age intervals, we recommend to perform spectroscopic measurements as soon as possible. The chemical reactions taking place in the blood stains are rapid in the beginning, but slower in a later stage⁵⁶. As a result, the accuracy of age estimations decreases with the age of the blood stain.

In the described case example (**Chapter 5**), it would have been interesting to know which person was shot first and what the time difference was between the different shots. Li et al demonstrated in a laboratory hyperspectral imaging setup that the age of blood stains can be determined with an accuracy of 1 hour within the first day after bleeding⁶⁸. If our measurements were performed immediately after discovery of the crime scene, it may have been possible to indicate the sequence of different blood stain patterns created around the victims (different blood stains found downstairs).

In forensic practice, the accuracy will depend on the actual age of the blood stain and knowledge of the environmental conditions. How this influences the evidential value depends on the hypotheses relevant to the case. Confidence intervals in casework are generally expected to be larger than intervals resulting from measurements performed in a laboratory setup.

9.8.f MOBILE ANALYSIS AT THE CRIME SCENE

The equipment used by crime scene investigators is ideally portable, wireless, waterproof, easily decontaminated and user-friendly. Recent technological advances enabled the development of fast, wireless, high resolution hyperspectral imaging systems, facilitating the transfer from the laboratory to the crime scene, as demonstrated in this thesis (Figure 9.4). The development of portable equipment enables the analysis of an unknown stain at the crime scene without waiting for results from the laboratory.



Figure 9.4. Photographs of a hyperspectral imaging system at a simulated crime scene.

Due to current developments hyperspectral imaging systems become smaller, more sensitive, user-friendly and cost effective. A next generation of snapshot systems is expected in the near future, consisting of a novel multispectral sensor integrating a tiled filter and a CMOS sensor. Similar to conventional Bayer filters used in colour imaging, a set of Fabry-Pérot filters can be chosen, filtering specific wavelengths needed for a certain application. While in the past spectral imaging technology developed from multispectral imaging using several broad wavelength bands, to hyperspectral imaging using many narrow wavelength bands, the new tiled filter based technique reduces the amount of wavelength bands again, but keeps the ability to use narrow wavelength bands. This evolution encourages the selection of wavelengths which are most relevant and informative to observe spectral differences. Prior knowledge about absorption properties, stepwise multiple linear regression, or multivariate

techniques such as Principal Component Analysis and Partial Least Squares can be explored for an optimal wavelength selection¹⁷⁹.

Another technology expected in the future is the use of adapted smartphones with additional filters, which can be used for the analysis of blood stains at the crime scene. Thanakiatkrai et al recently proposed to use smart phone cameras only for the age estimation of blood stains. Using an optimally controlled light box they successfully classified blood stains in broad age intervals. However, the described technique is expected to be highly sensitive to minimal changes in this setup, e.g. the camera used, the intensity of the light source, or the distance to the blood stain. Nevertheless, it is worthwhile to explore these new technologies for forensic analysis.

9.8.g CONCLUSION

In this thesis, we demonstrated several spectroscopic techniques for the non-destructive detection, identification and age estimation of blood stains at the crime scene. The non-destructive detection of latent blood stains, either by visible hyperspectral imaging or mid infrared imaging, facilitates bloodstain pattern analysis and the selection of relevant traces for DNA-analysis. Both visible and near infrared reflectance spectra show typical absorption properties of blood stain constituents, and can thus be used to discriminate blood from other substances. Subsequently, the age of blood stains can be estimated using these innovative techniques, providing investigators with new information which can be used to determine the moment a crime was committed, or whether certain blood stains are crime related. For more than a century, many research has been devoted to the development of techniques for age estimation of blood stains. However, to our knowledge, none of them have yet been implemented in standard forensic practice. We demonstrated a case example in which we successfully estimated the age of several blood stains. When introduced in criminal investigations, results can be used for incrimination or exclusion purposes and for elucidating criminal events.

10 - REFERENCES

1. Bremmer RH, Nadort A, van Leeuwen TG, van Gemert MJ, Aalders MC Age estimation of blood stains by hemoglobin derivative determination using reflectance spectroscopy. *Forensic Sci Int* 2011; 206: 166-171
2. Govender M, Chetty K, Bulcock H A review of hyperspectral remote sensing and its application in vegetation and water resource studies. *Water Sa* 2007; 33: 145-151
3. Gowen AA, O'Donnell CP, Cullen PJ, Downey G, Frias JM Hyperspectral imaging - an emerging process analytical tool for food quality and safety control. *Trends in Food Science & Technology* 2007; 18: 590-598
4. Gowen AA, O'Donnell CP, Cullen PJ, Bell SEJ Recent applications of Chemical Imaging to pharmaceutical process monitoring and quality control. *European Journal of Pharmaceutics and Biopharmaceutics* 2008; 69: 10-22
5. Levenson, R. M., Wachman, E. S., and Niu, W. Spectral imaging in biomedicine: a selective overview. M.R.Descour and S.S.Shen. *Imaging Spectrometry IV. Proceedings of SPIE 3438*, 300-312. 1998.
Ref Type: Conference Proceeding
6. Bremmer RH, Kanick SC, Laan N, Amelink A, van Leeuwen TG, Aalders MC Non-contact spectroscopic determination of large blood volume fractions in turbid media. *Biomed Opt Express* 2011; 2: 396-407
7. Suhre, D. R, Taylor, L. H., Singh, N. B., and Rosch, W. R. Comparison of acousto-optic tunable filters and acousto-optic dispersive filters for hyperspectral imaging. Mericsko, R. J. *27th AIPR Workshop: Advances in Computer-Assisted Recognition. Proceedings of SPIE 3584*, 142-147. 1999.
Ref Type: Conference Proceeding

8. Evans MD, Thai CN, Grant JC Development of a spectral imaging system based on a liquid crystal tunable filter. *Transactions of the Asac* 1998; 41: 1845-1852
9. Margalith, E. and Barnes, R. J. Spectral imaging device with tunable light source. Opotek, Inc. [US7233392]. 6-19-2007.
Ref Type: Patent
10. Qin J Instruments for Constructing Hyperspectral Imaging Systems. In: *Hyperspectral Imaging for Food Quality Analysis and Control*. Sun DW (ed). New York: Elsevier, 2010, 133-172
11. Kirkhus, T., Fismen, B. G., Tschudi, J., and O'Farrell, M. Calibration of a Multi-Object Spectrometer with Programmable and Arbitrary Field of View. *Applied Industrial Optics: Spectroscopy, Imaging and Metrology. Spectroscopy, Colour, & Imaging II* . 2010.
Ref Type: Conference Proceeding
12. Grahn HF, Geladi P *Techniques and Applications of Hyperspectral Image Analysis*. Chichester: John Wiley & Sons, Ltd, 2007
13. Geladi P, Burger J, Lestander T Hyperspectral imaging: calibration problems and solutions. *Chemometrics and Intelligent Laboratory Systems* 2004; 72: 209-217
14. Barnes RJ, Dhanoa MS, Lister SJ Standard Normal Variate Transformation and De-trending of Near-Infrared Diffuse Reflectance Spectra. *Appl Spectrosc* 1989; 43: 772-777
15. Burger, J. PhD thesis: Hyperspectral NIR image analysis: data exploration, correction and regression. 2006. Unit of Biomass Technology and Chemistry, Swedish University of Agricultural Sciences.
Ref Type: Thesis/Dissertation
16. Savitzky A, Golay MJE Smoothing and Differentiation of Data by Simplified Least Squares Procedures. *Anal Chem* 1964: 1627-1639

17. van der Meer F The effectiveness of spectral similarity measures for the analysis of hyperspectral imagery. *International Journal of Applied Earth Observation and Geoinformation* 2006; 8: 3-17
18. Edelman, G. J., van Leeuwen, T. G., and Aalders, M. C. G. Hyperspectral imaging of the crime scene for the automatic detection and identification of blood stains. *Algorithms and Technologies for Multispectral, Hyperspectral, and Ultraspectral Imagery XIX*, 87430A. *Proceedings of SPIE* . 2013.
Ref Type: Conference Proceeding
19. Edelman GJ, Manti V, van Ruth SM, van Leeuwen TG, Aalders MCG Identification and age estimation of blood stains on coloured backgrounds by near infrared spectroscopy. *Forensic Science International* 2012; 220: 239-244
20. Keshava N, Mustard JF Spectral unmixing. *Ieee Signal Processing Magazine* 2002; 19: 44-57
21. Alam, M. S., Elbakary, M. I., and Aslan, M. S. Object detection in hyperspectral imagery by using K-means clustering algorithm with pre-processing. Casasent, D. P. and Chao, T. *Optical Pattern Recognition XVIII. Proceedings of SPIE* . 2007.
Ref Type: Conference Proceeding
22. Wold S, Sjostrom M, Eriksson L PLS-regression: a basic tool of chemometrics. *Chemometrics and Intelligent Laboratory Systems* 2001; 58: 109-130
23. Shafri HZM, Suhaili A, Mansor S The Performance of Maximum Likelihood, Spectral Angle Mapper, Neural Network and Decision Tree Classifiers in Hyperspectral Image Analysis. *Journal of Computer Science* 2007; 3: 419-423
24. Alsberg BK, Loke T, Baarstad I **PryJector: A Device for In Situ Visualization of Chemical and Physical Property Distributions on Surfaces Using Projection and Hyperspectral Imaging.** *Journal of Forensic Sciences* 2011; 56: 976-983

25. Ng PH, Walker S, Tahtouh M, Reedy B Detection of illicit substances in fingerprints by infrared spectral imaging. *Anal Bioanal Chem* 2009; 394: 2039-2048
26. Ramotowski R Composition of Latent Print Residue. In: *Advances in Fingerprint Technology*. Lee Hc, Gaensslen R.E. (eds). Boca Raton, FL: CRC Press, 2001, 63-104
27. Bartick, E., Schwartz, R., Bhargava, R., Schaeberle, M., Fernandez, D., and Levin, I. Spectrochemical analysis and hyperspectral imaging of latent fingerprints. Baccino, E. 16th Meeting of the International Association of Forensic Sciences. 2002. Bologna, Monduzzi Editore. Ref Type: Conference Proceeding
28. Crane NJ, Bartick EG, Perlman RS, Huffman S Infrared spectroscopic imaging for noninvasive detection of latent fingerprints. *J Forensic Sci* 2007; 52: 48-53
29. Exline DL, Wallace C, Roux C, Lennard C, Nelson MP, Treado PJ Forensic applications of chemical imaging: latent fingerprint detection using visible absorption and luminescence. *J Forensic Sci* 2003; 48: 1047-1053
30. Payne G, Reedy B, Lennard C, Comber B, Exline D, Roux C A further study to investigate the detection and enhancement of latent fingerprints using visible absorption and luminescence chemical imaging. *Forensic Sci Int* 2005; 150: 33-51
31. Tahtouh M, Kalman JR, Roux C, Lennard C, Reedy BJ The detection and enhancement of latent fingermarks using infrared chemical imaging. *J Forensic Sci* 2005; 50: 64-72
32. Tahtouh M, Despland P, Shimmon R, Kalman JR, Reedy BJ The application of infrared chemical imaging to the detection and enhancement of latent fingerprints: method optimization and further findings. *J Forensic Sci* 2007; 52: 1089-1096
33. Bhargava R, Perlman RS, Fernandez DC, Levin IW, Bartick EG Non-invasive detection of superimposed latent fingerprints and inter-ridge

trace evidence by infrared spectroscopic imaging. *Anal Bioanal Chem* 2009; 394: 2069-2075

34. Champod C, Lennard C, Margot P, Stoilovic M Fingerprints and Other Ridge Skin Impressions. CRC Press, 2004
35. Miskelly GM, Wagner JH Using spectral information in forensic imaging. *Forensic Sci Int* 2005; 155: 112-118
36. Maynard P, Jenkins J, Edey C, Payne G, Lennard C, McDonagh A, Roux C Near infrared imaging for the improved detection of fingermarks on difficult surfaces. *Australian Journal of Forensic Sciences* 2009; 41: 43-62
37. Tahtouh M, Scott SA, Kalman JR, Reedy BJ Four novel alkyl 2-cyanoacrylate monomers and their use in latent fingermark detection by mid-infrared spectral imaging. *Forensic Sci Int* 2011; 207: 223-238
38. Grant A, Wilkinson TJ, Holman DR, Martin MC Identification of recently handled materials by analysis of latent human fingerprints using infrared spectromicroscopy. *Appl Spectrosc* 2005; 59: 1182-1187
39. Bhargava R, Perlman RS, Fernandez DC, Levin IW, Bartick EG Non-invasive detection of superimposed latent fingerprints and inter-ridge trace evidence by infrared spectroscopic imaging. *Anal Bioanal Chem* 2009; 394: 2069-2075
40. Emmons ED, Tripathi A, Guicheteau JA, Christesen SD, Fountain AW, III Raman chemical imaging of explosive-contaminated fingerprints. *Appl Spectrosc* 2009; 63: 1197-1203
41. Chen T, Schultz ZD, Levin IW Infrared spectroscopic imaging of latent fingerprints and associated forensic evidence. *Analyst* 2009; 134: 1902-1904
42. Kalasinsky KS, Magluilo J, Jr., Schaefer T Hair analysis by infrared microscopy for drugs of abuse. *Forensic Sci Int* 1993; 63: 253-260

43. Kalasinsky KS Drug distribution in human hair by infrared microscopy. *Cellular and Molecular Biology* 1998; 44: 81-87
44. Birngruber C, Ramsthaler F, Verhoff MA The colour(s) of human hair-forensic hair analysis with SpectraCube. *Forensic Sci Int* 2009; 185: e19-e23
45. Tramini P, Bonnet B, Sabatier R, Maury L A method of age estimation using Raman microspectrometry imaging of the human dentin. *Forensic Sci Int* 2001; 118: 1-9
46. Randeberg LL, Larsen EL, Svaasand LO Characterization of vascular structures and skin bruises using hyperspectral imaging, image analysis and diffusion theory. *Journal of Biophotonics* 2010; 3: 53-65
47. Payne G, Langlois N, Lennard C, Roux C Applying visible hyperspectral (chemical) imaging to estimate the age of bruises. *Med Sci Law* 2007; 47: 225-232
48. Stam B, van Gemert MJC, van Leeuwen TG, Teeuw AH, van der Wal AC, Aalders MCG Can colour inhomogeneity of bruises be used to establish their age? *J Biophotonics* 2011; 4: 759-767
49. Edelman GJ, van Leeuwen TG, Aalders MCG Hyperspectral imaging for the age estimation of blood stains at the crime scene. *Forensic Science International* 2012; 223: 72-77
50. Wolfe J, Exline DL Characterization of condom lubricant components using Raman spectroscopy and Raman chemical imaging. *J Forensic Sci* 2003; 48: 1065-1074
51. Payne G, Wallace C, Reedy B, Lennard C, Schuler R, Exline D, Roux C Visible and near-infrared chemical imaging methods for the analysis of selected forensic samples. *Talanta* 2005; 67: 334-344
52. Flynn K, O'Leary R, Lennard C, Roux C, Reedy BJ Forensic applications of infrared chemical imaging: multi-layered paint chips. *J Forensic Sci* 2005; 50: 832-841

53. Flynn K, O'Leary R, Roux C, Reedy BJ Forensic analysis of bicomponent fibers using infrared chemical imaging. *J Forensic Sci* 2006; 51: 586-596
54. Markstrom LJ, Mabbott GA Obtaining absorption spectra from single textile fibers using a liquid crystal tubable filter microspectrophotometer. *Forensic Science International* 2011; 209: 108-112
55. Kalacska ME, Bell LS, Sanchez-Azofeifa G, Caelli T The Application of Remote Sensing for Detecting Mass Graves: An Experimental Animal Case Study from Costa Rica. *Journal of Forensic Sciences* 2009; 54: 159-166
56. Bremmer RH, de Bruin DM, de Joode M, Buma WJ, van Leeuwen TG, Aalders MCG Biphasic Oxidation of oxy-hemoglobin in bloodstains. *PLoS One* 2012; 6: e21845
57. Gebhart SC, Majumder SK, Mahadevan-Jansen A Comparison of spectral variation from spectroscopy to spectral imaging. *Applied Optics* 2007; 46: 1343-1360
58. Tungol MW, Bartick EG, Montaser A Spectral Data-Base for the Identification of Fibers by Infrared Microscopy. *Spectrochimica Acta Part B-Atomic Spectroscopy* 1991; 46: e1535-e1544
59. Merrill RA, Bartick EG, Taylor JH Forensic discrimination of photocopy and printer toners. I. The development of an infrared spectral library. *Analytical and Bioanalytical Chemistry* 2003; 376: 1272-1278
60. Adler-Golden, S. M., Levine, R. Y., Matthew, M. W., Richtsmeier, S. C., Bernstein, L. S., Gruninger, J., Felde, G., Holke, M., Anderson, G., and Ratkowski, A. Shadow-insensitive material detection/classification with atmospherically corrected hyperspectral imagery. *SPIE* 4381 [Algorithms for Multispectral, Hyperspectral, and Ultraspectral Imagery VII], 460-469. 2001.
Ref Type: Conference Proceeding

61. Stoilovic M Detection of Semen and Blood Stains Using Polilight As A Light-Source. *Forensic Science International* 1991; 51: 289-296
62. Kunicki M Differentiating blue ballpoint pen inks. *Prob Forensic Sci LI* 2002: 56-70
63. Mokrzycki GM Advances in Document Examination: The Video Spectral Comparator 2000. *Forensic Science Communications* 1999; 1: 1-6
64. Atwater CS, Durina ME, Durina JP, Blackledge RD Visualization of gunshot residue patterns on dark clothing. *J Forensic Sci* 2006; 51: 1091-1095
65. Bremmer RH, Edelman G, Vegter TD, Bijvoets T, Aalders MCG Remote Spectroscopic Identification of Bloodstains. *Journal of Forensic Sciences* 2011; 56: 1471-1475
66. Botonjic-Sehic E, Brown CW, Lamontagne M, Tsaparikos M Forensic Application of Near-Infrared Spectroscopy: Aging of Bloodstains. *Spectroscopy* 2009; 24: 42-49
67. Li B, Beveridge P, O'Hare WT, Islam M The estimation of the age of a blood stain using reflectance spectroscopy with a microspectrophotometer, spectral pre-processing and linear discriminant analysis. *Forensic Science International* 2011; 212: 198-204
68. Li B, Beveridge P, O'Hare WT, Islam M The age estimation of blood stains up to 30 days old using visible wavelength hyperspectral image analysis and linear discriminant analysis. *Science and Justice* 2013; 53: 270-277
69. Peschel O, Muetzel E, Rothschild MA Blood stain pattern analysis. *Rechtsmedizin* 2008; 18: 131-145
70. Virkler K, Lednev IK Forensic body fluid identification: The Raman spectroscopic signature of saliva. *Analyst* 2010; 135: 512-517

71. Hodges CM, Akhavan J The Use of Fourier-Transform Raman-Spectroscopy in the Forensic Identification of Illicit Drugs and Explosives. *Spectrochimica Acta Part A-Molecular and Biomolecular Spectroscopy* 1990; 46: 303-307
72. McNesby KL, Pesce-Rodriguez RA Applications of vibrational spectroscopy in the study of explosives. In: *Handbook of Vibrational Spectroscopy*. Chalmers JM, Griffiths P.R. (eds). Chichester, England: John Wiley & Sons Ltd., 2002, 3152-3168
73. Malkoff, D. B. and Oliver, W. R. Hyperspectral imaging applied to forensic medicine. Bearman, G. H., Cabib, D., and Levenson, R. M. *Spectral imaging: Instrumentation, Applications and Analysis*. SPIE 3920, 108-116. 2000.
Ref Type: Conference Proceeding
74. Virkler K, Lednev IK Analysis of body fluids for forensic purposes: from laboratory testing to non-destructive rapid confirmatory identification at a crime scene. *Forensic Sci Int* 2009; 188: 1-17
75. Lomholt B, Keiding N Tetrabase, an alternative to benzidine and orthotolidine for detection of hemoglobin in urine. *The Lancet* 1977; 1: 608-609
76. Blum LJ, Esperanca P, Rocquefelte S A new high-performance reagent and procedure for latent blood stain detection based on luminol chemiluminescence. *Can Soc Forensic Sci J* 2006; 39: 20
77. Kent EJM, Elliot DA, Miskelly GM Inhibition of bleach-induced luminol chemiluminescence. *Journal of Forensic Sciences* 2003; 48: 64-67
78. Saferstein R *Criminalistics - an introduction to forensic science*. Prentice hall, 2004
79. James SH, Nordby JJ *Forensic Science: An Introduction to Scientific and Investigative Techniques*. Taylor&Francis, 2005

80. Zubakov D, Hanekamp E, Kokshoorn M, van IJcken W, Kayser M Stable RNA markers for identification of blood and saliva stains revealed from whole enome expression analysis of time-wise degraded samples. *Int J Legal Med* 2008; 122: 135-142
81. De Wael K, Lepot L, Gason F, Gilbert B In search of blood - Detection of minute particles using spectroscopic methods. *Forensic Science International* 2008; 180: 37-42
82. Zijlstra WG, Buursma A, Meeuwsen-Vanderroest WP Absorption spectra of human fetal and adult oxyhemoglobin, de-oxyhemoglobin, carboxyhemoglobin, and methemoglobin. *Clinical Chemistry* 1991; 37: 1633-1638
83. Nagababu E, Rifkind JM Formation of fluorescent heme degradation products during the oxidation of hemoglobin by hydrogen peroxide. *Biomedical and Biophysical Research Communications* 1998; 247: 592-596
84. Virkler K, Lednev IK Raman spectroscopic signature of blood and its potential application to forensic body fluid identification. *Analytical and Bioanalytical Chemistry* 2010; 396: 525-534
85. Kotowski TM, Grieve MC The use of microspectrophotometry to characterize microscopic amounts of blood. *J Forensic Sci* 1986; 31: 1079-1085
86. Gemert MJC, Welch AJ, Star WM One-dimensional transport theory. In: *Optical-thermal response of laser-irradiated tissue*. Welch AJ, Gemert M.J.C. (eds). New York: Springer science+business media, LLC, 1995, 47-72
87. Cheong W, Prahl S, Welch A A review of the optical properties of biological tissues. *IEEE Journal of quantum electronics* 1990; 26: 2166-2185
88. Inoue H, Takabe F, Iwasa M, Maeno Y, Seko Y A New Marker for Estimation of Bloodstain Age by High-Performance Liquid-Chromatography. *Forensic Science International* 1992; 57: 17-27

89. Miki T, Kai A, Ikeya M Electron-Spin Resonance of Bloodstains and Its Application to the Estimation of Time After Bleeding. *Forensic Science International* 1987; 35: 149-158
90. Fujita Y, Tsuchiya K, Abe S, Takiguchi Y, Kubo S, Sakurai H Estimation of the age of human bloodstains by electron paramagnetic resonance spectroscopy: Long-term controlled experiment on the effects of environmental factors. *Forensic Science International* 2005; 152: 39-43
91. Strasser S, Zink A, Kada G, Hinterdorfer P, Peschel O, Heckl WM, Nerlich AG, Thalhammer S Age determination of blood spots in forensic medicine by force spectroscopy. *Forensic Science International* 2007; 170: 8-14
92. Bauer M, Polzin S, Patzelt D Quantification of RNA degradation by semi-quantitative duplex and competitive RT-PCR: a possible indicator of the age of bloodstains? *Forensic Science International* 2003; 138: 94-103
93. Anderson S, Howard B, Hobbs GR, Bishop CP A method for determining the age of a bloodstain. *Forensic Science International* 2005; 148: 37-45
94. Bremmer RH, de Bruin KG, van Gemert MJC, van Leeuwen TG, Aalders MCG Forensic quest for age determination of bloodstains. *Forensic Science International* 2012; 216: 1-11
95. Barnes RJ, Dhanoa MS, Lister SJ Standard Normal Variate Transformation and De-trending of Near-Infrared Diffuse Reflectance Spectra. *Appl Spectrosc* 1989; 43: 772-777
96. Asakura T, Minakata K, Adachi K, Russell MO, Schwartz E Denatured Hemoglobin in Sickle Erythrocytes. *Journal of Clinical Investigation* 1977; 59: 633-640
97. Cover TM Citation Classic - Nearest Neighbor Pattern-Classification. *Current Contents/Engineering Technology & Applied Sciences* 1982: 20

98. Jain AK Data clustering: 50 years beyond K-means. *Pattern Recognition Letters* 2010; 31: 651-666
99. Woebkenberg NR, Mostardi RA, Ely DL, Worstell D Carboxyhemoglobin and Methemoglobin Levels in Residents Living in industrial and Nonindustrial Communities. *Environmental research* 2011; 26: 347-352
100. Teige B, Lundevall J, Fleischer E Carboxyhemoglobin Concentrations in Fire Victims and in Cases of Fatal Carbon-Monoxide Poisoning. *Zeitschrift fur Rechtsmedizin-Journal of Legal Medicine* 1977; 80: 17-21
101. Wald NJ, Idle M, Boreham J, Bailey A Carbon monoxide in breath in relation to smoking and carboxyhaemoglobin levels. *Thorax* 1981; 36: 366-369
102. Sears DA, Udden MM, Thomas LJ Carboxyhemoglobin levels in patients with sickle-cell anemia: Relationship to hemolytic and vasoocclusive severity. *American Journal of the Medical Sciences* 2001; 322: 345-348
103. Boyd S, Bertino MF, Seashols SJ Raman spectroscopy of blood samples for forensic applications. *Forensic Science International* 2011; 208: 124-128
104. Virkler K, Lednev IK Blood Species Identification for Forensic Purposes Using Raman Spectroscopy Combined with Advanced Statistical Analysis. *Analytical Chemistry* 2009; 81: 7773-7777
105. McLaughlin G, Sikirzhyski V, Lednev IK Circumventing substrate interference in the Raman spectroscopic identification of blood stains. *Forensic Science International* 2013; 231: 157-166
106. Maddala GS *Econometrics*. New York: McGraw-Hill, 1977
107. Bremmer RH, Nadort A, van Leeuwen TG, van Gemert MJ, Aalders MC Age estimation of blood stains by hemoglobin derivative

- determination using reflectance spectroscopy. *Forensic Sci Int* 2011; 206: 166-171
108. Bai J Estimation of a change point in multiple regression models. *The review of economics and statistics* 1997; 79: 551-563
 109. Colombo MF, Sanches R Hydration-dependent conformational states of hemoglobin - Equilibrium and kinetic behavior. *Biophysical Chemistry* 1990; 36: 33-39
 110. Tina Young A Photographic Comparison of Luminol, Fluorescein, and Bluestar. *Journal of Forensic Identification* 2006; 56: 906-912
 111. Perkins M The Application of Infrared Photography in Bloodstain Pattern Documentation of Clothing. *Journal of Forensic Identification* 2005; 55: 1-9
 112. Raymond MA, Hall RL An interesting application of infrared reflection photography to blood splash pattern interpretation. *Forensic Sci Int* 1986; 31: 189-194
 113. Lin ACY, Hsieh HM, Tsai LC, Linacre A, Lee JCI Forensic applications of infrared imaging for the detection and recording of latent evidence. *Journal of Forensic Sciences* 2007; 52: 1148-1150
 114. Schuler RL, Kish PE, Plese CA Preliminary Observations on the Ability of Hyperspectral Imaging to Provide Detection and Visualization of Bloodstain Patterns on Black Fabrics. *J Forensic Sci* 2012; 57: 1562-1569
 115. Rodarmel C, Shan J. Principal Component Analysis for Hyperspectral Image Classification. *Surveying and Land Information Systems* 2002; 62: 115-123
 116. Windig W, Guilment J Interactive Self-Modeling Mixture Analysis. *Analytical Chemistry* 1991; 63: 1425-1432

117. Edelman GJ, Gaston E, van Leeuwen, Cullen PJ, Aalders MC
Hyperspectral imaging for non-contact analysis of forensic traces.
Forensic Sci Int 2012; 223: 28-39
118. Lomax RG *Statistical concepts: a second course*. Mahwah: Lawrence
Erlbaum Associates, 2000
119. Jaumot J, Gargallo R, de Juan A, Tauler R A graphical user-friendly
interface for MCR-ALS: a new tool for multivariate curve resolution in
MATLAB. *Chemometrics and Intelligent Laboratory Systems* 2005; 76:
101-110
120. Budowle B, Leggitt JL, Defenbaugh DA, Keys KM, Malkiewicz SF The
presumptive reagent fluorescein for detection of dilute bloodstains and
subsequent STR typing of recovered DNA. *Journal of Forensic
Sciences* 2000; 45: 1090-1092
121. Barni F, Lewis SW, Berti A, Miskelly GM, Lago G Forensic application
of the luminol reaction as a presumptive test for latent blood detection.
Talanta 2007; 72: 896-913
122. Tobe SS, Watson N, Nic Daeid N Evaluation of six presumptive tests
for blood, their specificity, sensitivity, and effect on high molecular-
weight DNA. *Journal of Forensic Sciences* 2007; 52: 102-109
123. Virkler K, Lednev IK Analysis of body fluids for forensic purposes:
From laboratory testing to non-destructive rapid confirmatory
identification at a crime scene. *Forensic Science International* 2009;
188: 1-17
124. Weyer LG, Lo S-C *Spectra-Structure Correlations in the Near-infrared*.
In: *Handbook of Vibrational Spectroscopy*, 2006
125. Hall JW, Pollard A Near-infrared spectroscopic determination of
serum total proteins, albumin, globulins, and urea. *Clin Biochem* 1993;
26: 483-490

126. Inoue H, Takabe F, Iwasa M, Maeno Y, Seko Y A New Marker for Estimation of Bloodstain Age by High-Performance Liquid-Chromatography. *Forensic Science International* 1992; 57: 17-27
127. Strasser S, Zink A, Kada G, Hinterdorfer P, Peschel O, Heckl WM, Nerlich AG, Thalhammer S Age determination of blood spots in forensic medicine by force spectroscopy. *Forensic Science International* 2007; 170: 8-14
128. Bauer M, Polzin S, Patzelt D Quantification of RNA degradation by semi-quantitative duplex and competitive RT-PCR: a possible indicator of the age of bloodstains? *Forensic Science International* 2003; 138: 94-103
129. Anderson S, Howard B, Hobbs GR, Bishop CP A method for determining the age of a bloodstain. *Forensic Science International* 2005; 148: 37-45
130. Wood MFG, Cote D, Vitkin IA Combined optical intensity and polarization methodology for analyte concentration determination in simulated optically clear and turbid biological media. *Journal of Biomedical Optics* 2008; 13
131. Osborne BG, Fearn T, Hindle PH *Practical NIR Spectroscopy*. Harlow, UK: Longman, 1993
132. Schrader W, Meuer P, Popp J, Kiefer W, Menzebach JU, Schrader B Non-invasive glucose determination in the human eye. *Journal of Molecular Structure* 2005; 735-36: 299-306
133. Kasemsumran S, Du YP, Murayama K, Huehne M, Ozaki Y Simultaneous determination of human serum albumin, gamma-globulin, and glucose in a phosphate buffer solution by near-infrared spectroscopy with moving window partial least-squares regression. *Analyst* 2003; 128: 1471-1477
134. Hazen KH, Arnold MA, Small GW Measurement of glucose and other analytes in undiluted human serum with near-infrared transmission spectroscopy. *Analytica Chimica Acta* 1998; 371: 255-267

135. Peuchant E, Salles C, Jensen R Determination of Serum-Cholesterol by Near-Infrared Reflectance Spectrometry. *Analytical Chemistry* 1987; 59: 1816-1819
136. Chen J, Arnold MA, Small GW Comparison of combination and first overtone spectral regions for near-infrared calibration models for glucose and other biomolecules in aqueous solutions. *Analytical Chemistry* 2004; 76: 5405-5413
137. Sato T, Kawano S, Iwamoto M Near-Infrared Spectral Patterns of Fatty-Acid Analysis from Fats and Oils. *Journal of the American Oil Chemists Society* 1991; 68: 827-833
138. Kuenstner JT, Norris KH, McCarthy WF Measurement of Hemoglobin in Unlysed Blood by Near-Infrared Spectroscopy. *Applied Spectroscopy* 1994; 48: 484-488
139. Workman JJ Interpretive spectroscopy for near infrared. *Applied Spectroscopy Reviews* 1996; 31: 251-320
140. Roggan A, Friebel M, Dorschel K, Hahn A, Muller G Optical properties of circulating human blood in the wavelength range 400-2500 NM. *Journal of Biomedical Optics* 1999; 4: 36-46
141. Jacquemoud, S. and Ustin, S. L. Application of radiative transfer models to moisture content estimation and burned land mapping. 4th International Workshop on Remote Sensing and GIS Applications to Forest Fire Management. 2003.
Ref Type: Conference Proceeding
142. Kuenstner JT, Norris KH, Kalasinsky VF Spectrophotometry of Human Hemoglobin in the Midinfrared Region. *Biospectroscopy* 1997; 3: 225-232
143. Liu YL, Cho RK, Sakurai K, Miura T, Ozaki Y Studies on Spectra-Structure Correlations in Near-Infrared Spectra of Proteins and Polypeptides .1. A Marker Band for Hydrogen-Bonds. *Applied Spectroscopy* 1994; 48: 1249-1254

144. Kim YJ, Yoon G Prediction of glucose in whole blood by near-infrared spectroscopy: Influence of wavelength region, preprocessing, and hemoglobin concentration. *Journal of Biomedical Optics* 2006; 11
145. Burmeister JJ, Arnold MA Evaluation of measurement sites for noninvasive blood glucose sensing with near-infrared transmission spectroscopy. *Clinical Chemistry* 1999; 45: 1621-1627
146. Durand A, Devos O, Ruckebusch C, Huvenne JP Genetic algorithm optimisation combined with partial least squares regression and mutual information variable selection procedures in near-infrared quantitative analysis of cotton-viscose textiles. *Analytica Chimica Acta* 2007; 595: 72-79
147. Sikirzhitski V, Virkler K, Lednev IK Discriminant Analysis of Raman Spectra for Body Fluid Identification for Forensic Purposes. *Sensors* 2010; 10: 2869-2884
148. Kateb B, Yamamoto V, Yu C, Grundfest W, Gruen JP Infrared thermal imaging: A review of the literature and case report. *Neuroimage* 2009; 47: T154-T162
149. Gowen AA, Tiwari BK, Cullen PJ, McDonnell K, O'Donnell CP Applications of thermal imaging in food quality and safety assessment. *Trends in Food Science & Technology* 2010; 21: 190-200
150. Vadivambal R, Jayas DS Applications of Thermal Imaging in Agriculture and Food Industry-A Review. *Food and Bioprocess Technology* 2011; 4: 186-199
151. Khallaf A, Williams RW Postmortem Cooling of the Human Head - An Infrared Thermology Study. *Journal of the Forensic Science Society* 1991; 31: 7-19
152. van Iersel, M., Veerman, H., and van der Mark, W. Modelling a crime scene in 3D and adding thermal information. Huckridge, D. A. and Ebert, R. R. *Electro-Optical and Infrared Systems: Technology and Applications VI*. SPIE 7481, 74810M-74810M-11. 2009.
Ref Type: Conference Proceeding

153. Brooke H, Baranowski MR, McCutcheon JN, Morgan SL, Myrick ML Multimode Imaging in the Thermal Infrared for Chemical Contrast Enhancement. Part 3: Visualizing Blood on Fabrics. *Analytical Chemistry* 2010; 82: 8427-8431
154. Ammer K, Ring EFJ Application of thermal imaging in forensic medicine. *Imaging Science Journal* 2005; 53: 125-131
155. Gashi B, Edwards MR, Sermon PA, Courtney L, Harrison D, Xu Y Measurement of 9 mm cartridge case external temperatures and its forensic application. *Forensic Science International* 2010; 200: 21-27
156. Riga A Thermal analysis as an aid to forensics: Alkane melting and oxidative stability of wool. *Thermochimica Acta* 1998; 324: 151-163
157. Rozlosnik, A. E. Bringing up to date applications of infrared thermography in surveillance, safety and rescue. Dinwiddie, R. B. and LeMieux, D. H. *Thermosense XXII. SPIE 4020*, 387-405. 2000.
Ref Type: Conference Proceeding
158. Steketee J Spectral Emissivity of Skin and Pericardium. *Phys Med Biol* 1973; 18: 686-694
159. Watmough DJ, Phil D, Oliver R The emission of infrared radiation from human skin - implications for clinical thermography. *Br J Radiol* 1969; 42: 411-415
160. Bartl J, Baranek M Emissivity of aluminium and its importance for radiometric measurement. *Meas Phys Quant* 2004; 4
161. Watson K Two-temperature method for measuring emissivity. *Remote Sens Environ* 1992; 42: 117-121
162. Rozenbaum O, Meneses DD, Auger Y, Chermanne S, Echegut P A spectroscopic method to measure the spectral emissivity of semi-transparent materials up to high temperature. *Review of Scientific Instruments* 1999; 70: 4020-4025

163. Kruse PW A Comparison of the Limits to the Performance of Thermal and Photon Detector Imaging Arrays. *Infrared Physics & Technology* 1995; 36: 869-882
164. Balcerak, R. S. Uncooled IR Imaging: technology for the next generation. Andresen, B. F. and Scholl, M. S. *Infrared Technology and Applications XXV*. SPIE 3698, 110-118. 1999.
Ref Type: Conference Proceeding
165. Riedel, R. B., Coffin, J. S., and Prokoski, F. J. Forensic use of infrared video. *International Carnahan Conference on Security Technology*. IEEE , 108-112. 1992.
Ref Type: Conference Proceeding
166. Wickenheiser RA Trace DNA: A review, discussion of theory, and application of the transfer of trace quantities of DNA through skin contact. *Journal of Forensic Sciences* 2002; 47: 442-450
167. Henssge C Death Time-Estimation in Case Work .1. the Rectal Temperature Time of Death Nomogram. *Forensic Science International* 1988; 38: 209-236
168. Mall G, Hubig M, Eckl M, Buettner A, Eisenmenger W Modelling postmortem surface cooling in continuously changing environmental temperature. *Legal Medicine* 2002; 4: 164-173
169. Weyermann C, Ribaux O Situating forensic traces in time. *Science and Justice* 2012; 52: 68-75
170. Wang L, Jacques SL, Zheng L MCML - Monte Carlo modeling of light transport in multi-layered tissues. *Computer Methods and Programs in Biomedicine* 1995; 47: 131-146
171. Janchaysang S, Sumriddetchkajorn S, Buranasiri P Tunable filter-based multispectral imaging for detection of blood stains on construction material substrates. Part 1. Developing blood stain discrimination criteria. *Appl Opt* 2012; 51: 6984-6996

172. Lu M, Zhao L, Wang Y, You G, Kan X, Zhang Y, Zhang N, Wang B, Guo Y-J, Zhou H Measurement of the methemoglobin concentration using Raman spectroscopy. *Artificial cells, Nanomedicine, and Biotechnology* 2013; 1-7
173. Dasgupta R, Ahlawat S, Verma RS, Uppal A, Gupta PK Hemoglobin degradation in human erythrocytes with long-duration near-infrared laser exposure in Raman optical tweezers. *Journal of Biomedical Optics* 2010; 15: 055009
174. Hanson EK, Ballantyne J A blue spectral shift of the hemoglobin soret band correlates with the age (time since deposition) of dried bloodstains. *PLoS One* 2010; 5: e12830
175. Trombka JI, Schweitzer J, Selavka C, Dale M, Gahn N, Floyd S, Marie J, Hobson M, Zeosky J, Martin K, McClannahan T, Solomon P, Gottschang E Crime scene investigations using portable, non-destructive space exploration technology. *Forensic Sci Int* 2002; 123: 1-9
176. Weyermann C, Roux C, Champod C Initial Results on the Composition of Fingerprints and its Evolution as a Function of Time by GC/MS Analysis. *J Forensic Sci* 2011; 56: 102-108
177. Rosineide C.Simas, Gustavo B.Sanvido, Wanderson Romão, Priscila M.Lalli, Mario Benassi, Ildenize B.S.Cunha, Marcos N.Eberlin Ambient mass spectrometry: bringing MS into the "real world". *Anal Bioanal Chem* 2010; 398: 265-294
178. Espy RD, Manicke NE, Ouyang Z, Cooks RG Rapid analysis of whole blood by paper spray mass spectrometry for point-of-care therapeutic drug monitoring. *Analyst* 2012; 137: 2344-2349
179. Xiaobo Z, Jiewen Z, Povey MJW, Holmes M, Hanpin M Variables selection methods in near-infrared spectroscopy. *Analytica Chimica Acta* 2010; 667: 14-32

11 - SUMMARY

Blood stains are an important source of information in criminal investigations, as blood stain patterns can inform investigators about the activities causing the stains, and subsequent DNA-analysis can identify or exclude possible suspects. In this thesis, we demonstrated several spectroscopic techniques for the detection, identification and age estimation of blood stains, as outlined in **Chapter 1**. The introduction emphasizes the need for innovative techniques which aid crime scene investigation. Because existing spectroscopic techniques are rapid, portable, and non-destructive, the described techniques are highly suitable for crime scene analysis.

An interesting technique for the non-destructive analysis of forensic traces is hyperspectral imaging. In **Chapter 2**, we review the application of hyperspectral imaging for the visualization and chemical analysis of forensic traces and describe its advantages and main challenges. Because hyperspectral imaging integrates conventional imaging and spectroscopy, both spatial and spectral information are obtained simultaneously, enabling investigators to analyze the chemical composition of traces and visualize their spatial distribution at the same time.

Both probe based spectroscopy and hyperspectral imaging are introduced as an indicative test for the identification of blood stains in **Chapter 3**. We propose a light-transport model to indicate the presence of the haemoglobin oxidation products oxyhaemoglobin (HbO_2), methaemoglobin (MetHb), and hemichrome (HC) from reflectance spectra of blood stains, enabling investigators to distinguish blood from other samples. The sensitivity and specificity of the technique are investigated, and the practical applicability is demonstrated in forensic casework.

Apart from the presence of haemoglobin oxidation products, the proposed light-transport model can be used to calculate the relative concentrations of HbO_2 , MetHb and HC, which in turn can be used to estimate the age of a blood stain. In **Chapter 4** we successfully estimate the age of different blood stain patterns on white cotton backgrounds at a simulated crime scene using hyperspectral imaging. **Chapter 5** describes an adapted light-

transport model to correct for light absorptions of coloured backgrounds. Additionally, we describe a statistical approach to calculate an age interval for a questioned blood stain. The applicability of the new technique for blood stain age estimation in forensic casework and its possible value for criminal investigations is demonstrated in a case example. In the described homicide investigation, the results led to a more complete reconstruction of the timeline of events.

Chapter 6 covers the detection of latent blood stains on black backgrounds using visible hyperspectral imaging. At a crime scene, some blood stains may be invisible to the naked eye. Only after a stain is detected, it can be analysed further to be used as evidence in court, motivating the need for technology highlighting the contrast between a stain and its background. This chapter shows that blood stains can be distinguished from black fabrics based on the different absorption properties in the visible wavelength range.

In **Chapter 7** we analyse blood stains on black and coloured backgrounds using near infrared (NIR) spectroscopy. On these backgrounds, we successfully identify blood stains using correlation analysis and estimated their age using partial least squares regression analysis. Compared to visible spectroscopy, NIR spectroscopy provides more information about the chemical structure of samples, which is interesting for many forensic applications.

A final wavelength range explored in this thesis is the mid infrared or thermal wavelength range. All objects radiate infrared energy, invisible to the human eye, which can be converted into visible images by mid infrared cameras, thereby visualizing differences in temperature and/or emissivity of objects. **Chapter 8** provides an overview of the principles and instrumentation involved in mid infrared imaging. Difficulties concerning image interpretation are addressed. Reported forensic applications are reviewed and supported by practical illustrations, among which the detection of latent blood stains.

To conclude, all topics described above are discussed from a forensic practical point of view in **Chapter 9**. Emphasis is laid on further steps needed for the actual implementation of the described innovative techniques in standard forensic practice.

12 - SAMENVATTING

Bloedsporen bevatten belangrijke informatie voor criminalistisch onderzoek; bloedspoorpatronen geven aanwijzingen over de activiteiten die voorafgaand hebben plaatsgevonden en door middel van DNA analyse kan de donor worden geïdentificeerd. In dit proefschrift zijn verschillende spectroscopische technieken gebruikt voor de detectie, identificatie en leeftijdsbepaling van bloedsporen, zoals omschreven in **Hoofdstuk 1**. Deze introductie benadrukt de behoefte aan innovatieve technieken voor onderzoek op de plaats delict. Omdat bestaande spectroscopische technieken snel, draagbaar en niet destructief zijn, zijn de beschreven technieken erg geschikt voor sporenonderzoek op de plaats delict.

Een interessante techniek voor de niet destructieve analyse van forensische sporen is hyperspectrale beeldvorming. Verschillende toepassingen van hyperspectrale beeldvorming voor de visualisatie en chemische analyse van forensische sporen passeren in **Hoofdstuk 2** de revue. De voordelen en uitdagingen van deze techniek worden besproken. Hyperspectrale beeldvorming combineert conventionele fotografie met spectroscopie, waardoor zowel spatiële als spectrale informatie tegelijkertijd wordt vergaard. Dit geeft onderzoekers de mogelijkheid om de chemische samenstelling van sporen te analyseren en tegelijkertijd de verspreiding van verschillende sporen te visualiseren.

In **Hoofdstuk 3** worden spectroscopie en hyperspectrale beeldvorming geïntroduceerd als een indicatieve test voor de identificatie van bloedsporen. Door middel van een lichttransport model wordt de aanwezigheid van de hemoglobine oxidatieproducten oxyhemoglobine (HbO_2), methemoglobine (MetHb) en hemichroom (HC) aangetoond. Dit maakt het mogelijk om bloed te onderscheiden van soortgelijk gekleurde stoffen op basis van het reflectie spectrum. De gevoeligheid en specificiteit van deze techniek is onderzocht en de praktische bruikbaarheid is gedemonstreerd in een zaakvoorbeeld.

Behalve de aanwezigheid van oxidatieproducten van hemoglobine kan het voorgestelde lichttransport model ook worden gebruikt om de relatieve

hoeveelheid HbO₂, MetHb en HC te berekenen. Deze informatie kan worden gebruikt om de leeftijd van een bloedvlek te bepalen. In **Hoofdstuk 4** wordt de leeftijd van verschillende bloedspoorpatronen op wit katoen in een gesimuleerde plaats delict succesvol bepaald met behulp van hyperspectrale beeldvorming. **Hoofdstuk 5** beschrijft een aangepast lichttransport model, waarmee het mogelijk wordt om te corrigeren voor absorptie van licht door gekleurde ondergronden. Bovendien wordt een statistische benadering voor de berekening van een leeftijdsinterval van een bloedvlek beschreven. De toepasbaarheid van de nieuwe techniek voor bloeddatering in forensisch onderzoek en de mogelijke waarde in misdaadonderzoek is gedemonstreerd in een zaakvoorbeeld. In de beschreven moordzaak konden de resultaten helpen bij de reconstructie van een tijdlijn van gebeurtenissen.

Hoofdstuk 7 beschrijft de detectie van onzichtbare bloedvlekken op zwarte ondergronden met behulp van een hyperspectrale camera. Op een plaats delict zijn niet alle bloedvlekken met het blote oog zichtbaar. Pas nadat een vlek gedetecteerd is, kan een verdere analyse plaatsvinden, zodat de vlek als bewijsmiddel in een rechtszaak kan dienen. Daarom is er behoefte aan technologie waarmee het contrast tussen een vlek en de ondergrond wordt vergroot. Dit hoofdstuk laat zien dat bloedsporen kunnen worden onderscheiden van zwarte stoffen op basis van verschillende absorptie eigenschappen.

In **Hoofdstuk 7** analyseren we bloedvlekken op zwarte en gekleurde ondergronden met nabij infrarood (NIR) spectroscopie. Op deze ondergronden worden bloedvlekken succesvol geïdentificeerd door middel van een correlatie analyse. Ook wordt de leeftijd bepaald door middel van partial least squares regressie analyse. Vergeleken met zichtbare spectroscopie geeft NIR spectroscopie meer informatie over de chemische samenstelling van een stof, wat interessant kan zijn voor veel forensische toepassingen.

Het laatste golflengtegebied dat in dit proefschrift aan bod komt is het mid infrarode ofwel thermische bereik. Ieder object straalt infrarode energie uit, onzichtbaar voor het menselijk oog, wat kan worden geconverteerd in een zichtbaar beeld door een thermische camera. Daardoor worden verschillen in temperatuur en emissiviteit zichtbaar. **Hoofdstuk 8** geeft een overzicht van

het principe achter thermische camera's. Moeilijkheden bij de interpretatie van beelden worden besproken. Tot slot wordt een overzicht gegeven van uit de literatuur bekende forensische toepassingen. Het verhaal wordt ondersteund met een aantal praktische illustraties, waaronder de detectie van latente bloedsporen.

Alle onderwerpen die hierboven aan bod kwamen worden vanuit de forensische praktijk beschouwd in **Hoofdstuk 9**. De nadruk wordt daarbij gelegd op vervolgstappen die nodig zijn voor een daadwerkelijke implementatie van de beschreven innovatieve technieken in standaard forensisch onderzoek.

13 - CURRICULUM VITAE

Gerda Edelman (1980) completed her Masters degree in Physics at the Radboud University Nijmegen in 2004. In 2005 she worked as a high school physics teacher at the Open Schoolgemeenschap Bijlmer in Amsterdam and acquired a teacher degree in a post-Master education program at the University of Amsterdam (UvA). Gerda then completed the Forensic Science Master at the UvA in 2006 and graduated with honours. Following a successful internship she was employed as an applied scientist at the Netherlands Forensic Institute (NFI), where she worked on digital image analysis and crime scene reconstructions. Three years later, she chose to become a PhD student in the Department of Biomedical Engineering and Physics of the Academic Medical Center (AMC) in Amsterdam. Her research on the detection, identification and age estimation of blood stains at the crime scene using hyperspectral imaging resulted in this thesis. Gerda Edelman is currently employed as a researcher within the Mobile Forensic Team of the NFI. Her role is to improve existing and develop new, innovative techniques to be used by her crime scene investigation colleagues in the field.

14 - PORTFOLIO

AMC Graduate School for Medical Sciences PhD Portfolio – Summary of PhD training and teaching programme.

Name PhD student: Gerda Edelman
PhD period: December 2009 – June 2013
Name PhD supervisors: Maurice Aalders and Ton van Leeuwen

14.1. TRAINING

General courses

2011 Scientific writing in English for publication (1.5 ECTS)
2011 Practical biostatistics (1.1 ECTS)
2012 Advanced topics in biostatistics (2.1 ECTS)

Workshops

2010 IEEE-WHISPERS, Workshop on Hyperspectral Image and Signal Processing: Evolution in Remote Sensing, Reykjavik, Iceland (1.6 ECTS)
2011 IEEE-WHISPERS, Lisbon, Portugal (1.6 ECTS)
2012 IASIM-12 Hyperfest workshop, Sigulda, Latvia (2 ECTS)
2011 Hyperfest workshop, Riga, Latvia (1 ECTS)

Presentations

2010 – 2013 National chemistry meetings (1.4 ECTS)
2010 – 2013 National forensic meetings (1.4 ECTS)

(Inter)national conferences

2012 EAFS2012, European Association of Forensic Sciences, The Hague, The Netherlands (1.25 ECTS)
Oral presentation (0.5 ECTS)
2010 IASIM-10, International Association for Spectral Imaging,

- Dublin, Ireland (0.5 ECTS)
 Oral presentations (1 ECTS)
- 2012 IASIM-12, International Association for Spectral Imaging,
 Riga, Latvia (0.75 ECTS)
 Oral presentation (0.5 ECTS)
- 2013 SPIE Defense, Security, and Sensing, Baltimore, USA
 (1 ECTS)
 Oral presentation (0.5 ECTS)
- 2012 WSC-8, Winter symposium on chemometrics, Drakino, Russia
 (1 ECTS)
 Oral presentation (0.5 ECTS)
- 2010 IABPA, International Association of Bloodstain Pattern
 Analysts, Lisbon, Portugal (1 ECTS)

Other

- 2009 – 2013 Technical demonstrations (3 ECTS)
- 2012 Member of scientific committee, IASIM-12, International
 Association for Spectral Imaging, Riga, Latvia (1 ECTS)

14.2. TEACHING

Lecturing

- 2010 Observer based techniques, University of Amsterdam
 (0.5 ECTS)
- 2011 – 2013 CSI reality, University of Amsterdam (1 ECTS)

Supervising

- 2010 – 2013 Internships forensic science students (7 ECTS)
- 2011 – 2013 Practical traineeships physics students (1.2 ECTS)
- 2009 – 2013 Practical assignments for physics students (2 ECTS)
- 2010 – 2011 Practical assignments for medical students (1 ECTS)

15 - LIST OF PUBLICATIONS

Publications related to this thesis:

Edelman GJ, van Leeuwen TG, Aalders MCG. Visualization of latent blood stains using visible reflectance hyperspectral imaging and chemometrics. *Journal of Forensic Sciences*; in press.

Edelman GJ, van Leeuwen TG, Aalders MCG. Hyperspectral imaging of the crime scene for the automatic detection and identification of blood stains. *Proceedings of SPIE Defense Security and Sensing*; 2013.

Edelman GJ, Hoveling RJM, Roos M, van Leeuwen TG, Aalders MC. Infrared imaging of the crime scene: possibilities and pitfalls. *Journal of Forensic Sciences* 2013; 58(5):1156-62.

Edelman GJ, Manti V, van Ruth SM, van Leeuwen TG, Aalders MCG. Identification and age estimation of blood stains on coloured backgrounds by near infrared spectroscopy. *Forensic Science International* 2012;220(1-3):239-44.

Edelman GJ, Gaston E, van Leeuwen TG, Cullen PJ, Aalders MC. Hyperspectral imaging for non-contact analysis of forensic traces. *Forensic Science International* 2012;223(1-3):28-39.

Edelman GJ, van Leeuwen TG, Aalders MCG. Hyperspectral imaging for the age estimation of blood stains at the crime scene. *Forensic Science International* 2012;223(1-3):72-7.

Bremmer RH, Edelman G, Vegter TD, Bijvoets T, Aalders MCG. Remote spectroscopic identification of bloodstains. *Journal of Forensic Sciences* 2011;56(6):1471-5.

Publications not related to this thesis:

Edelman GJ, Lopatka M, Aalders MC. Objective colour classification of ecstasy tablets by hyperspectral imaging. *Journal of Forensic Sciences* 2013;58(4):881-6.

Edelman G, Alberink I, Hoogeboom B. Comparison of the performance of two methods for height estimation. *Journal of Forensic Sciences* 2010;55(2):358-65.

Edelman G, Bijhold J. Tracking people and cars using 3D modeling and CCTV. *Forensic Science International* 2010;202(1-3):26-35.

Edelman G, Alberink I. Estimation of body heights in digital images. In: Jamieson A, Moenssens A, editors. *Wiley Encyclopedia of Forensic Science*. 1 ed. Chichester: John Wiley & Sons; 2009;1624-32.

Edelman G, Alberink I. Height measurements in images: how to deal with measurement uncertainty correlated to actual height. *Law, probability & risk* 2009;9(2):91-102.

Edelman G, Alberink I. Comparison of body height estimation using bipeds or cylinders. *Forensic Science International* 2009;188(1-3):64-7.

16 - DANKWOORD

AT THE SOUND OF OUR STEPS HE GLANCED ROUND AND SPRANG TO HIS FEET WITH A CRY OF PLEASURE.

“I’VE FOUND IT! I’VE FOUND IT,” HE SHOUTED TO MY COMPANION, RUNNING TOWARDS US WITH A TEST-TUBE IN HIS HAND. “I HAVE FOUND A RE-AGENT WHICH IS PRECIPITATED BY HAEMOGLOBIN, AND BY NOTHING ELSE.”

HAD HE DISCOVERED A GOLD MINE, GREATER DELIGHT COULD NOT HAVE SHONE UPON HIS FEATURES.

“DR. WATSON, MR. SHERLOCK HOLMES,” SAID STAMFORD, INTRODUCING US. (...) “THE QUESTION NOW IS ABOUT HAEMOGLOBIN. NO DOUBT YOU SEE THE SIGNIFICANCE OF THIS DISCOVERY OF MINE?”

“IT IS INTERESTING, CHEMICALLY, NO DOUBT,” I ANSWERED, “BUT PRACTICALLY...”

A Study in Scarlet – Arthur Conan Doyle

In de bovenstaande passage ontdekt Sherlock Holmes een test, waarmee hij bloed kan identificeren. Hij is uitzinnig van vreugde, maar Dr. Watson zet hem al gauw weer met beide benen op de grond door te wijzen op de praktische bezwaren. Deze passage deed mij denken aan mijn promotie onderzoek. Het proefschrift is af, dus het dak kan eraf! Maar morgen, of overmorgen misschien, gaat het onderzoek gewoon door, om het volledig in de praktijk toepasbaar te maken.

Toen ik in december 2009 aan mijn promotie onderzoek begon, was er al een stevige basis gelegd. Het principe van de leeftijdsbepaling van bloedvlekken was al aangetoond. Aan mij de taak om de methode door te ontwikkelen van een laboratorium techniek naar een techniek die gebruikt kan worden op de plaats delict. Uiteraard was dit niet gelukt zonder de hulp en het enthousiasme van vele mensen om mij heen.

EDUCATION NEVER ENDS WATSON. IT IS A SERIES OF LESSONS WITH THE
GREATEST FOR THE LAST.

The Adventure of the Red Circle – Arthur Conan Doyle

Ik heb tijdens mijn promotie periode op het AMC ontzettend veel geleerd. Met name natuurlijk van mijn twee promotors. Maurice, jij ziet zelden problemen en altijd creatieve oplossingen. Hoe deprimerend mijn resultaten soms ook oogden, jij eindigde een bespreking vrijwel altijd met de woorden: “Nou, super!” Dat enthousiasme werkte erg aanstekelijk. Bedankt voor de prettige samenwerking! Ton, ik heb genoten van de vrijheid die je me hebt gegeven. Als we elkaar spraken, had je altijd een verhelderende, kritische blik op een idee, een experiment of een manuscript. Ook wil ik je bedanken voor de jaarlijkse uitjes naar de Jaap Eden baan waar we met de afdeling een Skeeve Skaes gingen rijden. Hartelijk dank ook aan Martin, die als emeritus hoogleraar altijd bereid was mee te denken of sommetjes op te lossen. Jetty, dankjewel voor de ondersteuning voorafgaand aan mijn verdediging en voor je flexibiliteit enkele uren voor een deadline.

NOTHING CLEARS UP A CASE SO MUCH AS STATING IT TO ANOTHER PERSON.

Silver Blaze – Arthur Conan Doyle

Mijn onderzoek werd mede mogelijk gemaakt door het CSI The Hague project. In het CSI lab hebben wij de techniek getest, doorontwikkeld en vooral heel vaak gedemonstreerd. De vragen van onder andere politici, NFI-ers, forensisch deskundigen en studenten leverden vaak nieuwe ideeën op. Bij deze wil ik graag Andro bedanken voor al zijn inzet in het project. Dankzij jou konden we onze techniek ‘uitrollen’ en bekendheid krijgen in binnen- en buitenland. Het eindfeestje met Beyoncé was legendarisch. Ook de altijd contente content-manager van CSI The Hague mag in dit dankwoord natuurlijk niet ontbreken. Jurrien, het was erg leuk om opnieuw met je samen te werken!

IT WAS WORTH A WOUND; IT WAS WORTH MANY WOUNDS; TO KNOW THE DEPTH OF LOYALTY AND LOVE WHICH LAY BEHIND THAT COLD MASK.

The Adventure of the Three Garridebs – Arthur Conan Doyle

Een belangrijke rol was ook weggelegd voor Henk, ons slachtoffer dat altijd bereid was te figureren op de gesimuleerde plaats delict (zie figuur 2.9). Ook tijdens borrels zorgde hij als danspartner voor de nodige hilariteit. Henk, bedankt!

Naast de demonstraties in het CSI lab, heb ik de afgelopen jaren regelmatig de kans gekregen om mijn onderzoek te presenteren op congressen en symposia. Ik heb daardoor allerlei interessante mensen leren kennen, van wie ik veel heb geleerd en met wie ik van alles heb beleefd. Paardrijden in IJsland, de handstand oefenen in Lissabon, bobsleeën en een feestje geven in mijn penthouse in Letland, sneeuwscooteren in Rusland, de koningin ontmoeten in Den Haag, de laatste koninginnedag vieren in Baltimore... allemaal geweldige ervaringen! Op dat laatste na dan.

Maar ook voor mijn proefschrift hebben mijn reizen concreet iets opgeleverd. Hoofdstuk 2 is tot stand gekomen doordat PJ mij in de kroeg in Dublin voorstelde samen een review paper te schrijven. Anderhalf jaar en een aantal skype-sessies met PJ en Edurne later was het manuscript af. Ook hoofdstuk 7 heeft zijn oorsprong in Dublin. In een andere bar ontmoette ik Vicky, die mij vriendelijk aanbood gebruik te maken van een nabij infrarood spectrometer. Toen haar dochter een bloedneus had, ging zij vol enthousiasme van start met een eerste meting aan een bebloede zakdoek, waarna ik een maand lang regelmatig metingen kon doen op het Rikilt in Wageningen. Voor de analyse van data van spectrale camera's heb ik veel opgestoken van de allereerste Hyperfest workshop, georganiseerd door James. Jimi, hartelijk dank voor de gastvrije ontvangst in je villa aan de rivier, vlakbij het strand, met pooltafel en sauna in de kelder. Aoife en Federico, het was leuk om jullie in allerlei landen te ontmoeten. Ik heb veel van jullie geleerd! Kodi, bedankt dat je

me elke ochtend opgewekt kwispelend wakker kwam maken voor een wandeling naar het strand.

THERE IS NOTHING MORE STIMULATING THAN A CASE WHERE
EVERYTHING GOES AGAINST YOU.

The Hound of the Baskervilles – Arthur Conan Doyle

Om op verzoek van de politie metingen te doen in moordzaken, werd het FTS crime scene team opgericht. Ingevroren bloed, beschimmelde bloedvlekken, bloedvlekken die stinken naar kattenpis. Een bloedvlekje van nog geen millimeter op het plafond, bloed op een donkerblauw T-shirt of op een mahoniehouten vloer; de zaken die we aangedragen kregen zorgden steeds weer voor nieuwe uitdagingen. En om de situatie nog iets complexer te maken, werd onze spiksplinternieuwe spectrale camera (gebruikt in hoofdstuk 4) gestolen, net als de geleende thermische camera (gebruikt in hoofdstuk 8). Toch kwamen we hierdoor steeds een stap verder. De omstandigheden in de zaken leverden mooie onderzoeksvragen op en door de diefstal van de camera's kreeg de ontwikkeling van een nieuwe draadloze camera meer prioriteit. De nieuwe camera (gebruikt in hoofdstuk 6) bewees meteen tegen een stootje te kunnen, want ook nadat hij bij een botsing door de auto was geslingerd, deed hij het nog prima! Ivo, Mercedes, Jan, Marilyn, Maurice en Richelle: bedankt voor de leuke tijd bij FTS!

A SANDWICH AND A CUP OF COFFEE, AND THEN OFF TO VIOLIN-LAND,
WHERE ALL IS SWEETNESS AND DELICACY AND HARMONY, AND THERE ARE
NO RED-HEADED CLIENTS TO VEX US WITH THEIR CONUNDRUMS.

The Adventures of Sherlock Holmes – Arthur Conan Doyle

Een kopje koffie met een muffin op het voetenplein, lunchen bij de Basiliek of de polonaise lopen bij een optreden van Danny de Munk. Een werkdag zou maar wat saai zijn zonder leuke collega's om je heen. Edwin, jij zorgde altijd voor een vrolijke noot in onze kelder. En je was natuurlijk een fantastische

manager van de jaarlijkse labschoonmaak! Richelle, wat mij betreft ben jij de medewerker van de week! Ik kan me geen betere paranimf voorstellen! Ook de rest van de keldercrew wil ik bedanken voor de gezelligheid: Annemieke, Kai, Jasmin, Saskia, wat moet een mens met daglicht als jullie altijd het zonnetje in huis zijn? Angela, zonder jou was dit proefschrift natuurlijk nooit tot stand gekomen. Bedankt voor alle keren dat je bloed hebt willen afnemen! Judith, bedankt voor het weer oplappen van een bezweken student na het bloed prikken. Daar gaan we zeker nog eens op proosten onder het genot van een goed concert. Nienke en Annemarie, jullie waren altijd een goede reden om eens boven te komen buurten. De volgende keer kom ik graag eens langs down under in Den Bosch of Sydney.

André en Thamar, wat leuk dat wij jaren na onze studie weer herenigd werden op het AMC. Ik had destijds durven wedden om een kratje bier dat ik nooit zou gaan promoveren. Onze dates op het Voetenplein of in het Oude Gasthuis waren weer als vanouds! Dr Dre, het was ook erg leuk om samen met jou Amsterdam te herontdekken. Van De Gracht naar Maloe Melo, via de warp zone naar de Korsakoff, steeds weer een level verder tot de uitsmijter er een einde aan maakte. Op de volgende promotie! Dirk, iets voor jou misschien?

THE WORLD IS FULL OF OBVIOUS THINGS WHICH NOBODY BY ANY CHANCE
EVER OBSERVES

The Hound of the Baskervilles – Arthur Conan Doyle

De technieken omschreven in dit proefschrift kunnen het menselijk observatie vermogen ondersteunen bij het onderzoek op de plaats delict. De laatste loodjes heb ik afgemaakt naast mijn nieuwe functie binnen het Mobiel Forensisch Team van het NFI. Bij deze wil ik ook mijn nieuwe collega's hartelijk bedanken. Gerard, fijn dat je me de kans gaf om mijn proefschrift af te maken naast mijn nieuwe baan. Matthijs, Jurrien en Paul, samen met jullie ga ik graag de uitdaging aan om nieuwe technieken te ontwikkelen voor sporenonderzoek. Ook de input en praktijkervaring van sporendeskundigen is

daarbij heel waardevol, wat al bleek in hoofdstuk 5 en 8, waaraan Martin een nuttige bijdrage heeft geleverd. Martin, Fetze, Paul, Josita, Marcel, Léon en Dennis, mede dankzij jullie ga ik elke dag met veel plezier naar mijn werk! Annabel, hartelijk bedankt voor je inzet voor de statistische onderbouwing van hoofdstuk 5. Ik hoop nog lang met je te kunnen samenwerken. Ook Elisa wil ik bedanken voor de prettige samenwerking. Ik ben blij dat het onderzoek naar de leeftijd van bloedvlekken in ons nieuwe project een vervolg gaat krijgen. Ivo en Ingrid, ik kom graag nog eens proosten op mijn proefschrift bij jullie aan de borreltafel.

“HOLMES AND WATSON ARE ON A CAMPING TRIP. IN THE MIDDLE OF THE NIGHT HOLMES WAKES UP AND GIVES DR. WATSON A NUDGE. "WATSON" HE SAYS, "LOOK UP IN THE SKY AND TELL ME WHAT YOU SEE."

"I SEE MILLIONS OF STARS, HOLMES," SAYS WATSON.

"AND WHAT DO YOU CONCLUDE FROM THAT, WATSON?"

WATSON THINKS FOR A MOMENT. "WELL," HE SAYS, "ASTRONOMICALLY, IT TELLS ME THAT THERE ARE MILLIONS OF GALAXIES AND POTENTIALLY BILLIONS OF PLANETS. ASTROLOGICALLY, I OBSERVE THAT SATURN IS IN LEO. HOROLOGICALLY, I DEDUCE THAT THE TIME IS APPROXIMATELY A QUARTER PAST THREE. METEROLOGICALLY, I SUSPECT THAT WE WILL HAVE A BEAUTIFUL DAY TOMORROW. THEOLOGICALLY, I SEE THAT GOD IS ALL-POWERFUL, AND WE ARE SMALL AND INSIGNIFICANT. UH, WHAT DOES IT TELL YOU, HOLMES?"

"WATSON, YOU IDIOT! SOMEONE HAS STOLEN OUR TENT!"

Plato and a Platypus Walk Into a Bar – Thomas Cathcart and Daniel Klein

En natuurlijk is het ook fijn om niet met wetenschap bezig te zijn! Gelukkig had ik daarvoor uitgebreid de gelegenheid. Voetballen, snowboarden, borrelen in Amsterdam, Brussel of Düsseldorf, concerten bezoeken, bootje varen. Bij deze wil ik graag al mijn vrienden bedanken. Niet omdat jullie iets met mijn proefschrift te maken hebben gehad, maar gewoon omdat het kan. Ik schrijf waarschijnlijk maar een keer in mijn leven een dankwoord en daarin mogen

jullie natuurlijk niet ontbreken. Steph, leuk dat je mijn paranimf wilde zijn! Het gebeurt niet vaak dat ik glaasjes water van je krijg.

Mijn familie ben ik natuurlijk ook eeuwig dankbaar. Loulou, jij bracht mij jaren geleden op het idee om het college forensische wetenschappen te gaan volgen. Vanaf dat moment wilde ik niks anders meer. Nellie, toen ik je eens vertelde dat ik een dag vrij had genomen om aan mijn proefschrift te werken, maar in plaats daarvan de halve dag had liggen slapen, had jij de bemoedigende woorden: “Dan had je de rust vast hard nodig”. Dat zijn teksten die alleen moeders kunnen zeggen. Dankjewel daarvoor. Wist je trouwens dat de lapjes uit hoofdstuk 6 van jouw oude kleding komen? Theo, zonder over bloed te willen praten had je toch altijd interesse in mijn onderzoek. Bedankt voor de support! Rest mij nog een speciaal persoon te bedanken, maar Paul, jou bedank ik liever persoonlijk.

